

## TECHNICAL REPORT STANDARD TITLE PAGE

1. REPORT NO. <b>WA-RD 482.1</b>	2. GOVERNMENT ACCESSION NO.	3. RECIPIENT'S CATALOG NO.	
4. TITLE AND SUBTITLE <b>Retrofit of Split Bridge Columns</b>	5. REPORT DATE <b>February 11, 2000</b>		
	6. PERFORMING ORGANIZATION CODE		
7. AUTHOR(S) <b>David I. McLean, Moein H. El-Aaarag and Paul D. Rogness</b>		8. PERFORMING ORGANIZATION REPORT NO.	
9. PERFORMING ORGANIZATION NAME AND ADDRESS <b>Washington State Transportation Center (TRAC) Civil and Environmental Engineering; Sloan Hall, Room 101 Washington State University Pullman, Washington 99164-2910</b>		10. WORK UNIT NO.	
		11. CONTRACT OR GRANT NO. <b>T9902-23</b>	
12. SPONSORING AGENCY NAME AND ADDRESS <b>Research Office Washington State Department of Transportation Transportation Building, MS 7370 Olympia, Washington 98504-7370 Keith Anderson, Project Manager, 360-709-5405</b>		13. TYPE OF REPORT AND PERIOD COVERED <b>Draft Report</b>	
		14. SPONSORING AGENCY CODE	
15. SUPPLEMENTARY NOTES <b>This study was conducted in cooperation with the U.S. Department of Transportation, Federal Highway Administration.</b>			
16. ABSTRACT <p>Many older bridges in Washington State contain split reinforced concrete columns as common members between adjacent bridge sections. The split detail was incorporated in columns to allow for movements in the bridge due to temperature and shrinkage effects. It is expected that these split columns will perform poorly in the event of a significant earthquake. This study investigated retrofitting measures for improving the seismic performance of existing split columns.</p> <p>Experimental tests were conducted on one-third scale split column specimens which were representative of the split columns present in the Spokane Street Overcrossing near Seattle. Two test setups were used to examine vulnerabilities in the split columns associated with seismic loading in the longitudinal and transverse directions of the bridge. The specimens were subjected to increasing levels of cycled inelastic lateral displacements. Various retrofit measures were evaluated. Specimen performance was evaluated on the basis of load capacity, displacement ductility, and hysteretic behavior.</p> <p>Tests on specimens representing as-built conditions revealed vulnerabilities that have previously been observed in the field or are expected to occur during a major earthquake. Poor performance evident in the as-built specimens included crack propagation from the base of the split, lap splice degradation, and shear failure in the split sections.</p> <p>Retrofit design focused on enhancing the column seismic performance while at the same time preserving as much of the gap between the split sections as possible. Procedures were developed for the design of steel jacketing as a retrofit measure for the split columns. Circular jacketing was used for the section below the split and for retrofitting a deficient lap splice. "D" shaped jackets were used for the split sections to provide confinement in flexural hinging regions and to increase shear strength. Tests on specimens retrofitted with the steel jacketing showed significant improvements in performance when compared to that for the as-built specimens.</p> <p>Three companies who manufacture composite retrofit systems were invited to participate in this project. Each company was provided with unretrofitted specimens to which they designed and installed their company's retrofit system. While some differences in performance were obtained with the various retrofit systems, all retrofitted specimens showed significant improvements in performance when compared to that for the as-built specimen. Performance differences in the retrofitted specimens were attributed to the different design procedures and assumptions used by each retrofit company.</p>			
17. KEY WORDS <b>Key words:</b>		18. DISTRIBUTION STATEMENT <b>No restrictions. This document is available to the public through the National Technical Information Service, Springfield, VA 22616</b>	
19. SECURITY CLASSIF. (of this report)  <b>None</b>	20. SECURITY CLASSIF. (of this page)  <b>None</b>	21. NO. OF PAGES	22. PRICE

**Research Report**

Research Project 9902-26  
Split Columns

**RETROFIT OF SPLIT BRIDGE COLUMNS**

by

David I. McLean  
Professor

Moein H. El-Aaarag  
Graduate Student

Paul D. Rogness  
Graduate Student

**Washington State Transportation Center (TRAC)**  
Department of Civil and Environmental Engineering  
Washington State University  
Pullman, Washington 99164-2910

Washington State Department of Transportation  
Technical Monitor  
Hongzhi Zhang  
Bridge and Structures Branch Engineer

Prepared for

**Washington State Transportation Commission**  
Department of Transportation  
and in cooperation with  
**U.S. Department of Transportation**  
Federal Highway Administration

February, 2000

## **DISCLAIMER**

The contents of this report reflect the views of the authors, who are responsible for the facts and the accuracy of the data presented herein. The contents do not necessarily reflect the official views or policies of the Washington State Transportation Commission, Department of Transportation, or the Federal Highway Administration. This report does not constitute a standard, specification, or regulation.

## TABLE OF CONTENTS

<u>Section</u>	<u>Page</u>
<b>Executive Summa Introduction .....</b>	<b>vii</b>
<b>Introduction.....</b>	<b>1</b>
Introduction and Background .....	1
Research Objectives .....	3
<b>Previous Research and Current Practice.....</b>	<b>3</b>
Column Deficiencies.....	3
Column Retrofitting.....	4
Steel Jacket Retrofitting .....	4
Composite Material Retrofitting.....	4
<b>Experimental Testing Program.....</b>	<b>14</b>
Test Specimens and Parameters.....	14
Test Setup and Procedures.....	16
<b>Research Findings and Discussion.....</b>	<b>20</b>
Out-of-Phase, Flexure-Critical Test Results .....	20
Specimen AB1 (As-Built) .....	20
Specimen SJ1 (Steel Jacket Retrofit).....	23
Specimen FW1 (Fyfe Company Retrofit).....	29
Specimen FW2 (Sumitomo Retrofit).....	34
Specimen FW3 (XXSys Retrofit).....	38
Comparison of Out-of-Phase, Flexure-Critical Specimen Performance .....	45
Out-of-Phase, Shear-Critical Test Results .....	47
Specimen AB3 (As-Built) .....	47
Specimen SJ3 (Steel Jacket Retrofit).....	49
Out-of-Phase, Footing Critical Test Results (Specimen SJ2) .....	54
Transverse Test Results .....	55
Specimen AB2 (As-Built) .....	55
Specimen SJ4 (Steel Jacket Retrofit).....	60
Specimen FW4 (Fyfe Company Retrofit).....	65
Specimen FW5 (Sumitomo Retrofit).....	65
Specimen FW5 (XXSys Retrofit).....	69
Comparison of Transverse Specimen Performance .....	75
<b>Conclusions.....</b>	<b>79</b>
<b>Recommendations/Applications/Implementation.....</b>	<b>80</b>
<b>Acknowledgments .....</b>	<b>82</b>
<b>References.....</b>	<b>83</b>
<b>Appendix A Fyfe Company Retrofit Design Calculations .....</b>	<b>A-1</b>
<b>Appendix B Sumitomo Retrofit Design Calculations .....</b>	<b>B-1</b>
<b>Appendix C XXSys Retrofit Design Calculations .....</b>	<b>C-1</b>

## LIST OF FIGURES

<u>Figure</u>	<u>Page</u>
1. Split Concrete Column from Spokane Street Overcrossing .....	2
2. Crack Propagation from the Base of the Split Sections.....	2
3. Steel Jacket Thickness for Hinge Confinement in a Circular Column .....	7
4. Steel Jacket Thickness for Lap Splice Retrofit in a Circular Column .....	7
5. Single Bending Retrofit Regions.....	9
6. Double Bending Retrofit Regions .....	9
7. Dimensions Used to Calculate $D_c$ .....	10
8. Out-of-Phase Test Setup.....	18
9. Transverse Test Setup.....	19
10. Details of Specimen AB1 .....	22
11. Specimen AB1 Testing Photographs.....	23
12. Load-Displacement Curves for Specimen AB1 .....	24
13. Basis of Retrofit to Prevent Crack Propagation from Split .....	26
14. “D” Section Steel Jacket Retrofit of Split Sections .....	26
15. Retrofit Details for Specimen SJ1 .....	27
16. Specimen SJ1 Test Photographs.....	28
17. Load-Displacement Curves for Specimen SJ1 .....	29
18. Retrofit Details for Specimen FW1 .....	30
19. Fyfe Company Retrofit Installation Photographs.....	32
20. Specimen FW1 Test Photographs.....	33
21. Load-Displacement Curves for Specimen FW1 .....	34
22. Retrofit Details for Specimen FW2 .....	36
23. Sumitomo Retrofit Installation Photographs .....	38
24. Specimen FW2 Test Photographs.....	39
25. Load-Displacement Curves for Specimen FW2 .....	40
26. Retrofit Details for Specimen FW3 .....	30
27. XXSysy Retrofit Installation Photographs .....	42
28. Specimen FW3 Test Photographs.....	44
29. Load-Displacement Curves for Specimen FW4 .....	45
30. Load-Displacement Envelope of Out-of-Phase, Flexure-Critical Specimens .....	46
31. Details for Specimen AB3.....	48
32. Specimen AB3 Test Photographs.....	49
33. Load-Displacement Curves for Specimen AB3 .....	50
34. Retrofit Details for Specimen SJ3 .....	51
35. Specimen SJ3 Test Photographs.....	52
36. Load-Displacement Curves for Specimen SJ3 .....	53
37. Retrofit Details for Specimen SJ2 .....	54
38. Specimen SJ2 Test Photographs.....	54
39. Load-Displacement Curves for Specimen SJ2 .....	54
40. Details for Specimen AB2.....	48
41. Specimen AB2 Test Photographs.....	49
42. Load-Displacement Curves for Specimen AB2 .....	50
43. Retrofit Details for Specimen SJ4 .....	27
44. Specimen SJ4 Test Photographs.....	28
45. Load-Displacement Curves for Specimen SJ4 .....	29
46. Retrofit Details for Specimen FW4 .....	30
47. Specimen FW4 Test Photographs.....	33
48. Load-Displacement Curves for Specimen FW4 .....	34
49. Retrofit Details for Specimen FW5 .....	36
50. Specimen FW5 Test Photographs.....	39

## LIST OF FIGURES

<u>Figure</u>	<u>Page</u>
1. Split Concrete Column from Spokane Street Overcrossing.....	2
2. Crack Propagation from the Base of the Split Sections.....	2
3. Steel Jacket Thickness for Hinge Confinement in a Circular Column.....	7
4. Steel Jacket Thickness for Lap Splice Retrofit in a Circular Column.....	7
5. Single Bending Retrofit Regions.....	9
6. Double Bending Retrofit Regions.....	9
7. Dimensions Used to Calculate $D_e$ .....	10
8. Out-of-Phase Test Setup.....	18
9. Transverse Test Setup.....	19
10. Details of Specimen AB1.....	21
11. Specimen AB1 Testing Photographs.....	22
12. Load-Displacement Curves for Specimen AB1.....	24
13. Basis of Retrofit to Prevent Crack Propagation from Split.....	26
14. "D" Section Steel Jacket Retrofit of Split Sections.....	26
15. Retrofit Details for Specimen SJ1.....	27
16. Specimen SJ1 Test Photographs.....	28
17. Load-Displacement Curves for Specimen SJ1.....	29
18. Retrofit Details for Specimen FW1.....	30
19. Fyfe Company Retrofit Installation Photographs.....	32
20. Specimen FW1 Test Photographs.....	33
21. Load-Displacement Curves for Specimen FW1.....	34
22. Retrofit Details for Specimen FW2.....	36
23. Sumitomo Retrofit Installation Photographs.....	37
24. Specimen FW2 Test Photographs.....	39
25. Load-Displacement Curves for Specimen FW2.....	40
26. Retrofit Details for Specimen FW3.....	42
27. XXSys Retrofit Installation Photographs.....	43
28. Specimen FW3 Test Photographs.....	44
29. Load-Displacement Curves for Specimen FW4.....	45
30. Load-Displacement Envelope of Out-of-Phase, Flexure-Critical Specimens.....	47
31. Details for Specimen AB3.....	48
32. Specimen AB3 Test Photographs.....	50
33. Load-Displacement Curves for Specimen AB3.....	51
34. Retrofit Details for Specimen SJ3.....	52
35. Specimen SJ3 Test Photographs.....	53
36. Load-Displacement Curves for Specimen SJ3.....	54
37. Retrofit Details for Specimen SJ2.....	56
38. Specimen SJ2 Test Photographs.....	57
39. Load-Displacement Curves for Specimen SJ2.....	58
40. Details for Specimen AB2.....	59
41. Specimen AB2 Test Photographs.....	61
42. Load-Displacement Curves for Specimen AB2.....	62
43. Retrofit Details for Specimen SJ4.....	63
44. Specimen SJ4 Test Photographs.....	64
45. Load-Displacement Curves for Specimen SJ4.....	64
46. Retrofit Details for Specimen FW4.....	66
47. Specimen FW4 Test Photographs.....	67
48. Load-Displacement Curves for Specimen FW4.....	68
49. Retrofit Details for Specimen FW5.....	70
50. Specimen FW5 Test Photographs.....	71
51. Load-Displacement Curves for Specimen FW5.....	72

52.	Retrofit Details for Specimen FW6 .....	73
53.	Specimen FW6 Test Photographs.....	74
54.	Load-Displacement Curves for Specimen FW6.....	75
55.	Load-Displacement Envelope of Transverse Specimens .....	76

## LIST OF TABLES

<u>Table</u>		<u>Page</u>
1.	Summary of the Test Specimens.....	15
2.	Properties of Composite Materials .....	16
3.	Summary of Out-of-Phase, Flexure-Critical Test Results.....	45
4.	Comparison of Relative Confinement Pressures in Composite Out-of-Phase Specimens.....	46
5.	Summary of Transverse Test Results.....	75
6.	Comparison of Relative Confinement Pressures in Composite Transverse Specimens .....	77

## EXECUTIVE SUMMARY

Many older bridges in Washington State contain split reinforced concrete columns as common members between adjacent bridge sections. The split detail was incorporated in columns to allow for movements in the bridge due to temperature and shrinkage effects. It is expected that these split columns will perform poorly in the event of a significant earthquake. This study investigated retrofitting measures for improving the seismic performance of existing split columns.

Experimental tests were conducted on one-third scale split column specimens which were representative of the split columns present in the Spokane Street Overcrossing near Seattle. Two test setups were used to examine vulnerabilities in the split columns associated with seismic loading in the longitudinal and transverse directions of the bridge. The specimens were subjected to increasing levels of cycled inelastic lateral displacements. Various retrofit measures were evaluated. Specimen performance was evaluated on the basis of load capacity, displacement ductility, and hysteretic behavior.

Tests on specimens representing as-built conditions revealed vulnerabilities that have previously been observed in the field or are expected to occur during a major earthquake. Poor performance evident in the as-built specimens included crack propagation from the base of the split, lap splice degradation, and shear failure in the split sections.

Retrofit design focused on enhancing the column seismic performance while at the same time preserving as much of the gap between the split sections as possible. Procedures were developed for the design of steel jacketing as a retrofit measure for the split columns. Circular jacketing was used for the section below the split and for retrofitting a deficient lap splice. "D" shaped jackets were used for the split sections to provide confinement in flexural hinging regions and to increase shear strength. Tests on specimens retrofitted with the steel jacketing showed significant improvements in performance when compared to that for the as-built specimens.

Three companies who manufacture composite retrofit systems were invited to participate in this project. Each company was provided with unretrofitted specimens to which they designed and installed their company's retrofit system. While some differences in performance were obtained with the various retrofit systems, all retrofitted specimens showed significant improvements in performance when compared to that for the as-built specimen. Performance differences in the retrofitted specimens were attributed to the different design procedures and assumptions used by each retrofit company.



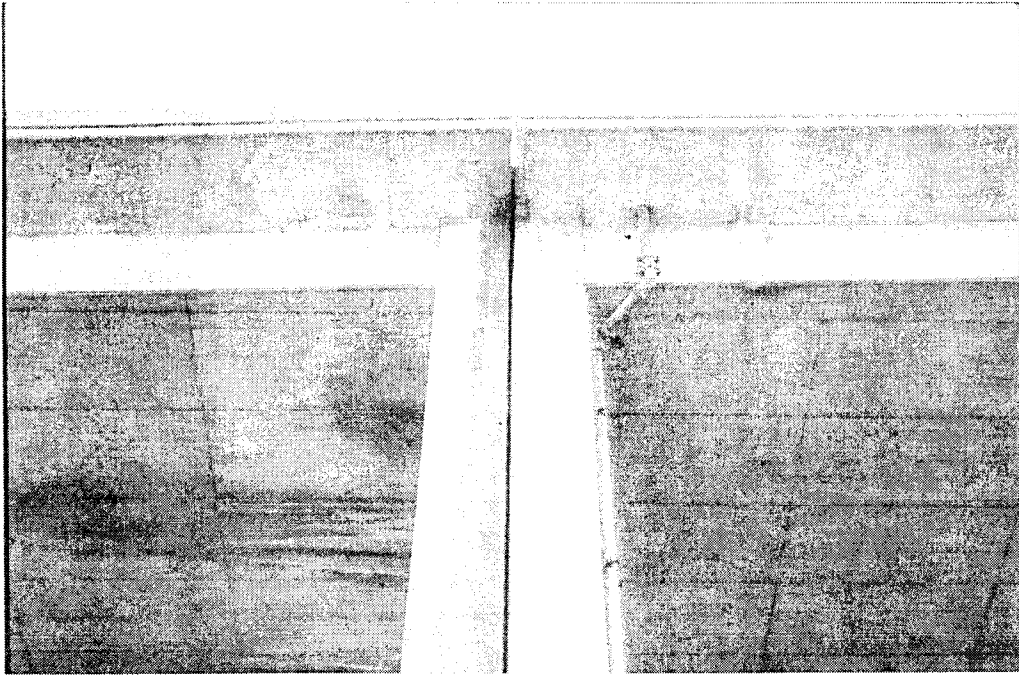


Figure 1 Split Concrete Column from Spokane Street Overcrossing



Figure 2 Crack Propagation from the Base of the Split Sections

composite fiber wraps provided by three different companies were tested. Specimen performance was evaluated in terms of load capacity, ductility and energy dissipation.

## **RESEARCH OBJECTIVES**

The objectives of this study were as follows:

1. to identify the seismic vulnerabilities in split columns typical of those present in the Spokane Street Overcrossing;
2. to evaluate steel jacketing as a retrofit for improving the performance of split columns;
3. to evaluate three commercial composite wrap retrofit systems for improving the performance of split columns; and
4. to draw conclusions on the feasibility and effectiveness of the various retrofit systems and make recommendations for methods to improve the seismic performance of split reinforced concrete bridge columns.

## **PREVIOUS RESEARCH AND CURRENT PRACTICE**

### **COLUMN DEFICIENCIES**

A common deficiency found in older bridge columns is an insufficient amount of transverse reinforcement. Typically, No. 3 or No. 4 hoops at 0.3 m (12 in.) on center were used in columns, regardless of the column cross-sectional dimensions, and the hoops had short extensions and anchorage only by lapping the ends in the cover concrete. Intermediate ties were rarely used. These details result in many older columns being susceptible to shear failures, and little confinement is provided for developing the full flexural capacity or preventing buckling of the longitudinal reinforcement.

Another detail commonly used in older bridges is splicing of the longitudinal bars at the bottom of the columns. Often, starter bars were extended only 20 longitudinal bar diameters ( $d_b$ ) from the foundations, which does not provide sufficient length to develop the yield strength of the reinforcement, thus leading to bond failure. These deficiencies result in a high potential for flexural strength degradation at splice locations in the event of a large earthquake.

A number of older bridges in Washington State have split reinforced concrete columns. The split columns are used as a common column between two adjacent bridge sections, typically with a 5-cm (2-in.) gap over some portion of the total column height. The purpose of the split is, through flexing of the split sections of the column, to allow movement of the bridge superstructure due to temperature and shrinkage effects. Generally, no special detailing was used at the base of the split, introducing the potential for crack propagation and column failure under seismic loading. Further, because the split columns were built prior to 1971, all of the deficiencies common in older columns are also present in the split columns.

Procedures for assessing column vulnerabilities have been developed, e.g., Priestley and Seible (1994), and Priestley, Seible and Calvi (1996). Assessments must be made of all potential failure modes, including flexural strength assessment, shear strength assessment, and potential for splice degradation. In the case of split columns, the potential for the split to open must also be evaluated. The lowest mechanism in terms of strength and/or displacement will determine the actual expected response of the column. The assessments of column vulnerability determine the retrofitting required for the column in order to obtain a satisfactory response of the bridge.

## **COLUMN RETROFITTING**

### **Steel Jacket Retrofitting**

Previous research (Priestley and Seible, 1991; Chai, Priestley and Seible, 1991) has shown that steel jacketing is an effective column retrofit method for deficient reinforced concrete columns. Steel jackets provide deficient columns with the necessary confinement and are approximately equivalent to external, closely spaced spiral reinforcement. Steel jacket retrofitting was originally developed for retrofitting circular columns using two semi-circular shells of steel rolled typically 2.5 cm (1.0 in.) larger than the column radius. After the two shells are welded together around the column, the gap between the jacket and the column is filled with grout. A clearance of approximately 5 cm (2 in.) between the ends of the jacket and any supporting members, such as the footing and cap beam, is typically specified in order to prevent the jacket from bearing against the member at large drift angles. For rectangular columns, research has shown that elliptical jackets are most successful. The tension action developed with an elliptical jacket increases the lateral stiffness of the cross

section, producing effective confinement. In contrast, rectangular steel jackets provide confinement through bending action of the jacket sides, which is relatively more flexible than the tension action with elliptical jackets. Test results have shown that jacketing of the columns can improve the hinge and/or splice region performance (partial height jacketing) and column shear performance (full height jacketing).

Priestley, et al (1996) have developed equations for the design of circular and elliptical steel jackets. For a circular column, the required retrofit jacket thickness to provide confinement of flexural plastic hinge region is a function of the maximum ductility required of the hinge. The thickness,  $t_j$ , is given by:

$$t_j = \frac{0.18(\varepsilon_{cm} - 0.004)Df'_{cc}}{f_{yj}\varepsilon_{sm}} \quad (\text{Equation 1})$$

where  $\varepsilon_{cm}$  is the maximum compressive strain required in the hinge,  $D$  is the jacket diameter,  $f'_{cc}$  is the confined concrete compressive strength,  $f_{yj}$  is the jacket yield strength, and  $\varepsilon_{sm}$  is the jacket strain at maximum stress. Design charts for required jacket thickness in a flexural hinge region are given in Figure 3 for two common longitudinal bar sizes based upon providing confinement to develop extreme deformation capability, Grade 40 bars, and A36 jackets.

Tests (Priestley, et al, 1996) have shown that the confinement required to provide slippage of bars in a lap splice is based upon restricting the radial dilation strain in to less than 0.0015. Based upon this criterion, the required jacket thickness for a circular column to develop a splice is given by:

$$t_j = 0.61 \frac{A_b f_{yl} D}{p l_s (0.0015 E_{sj})} \quad (\text{Equation 2})$$

where  $A_b$  is the splice bar area,  $f_{yl}$  the bar yield strength,  $p$  the failure perimeter around one bar if a splice failure should occur,  $l_s$  the splice length, and  $E_{sj}$  the modulus of elasticity for the steel jacket. The quantity  $0.0015 E_{sj}$  should not be taken as greater than the yield strength of the jacket. For circular columns, the perimeter  $p$  is given by:

$$p = \frac{\pi D'}{2n} + 2(d_b + c) \leq 2\sqrt{2}(c + d_b) \quad (\text{Equation 3})$$

where  $n$  is the number of longitudinal bars of diameter  $d_b$  evenly spaced around the core of diameter  $D'$ , with cover  $c$ . Design charts for required jacket thickness to confine a splice in a circular column are given in Figure

4 for two common longitudinal bar sizes, Grade 40 bars, a lap splice of  $20d_b$ , and A36 jackets. Note that the requirements for confinement of a plastic hinge and for confinement of a lap splice are not additive. Thus, the greater of equation 1 or equation 2 will control the required jacket thickness.

The contribution to the column shear strength,  $V_{sj}$ , provided by a circular steel jacket, based upon an assumed shear crack angle of  $35^\circ$ , is given by (Priestley, et al, 1996):

$$V_{sj} = \frac{\pi}{2} t_j f_{yj} D C \cot 35^\circ \quad (\text{Equation 4})$$

Equation 4 can be used to determine the thickness of jacket required to satisfy shear strength requirements.

For rectangular column, an elliptical steel jacket is recommended (Priestley, et al, 1996). Consider an elliptical steel jacket applied around a rectangular column, with a radius in the strong-axis direction of  $R_1$ , a radius in the weak-axis direction of  $R_3$ , and a radius to the column corner of  $R_2$ . The equations developed for the design of circular jackets can be used for elliptical jackets by using an average radius of the jacket,  $R$ , in both the strong and weak axis directions and substituting  $D = 2R$  into the previous equations. Thus:

$$R = \frac{R_1 + R_2}{2} \quad \text{for strong-axis direction} \quad (\text{Equation 5a})$$

$$R = \frac{R_3 + R_2}{2} \quad \text{for weak-axis direction} \quad (\text{Equation 5b})$$

The effective confining pressure from an elliptical jacket will be less in the weak direction of the column. However, it is typically the strong axis direction that is critical for most bridges (Priestley, et al, 1996).

### **Composite Material Retrofitting**

Currently, there are two types of composite material retrofit systems that are commercially available: carbon fiber/epoxy jackets and fiberglass/epoxy jackets. For both of these systems, the composite material is saturated in an epoxy and wrapped around the column. The fibers are typically oriented at  $90^\circ$  to the columns longitudinal axis. The material provides the column with exterior confinement analogous to the interior confinement provided by transverse reinforcement.

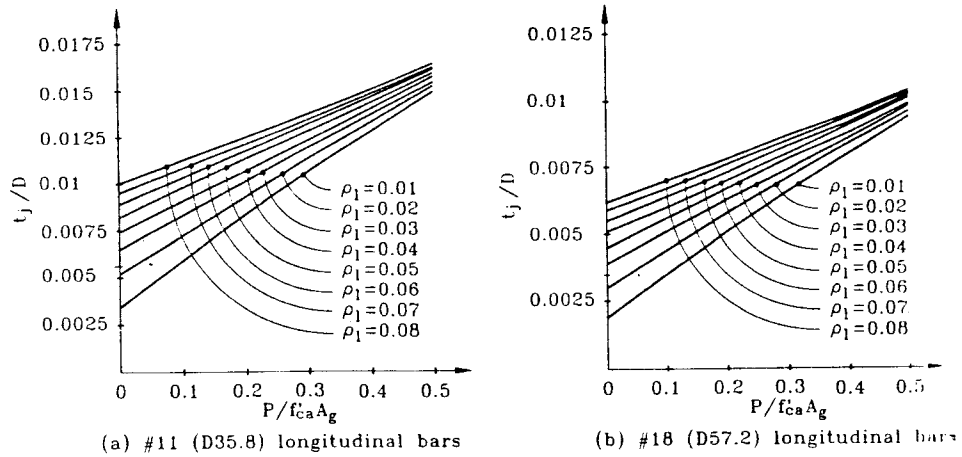


Figure 3 Steel Jacket Thickness For Hinge Confinement In A Circular Column (from Priestley, et al, 1996)

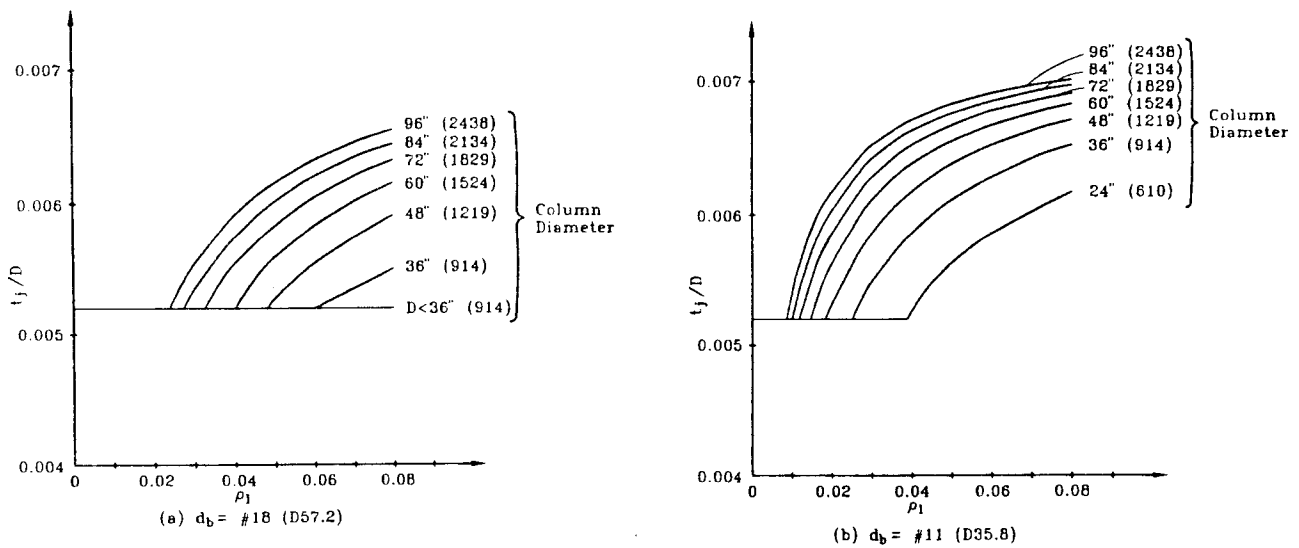


Figure 4 Steel Jacket Thickness For Lap Splice Retrofit In A Circular Column (from Priestley, et al, 1996)

Composite material retrofit systems can be effective for both circular and rectangular columns. Typically, the corners of rectangular columns are rounded to a 5-cm (2-in.) radius prior to retrofitting in order to avoid the possibility of damage to the fibers (Seible, et al, 1995). Circular jackets provide the column with a continuous confinement stress while rectangular jackets only provide confinement stress at the corners. Circular columns usually require smaller jacket thicknesses. A circular or elliptical concrete shell may be placed around a rectangular column prior to retrofit in order to increase the effectiveness of the composite material jacket (Seible, et al, 1995).

Design guidelines for composite material retrofit systems can be found, for example, in the ACTT-95/08 provisions entitled *Earthquake Retrofit of Bridge Columns with Continuous Carbon Fiber Jackets* (Seible, et al, 1995) and *Seismic Retrofit of Bridge Columns Using High Strength Fiberglass/Epoxy Jackets* (SEQAD, 1993). The same basic design equations are found in both of these documents. Research projects conducted at the University of California, San Diego, provide the basis for these design equations. In both documents, the only two composite material properties that must be known for design are the ultimate tensile stress,  $f_{jt}$ , and the modulus of elasticity,  $E_j$ . Linear elasticity of the material is assumed.

For each mode of failure, a required jacket thickness must be determined. Each failure mode affects different regions of the column and each of these regions needs to be evaluated. Figures 5 and 6 define these regions for columns subject to single bending and double bending. In these figures,

- $L_s$  = lap splice length;
- $L_{c1}$  = primary confinement region for plastic hinge;
- $L_{c2}$  = secondary confinement region for plastic hinge;
- $L_{vi}$  = shear region inside plastic hinge; and
- $L_{v0}$  = shear region outside plastic hinge.

The three structural deficiencies that need to be addressed are confinement of flexural hinges, confinement of lap splices, and shear strength. The following design guidelines may be used for carbon fiber or fiberglass epoxy retrofit systems (Seible, et al, 1995 and SEQAD, 1993).

The level of confinement provided by the composite material jacket in flexure plastic hinge region must meet two requirements. First, it must increase the concrete's ultimate compression strain,  $\epsilon_{cu}$ , allowing the inelastic rotation capacity to reach the desired level of ductility. Second, it must prevent buckling of the longitudinal reinforcement. A required jacket thickness is determined for each requirement. The design jacket

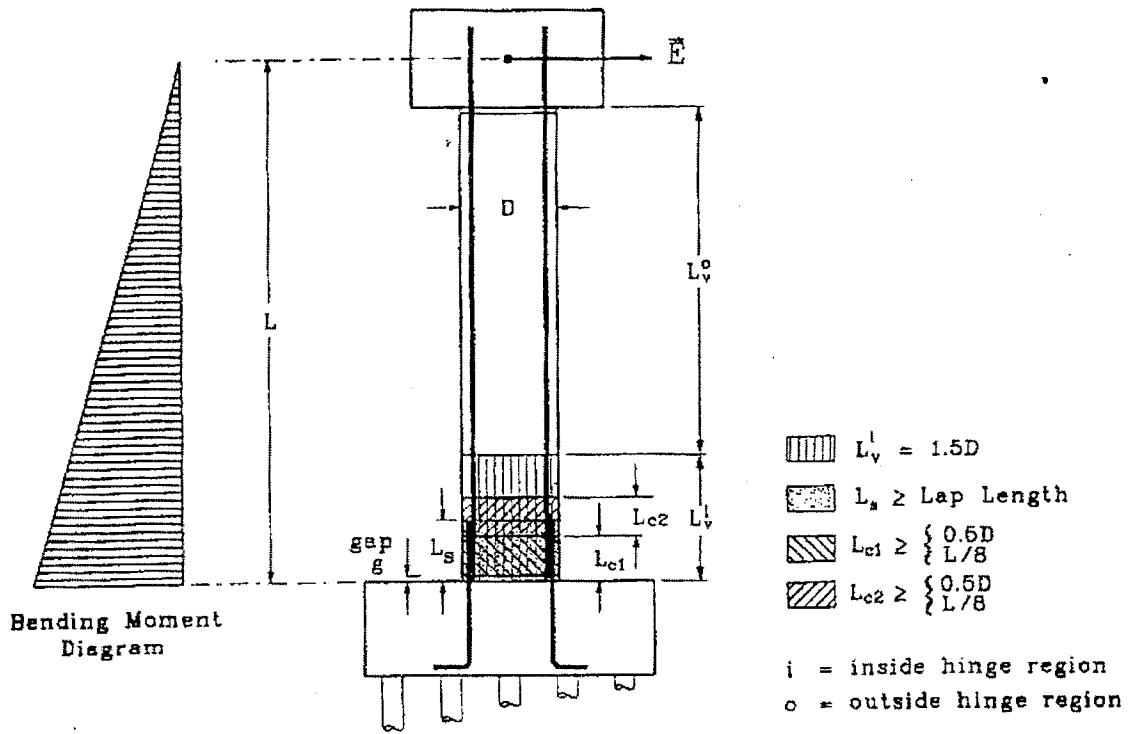


Figure 5 Single Bending Retrofit Regions (Seible, et al, 1995)

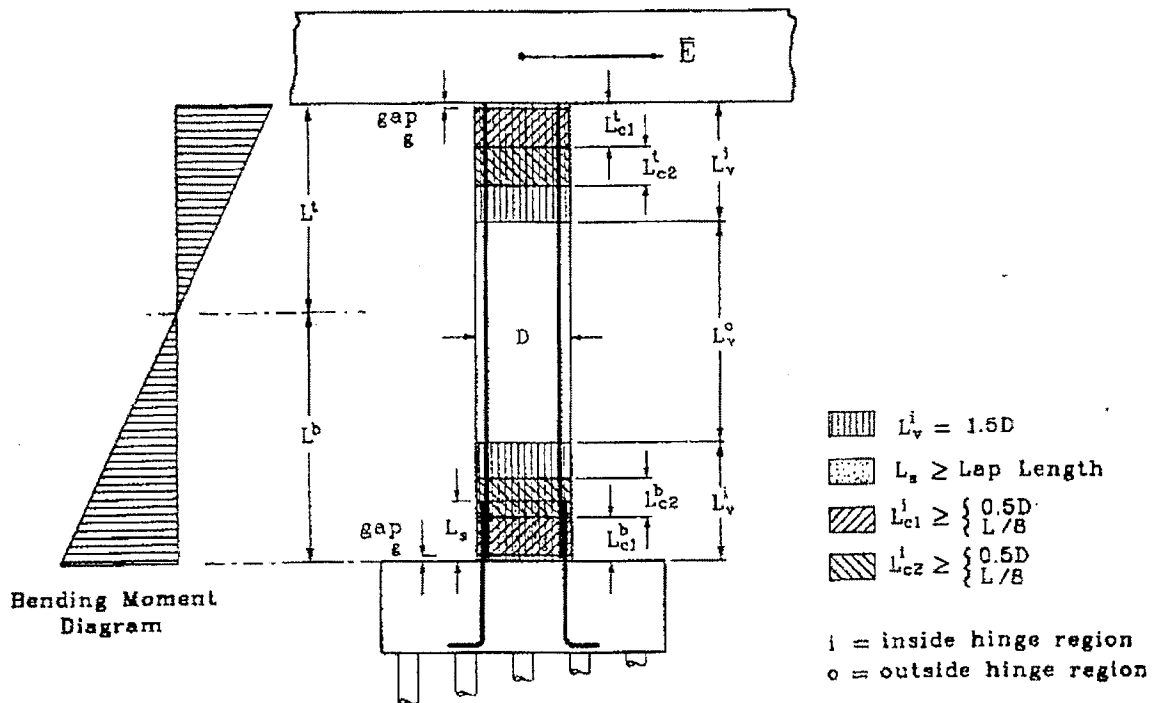


Figure 6 Double Bending Retrofit Regions (Seible, et al, 1995)

thickness,  $t_j$ , is the larger of these two thicknesses (Seible, et al, 1995).

The equations for both design requirements depend on the volumetric reinforcement ratio of the composite material jacket,  $\rho_j$ , as defined by Equation 6.

$$\rho_j = \frac{A_{jacket}}{A_{concrete}} = \frac{t_j \pi D}{\frac{\pi D^2}{4}} = \frac{4t_j}{D} \quad \text{for circular columns} \quad (\text{Equation 6})$$

$D$  is the diameter of a circular column. The same equation is used for rectangular columns fitted with elliptical jackets, but  $D$  is replaced with the effective column diameter  $D_e$  (Seible, et al, 1995). Figure 7 illustrates the dimensions needed to calculate  $D_e$  using Equations 7 through Equation 10.

$$k = \left( \frac{A}{B} \right)^{\frac{2}{3}} \quad (\text{Equation 7})$$

$$a = kb \quad (\text{Equation 8})$$

$$b = \sqrt{\left( \frac{A}{2k} \right)^2 + \left( \frac{B}{2} \right)^2} \quad (\text{Equation 9})$$

$$D_e = \frac{b^2}{a} + \frac{a^2}{b} \quad (\text{Equation 10})$$

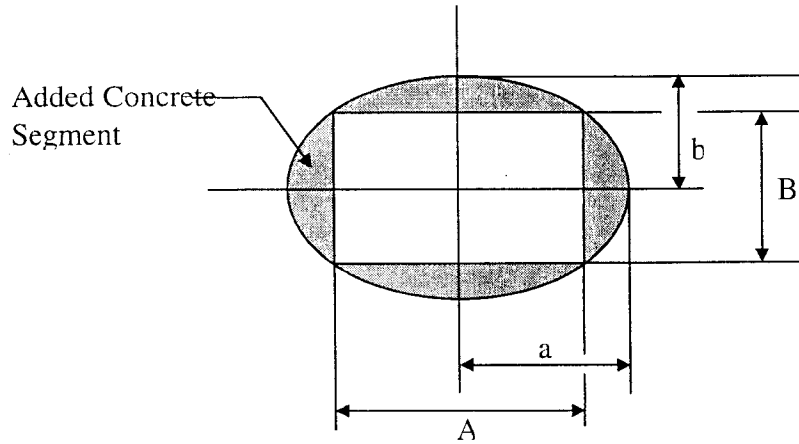


Figure 7 Dimensions Used to Calculate  $D_e$  (Seible, et al, 1995)

When designing the jacket, the required ultimate compression strain is calculated based on the desired ductility level. The design jacket thickness required to increase the ultimate concrete compression strain depends on the relationship between ultimate strain,  $\epsilon_{cu}$ , and the level of confinement. Testing of both fiberglass/epoxy and carbon fiber/epoxy jacketed columns has led to the following equation for the jacket thickness (Seible, et al, 1995):

$$t_j = \frac{0.1D(\epsilon_{cu} - 0.004)f'_{cc}}{f_{ju}\epsilon_{ju}} \quad (\text{Equation 11})$$

$f'_{cc}$  is the compression strength of the confined concrete and can conservatively be taken as  $1.5f'_c$  (Seible, et al, 1995). Test results indicate that jackets installed on rectangular columns without the formation of an elliptical shell can also be effective (Seible, et al, 1995). However, testing was limited to rectangular columns with side aspect ratios of 1.5 or less. Again,  $D_c$  is used to calculate  $\rho_j$ , but it is recommended that the required thickness then be doubled to account for the reduced effectiveness of the jacket.

Priestley, et al (1996) proposed an alternative method for determining the thickness required for a rectangular jacket to increase the ultimate concrete compression strain in the plastic hinge regions of rectangular columns. Rather than designing the retrofit using an equivalent column diameter, then doubling the thickness, the reduced effectiveness of rectangular jackets is incorporated into the development of the relationships for required jacket thickness. For a rectangular column with cross-section dimensions  $b$  by  $h$ , the required jacket thickness is given by:

$$t_j = \left[ \frac{bh}{b+h} \right] \frac{0.8D(\epsilon_{cu} - 0.004)f'_{cc}}{2f_{ju}\epsilon_{ju}} \quad (\text{Equation 12})$$

For long slender columns, a required jacket thickness also needs to be determined to prevent global buckling of the longitudinal reinforcement. This applies to any column with a distance between the maximum moment location and the point of inflection that is greater than four times the column's diameter or effective diameter. The required jacket thickness is given by (Seible, et al, 1995):

$$t_j = \frac{nD}{E_j} \quad (\text{Equation 13})$$

where  $n$  is the number of longitudinal bars,  $D$  is expressed in inches and  $E_j$  is expressed in ksi.

The design jacket thickness for flexure hinge confinement is the larger of the values calculated from Equation 11 or 12 and Equation 13. The jacket must cover the primary plastic hinge confinement region,  $L_{c1}$ . In addition, a jacket thickness of  $0.5t_j$  must cover the secondary plastic hinge confinement region,  $L_{c2}$ . The primary and secondary plastic hinge confinement regions are based on the expected plastic hinge length, determined from the column geometry in the loading direction, as show in Figures 5 and 6 (Seible, et al, 1995)

The design of composite material jackets to prevent lap splice failures is based upon the tensile stress developed in the jacket being capable of preventing the debonding of the lap splice starter bars from the concrete core (Seible, et al, 1995). In order to reach a stress level of 1.4 times yield stress,  $f_y$ , in the longitudinal steel, an internal lateral pressure as given by Equation 13 is required (Seible, et al, 1995).

$$f_l = \frac{A_s f_y}{\left( \frac{p}{2n} + 2(d_b + cc) \right) L_s} \quad (\text{Equation 13})$$

$A_s$  is the area of the longitudinal reinforcement,  $p$  is the length of the inside crack along the longitudinal reinforcement,  $n$  is the number of longitudinal reinforcing bars,  $d_b$  is the longitudinal bar diameter,  $cc$  is the concrete cover to the outside edge of the longitudinal bars, and  $L_s$  is the length of the lap splice. The required jacket thickness to produce a confining stress of  $f_l$  is given by:

$$t_j = \frac{D f_l}{2 f_j} \quad (\text{Equation 14})$$

Debonding of the lap splice starter bars will occur before the strain in the jacket reaches its ultimate strain. Tests have indicated that debonding will occur at jacket strains ranging from 0.001 to 0.002. A strain limit of 0.001 is therefore proposed for design (Seible, et al, 1995). The limiting jacket stress is then given by Equation 15.

$$f_j = 0.001 E_j \quad (\text{Equation 15})$$

Combining Equation 14 with Equations 13 and 15 provides the required jacket thickness for lap splice confinement as:

$$t_j = 500 \frac{Df_t}{E_j} \quad (\text{Equation 16})$$

Typically, the confinement contribution from transverse reinforcement is small compared to that of the jacket, and it is usually ignored when designing the jacket (Seible, et al, 1995). Similar to the plastic hinge design, the design equations for lap splice confinement are based on circular cross-sections. For rectangular cross-sections, it is recommended that an elliptical concrete shell be placed around the column. The design is then identical to the circular cross-section, but the effective column diameter,  $D_e$ , is used in place of  $D$  (Seible, et al, 1995). The calculation of  $D_e$  is shown in Figure 7 and Equations 7 to 10. Rectangular jackets installed directly to rectangular columns can be effective only if controlled debonding is permissible (Seible, et al, 1995). Although the jacket will provide confinement stresses only at the corners, it will prevent the concrete cover from spalling off. The jacket thickness is then designed using the effective column diameter and increased by a factor of 2 (Seible, et al, 1995). The jacket should cover the entire lap splice region.

The contribution to shear strength from the addition of a composite material jacket,  $V_j$ , is given by Equations 17 and 18 (Seible, et al, 1995).

$$V_j = \frac{\pi}{2} f_{jd} t_j D \cot \theta \quad \text{circular columns} \quad (\text{Equation 17})$$

$$V_j = 2 f_{jd} t_j D \cot \theta \quad \text{rectangular columns} \quad (\text{Equation 18})$$

In Equations 17 and 18,  $t_j$  is the jacket thickness,  $D$  is the column dimension in the direction of loading, and  $\theta$  is the inclination of the shear crack or principal compression strut. The design stress level for the jacket,  $f_{jd}$ , is calculated to be less than the ultimate stress capacity of the composite material,  $f_{ju}$ , due to limitations imposed by the concrete. When dilation strain in the concrete exceeds 0.004, the contribution of the concrete to shear capacity,  $V_c$ , decreases quickly due to aggregate interlock degradation (Priestley, et al, 1996). This strain is less than the ultimate strain limit for fiberglass or carbon fiber composite materials. The stress  $f_{jd}$  is therefore

determined using an allowable strain of 0.004, as shown in Equation 19.

$$f_{jd} = 0.004E_j \quad (\text{Equation 19})$$

Design of the composite material shell must ensure that  $V_j$  compensates for the shear capacity deficient in the unretrofitted column, as shown by Equation 20.

$$V_j \geq \frac{V_o}{\phi} - (V_c + V_s + V_p) \quad (\text{Equation 20})$$

$V_o$  can be estimated as 1.5 times the shear capacity of the column at a displacement ductility level,  $\mu_\Delta$ , of 1.0 and  $\phi$  is taken as 0.85 (Seible, et al, 1995).

## EXPERIMENTAL TESTING PROGRAM

### TEST SPECIMENS AND PARAMETERS

The test specimens of this study were constructed to be representative of the split columns present in the Spokane Street Overcrossing. Specific details in the columns vary, so the dimensions and reinforcing schemes of the test specimens of this study were chosen to be typical of the details of the split columns in the bridge and to reveal several potential modes of failure. The test specimens were one-third scale representations of the actual columns. However, the 5-cm (2-in.) split present in the columns was not scaled down in the test specimens due to retrofit installation limitations. For all but one of the specimens, the footings were oversized and over-reinforced to ensure that failures occurred in the columns.

Table 2 provides a summary of the test specimen parameters. A total of 13 columns were tested. Eight of the specimens were subjected to loading corresponding to opening of the split in the longitudinal direction of the bridge (out-of-phase movement of the split sections). Vulnerabilities in the out-of-phase specimens included crack propagation from the base of the split, flexural hinge failure in the split sections, and shear failure in the split sections. The other five specimens were subjected to loading corresponding to parallel movement of the split section transverse to the bridge. The vulnerabilities of the transverse specimens were lap splice failure at the base of the column and plastic hinge failure in the split sections.

Table 1 Summary of Test Specimens

Specimen	Loading Configuration	Vulnerability	Retrofit	Split Height in m (ft)	Longitudinal Reinforcement Ratio ( $\rho$ )
AB1	Out-of-phase	Split propagation and hinging in split sections	None (as-built)	1.5 (5)	0.013
AB2	Transverse	Lap splice degradation	None (as-built)	2.4 (8) Full height	0.013
AB3	Out-of-phase	Shear in split sections	Bottom section only	1.2 (4)	0.037
SJ1	Out-of-phase	Split propagation and hinging in split sections	Full-height steel jacket	1.5 (5)	0.013
SJ2	Out-of-phase	Split propagation into footing	Full-height steel jacket	2.4 (8) Full height	0.013
SJ3	Out-of-phase	Shear in split sections	Full-height steel jacket	1.2 (4)	0.037
SJ4	Transverse	Lap splice degradation	Full-height steel jacket	2.4 (8) Full height	0.013
FW1	Out-of-phase	Split propagation and hinging in split sections	Fyfe Company	1.5 (5)	0.013
FW2	Out-of-phase	Split propagation and hinging in split sections	Sumitomo	1.5 (5)	0.013
FW3	Out-of-phase	Split propagation and hinging in split sections	XXSys	1.5 (5)	0.013
FW4	Transverse	Lap splice degradation	Fyfe Company	2.4 (8) Full height	0.013
FW5	Transverse	Lap splice degradation	Sumitomo	2.4 (8) Full height	0.013
FW6	Transverse	Lap splice degradation	XXSys	2.4 (8) Full height	0.013

Three specimens were left unretrofitted in order to characterize the expected response of the as-built split bridge columns. The remaining specimens were constructed similarly to the as-built specimens, but were retrofitted using steel jacketing or composite fiber wraps. Three companies which manufacture composite retrofit systems agreed to participate in this project. The companies designed and installed their retrofit product on split column specimens constructed by WSU. Fyfe Company installed a fiberglass/epoxy system. XXSys Technologies and the Sumitomo Corporation of America both installed a carbon fiber/epoxy system. The composite retrofit design equations presented earlier were used by all three companies for the retrofit design.

However, the respective designs of the three companies varied due to designer preferences and the properties of the different composite materials. Specific specimen and retrofit details are presented for each specimen along with the discussion on results in later sections. Further details of the composite retrofit design and construction are presented in Appendices A, B and C.

The concrete used in the specimens had an average measured compressive strength at the time of testing of approximately 31 MPa (4500 psi). The longitudinal steel was Grade 40 with an average yield strength of 386 MPa (56 ksi). The transverse reinforcement was 1006 annealed steel with an average yield strength of 380 MPa (55 ksi). The steel retrofit jackets were rolled from 3.2-mm (0.125-in.) thick steel sheets with a measured yield strength of 248 MPa (36 ksi). Grout used with the steel jacketing retrofit had an average compressive strength of approximately 45 MPa (6500 psi), measured at the time of testing. Table 2 lists the properties of each company's composite material as supplied by each respective company. Additional details of the testing program are given in El Aarag (1999) and Rogness (1999).

Table 2 Properties of Composite Materials

Company	Type of Composite Material	Material Thickness per Layer (in.)	Ultimate Stress (ksi)	Elastic Modulus (ksi)
Fyfe Company	Fiberglass/epoxy	0.051	60	3250
XXSys Technologies	Carbon-fiber/epoxy	Varies	120	12000
Sumitomo Corporation	Carbon-fiber/epoxy	0.0066	331	33400

### **TEST SETUP AND PROCEDURE**

The two test setups used in this study are shown in Figures 8 and 9. The specimens were subjected to reversed cyclic lateral loading based upon increasing levels of lateral displacements. To simplify testing, no axial loading was applied to the specimens. While the omission of axial loads will have some effect on response, it was felt that this effect would be relatively small and not adversely impact the conclusions drawn from this study. For all but one specimen, the column caps and footings were over-sized and over-reinforced

relative to the details in the actual bridge in order to force damage into the columns. Specimen SJ2 incorporated a footing with dimensions and reinforcement representative of the actual footings to investigate the ability of the retrofit measures to prevent split propagation into the footing. All specimens were bolted to a laboratory strong floor using high-strength steel rods.

The out-of-phase test setup shown in Figure 8 was utilized to simulate seismic loading in the longitudinal direction of the bridge associated with the two bridge decks that the split column support moving in opposite directions, causing the column split to open and close. This test setup produces a double bending condition in the column with maximum moments occurring at the top and bottom of the split sections. The columns were subjected to displacement-controlled, reversed-cyclic lateral loading. The loading was pseudo-static and controlled manually. At each displacement interval, 3 cycles of loading were completed. Lateral displacements were applied to 0.64 cm (0.25 in.), increased by 0.64-cm (0.25-in.) increments up to 5.1 cm (2 in.), then increased by 1.2-cm (0.5-in.) increments until a displacement of 13 cm (6 in.) was reached or the column failed. When the two split sections were being pulled together, displacements were stopped at 1.9 cm (0.75 in.) due to limitations from the split width and testing hardware. Failure was defined as a 20% drop in load capacity from the peak applied load. Load and displacement data were collected at one-second intervals from the three load cells and the LVDT.

The transverse test setup shown in Figure 9 was utilized to simulate loading in the transverse direction of the bridge where both of the split sections move in the same direction perpendicular to the bridge's longitudinal axis. The test setup creates a single bending condition in the column. Bending moments vary linearly from zero at the applied load to a maximum at the base of the column. The transverse specimens were subjected to displacement-controlled, reversed-cyclic lateral loading. The loading rate was pseudo-static and controlled manually. At each displacement interval, 3 cycles of loading were completed. Lateral displacements were applied to  $\pm 1.3$ -cm (0.5 in.), then increased by  $\pm 1.3$ -cm (0.5-in.) intervals up to 7.6cm ( $\pm 3$  in.). Displacements were then increased by 2.5-cm (1-in.) intervals until the column failed. Failure was defined as a 20% drop in load capacity from the peak applied load. Load and displacement data were collected at 1-second intervals from the actuator load cell and LVDT.

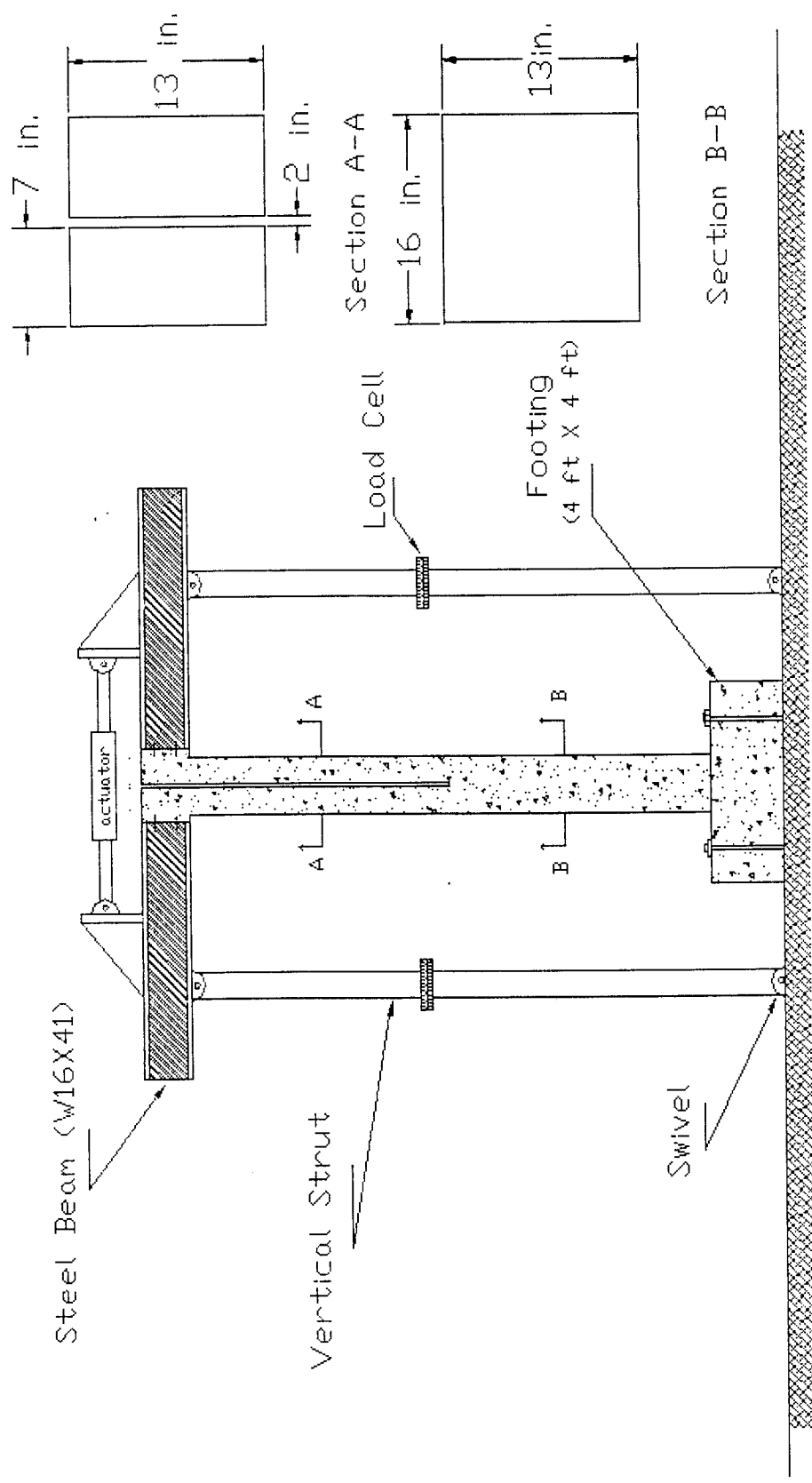


Figure 8 Out-of-Phase Test Setup

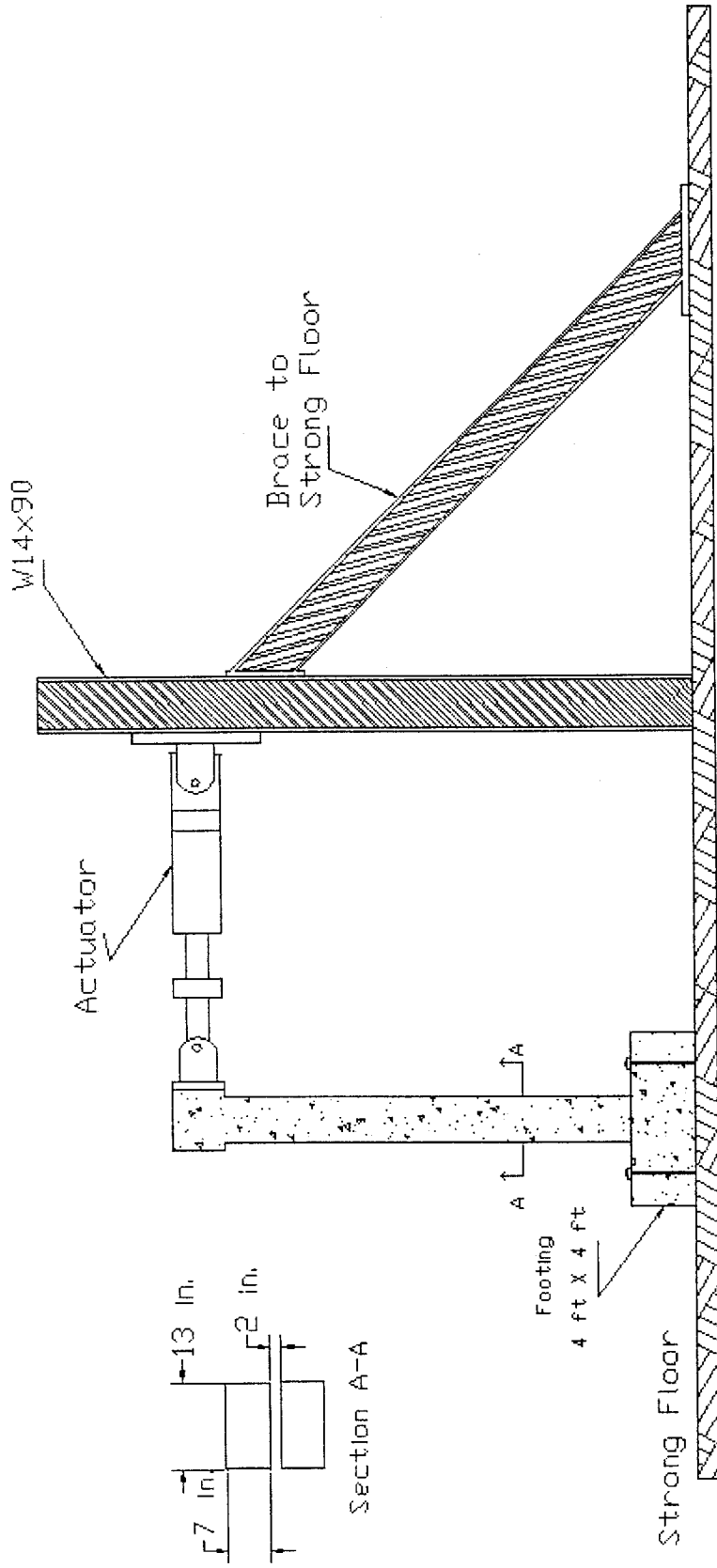


Figure 9 Transverse Test Setup

## RESEARCH FINDINGS AND DISCUSSION

In this section, results of the experimental tests are summarized. The results are grouped based upon the test setup and the vulnerability under investigation. For each specimen, specific details of the column construction and, if applicable, retrofit design are discussed. The seismic performance of each specimen was evaluated based on displacement ductility capacity and energy dissipation. Displacement ductility capacity,  $\mu_{\Delta}$ , is the ratio of the measured displacement at failure, defined as a 20% drop in peak load, to the yield displacement. Yield displacement was determined after testing by fitting a bilinear load-displacement approximation to the experimental hysteresis curves, as outlined by Priestley, et al (1996). The energy dissipation of each specimen was measured by calculating the total area under the load-displacement hysteresis curves. Results from the as-built and retrofitted specimens are compared. Conclusions about observed column behavior and retrofit effectiveness are made.

### OUT-OF-PHASE, FLEXURE-CRITICAL TEST RESULTS

The out-of-phase, flexure-critical specimens are susceptible to crack propagation from the base of the split and flexural hinging failure at the top and bottom of the split sections once the cover concrete spalls. The experimental yield displacement for the out-of-phase, flexure-critical specimens was determined from the hysteresis curves for the retrofitted specimens to be 1.5 cm (0.6 in.).

#### Specimen AB1(As-Built)

Specimen AB1 was constructed to be representative of a typical split column in the Spokane Street Overcrossing with a split over approximately half of the column height. Details of the specimen are given in Figure 10. The column longitudinal reinforcing ratio was 0.013. Specimen AB1 was tested under out-of-phase loading and was expected to be vulnerable to crack propagation from the base of the split as well as the possibility of rapid flexural hinge degradation at the top and bottom of the split sections once the concrete cover spalls.

Specimen AB1 reached a maximum displacement of 13 cm (5 in.) with no significant drop in load. However, the specimen did experience very significant damage as shown in Figure 11. A crack began to

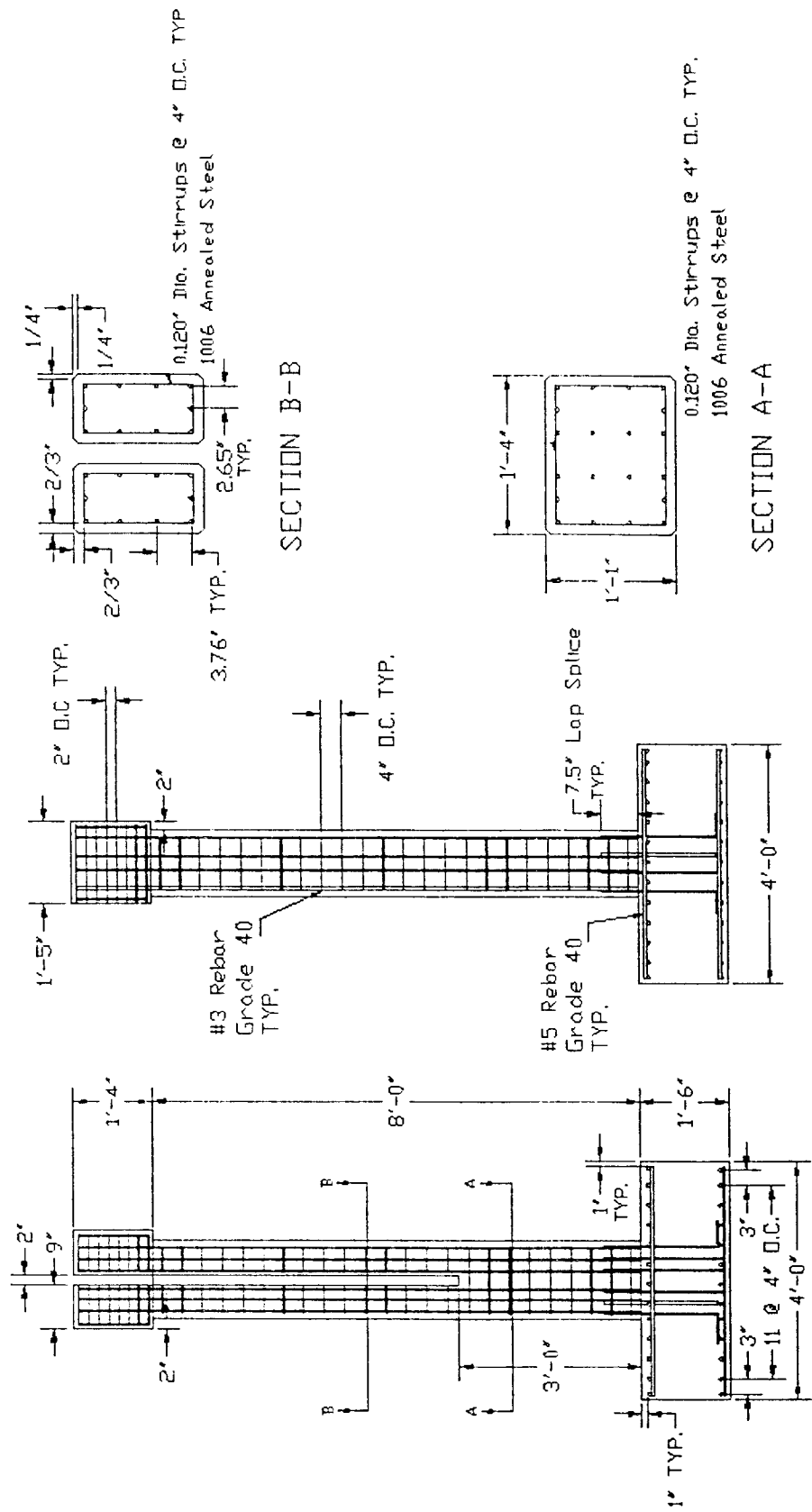
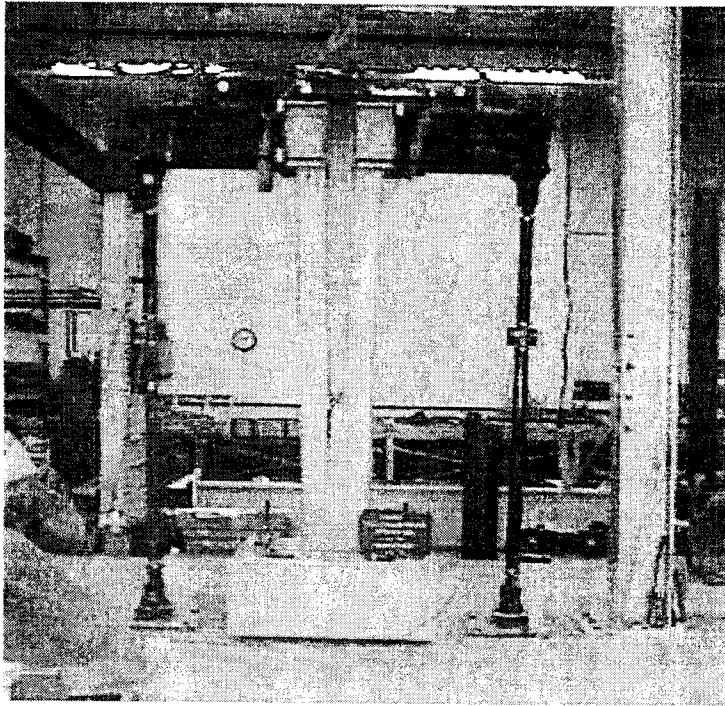
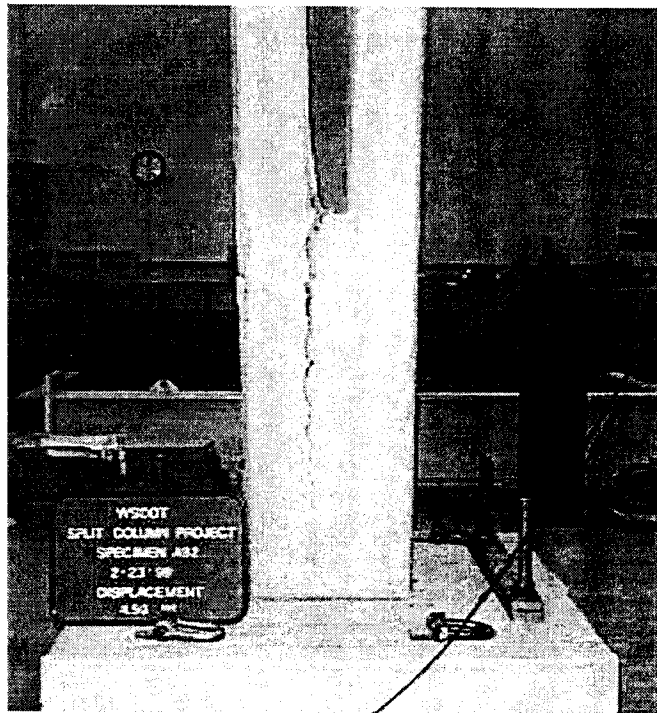


Figure 10 Details of Specimen AB1



(a) Testing of Specimen AB1



(b) Crack Propagation at the Base of the Split

Figure 11 Specimen AB1 Testing Photographs

propagate from the base of the split at the first loading cycle and continued to propagate as testing continued, eventually reaching a depth of 0.76 m (2.5 ft) with a maximum width of 5 cm (2 in.). The specimen resisted a peak lateral load of 22 kN (4.96 kips) at a displacement of 9.9 cm (3.9 in.) and continued to reach approximately the same peak load at each successive maximum displacement. The stability of the lateral load can be attributed to the increasing flexibility of the split sections. As the split propagated into the unsplit section, the effective length of the split section increased, causing an increase in column flexibility. Crack propagation from the base of the split was the only damage that developed in the specimen, as shown in Figure 11. There was no evidence of flexural hinge formation at the top or bottom of either split section. The displacement ductility of the specimen could not be determined because of the changing effective length and lateral stiffness of the split sections due to crack propagation.

The load-displacement hysteresis curves for Specimen AB1 are shown in Figure 12. The relatively narrow loops indicate that the split sections did not experience plastic deformations, resulting in low energy dissipation. This behavior could result in a pounding mechanism developing between the two split sections, which could potentially cause catastrophic failure in the bridge. In addition, with the presence of axial loads, which were not incorporated in this study, greater damage in the split columns would be expected.

### **Specimen SJ1 (Steel Jacket Retrofit)**

Specimen SJ1 was constructed identically to the as-built specimen AB1, except that the specimen was retrofitted with steel jacketing to prevent crack propagation from the base of the split and to provide confinement around potential flexural hinging regions. Based upon previous studies, circular or elliptical jackets provide better confinement than rectangular jackets. A circular jacket was selected for the retrofitting the bottom non-split section. The jacket was designed to prevent opening of the split by carrying the maximum shear force transferred from the split sections. With reference to Figure 13, equilibrium requires:

$$2t_j f_s Y = V_p \quad (\text{Equation 21})$$

where  $V_p$  is the shear force required to develop a full plastic hinge in a single split section,  $t_j$  is the required steel jacket thickness, and  $f_s$  is the average steel stress introduced in the retrofit jacket to resist crack opening.

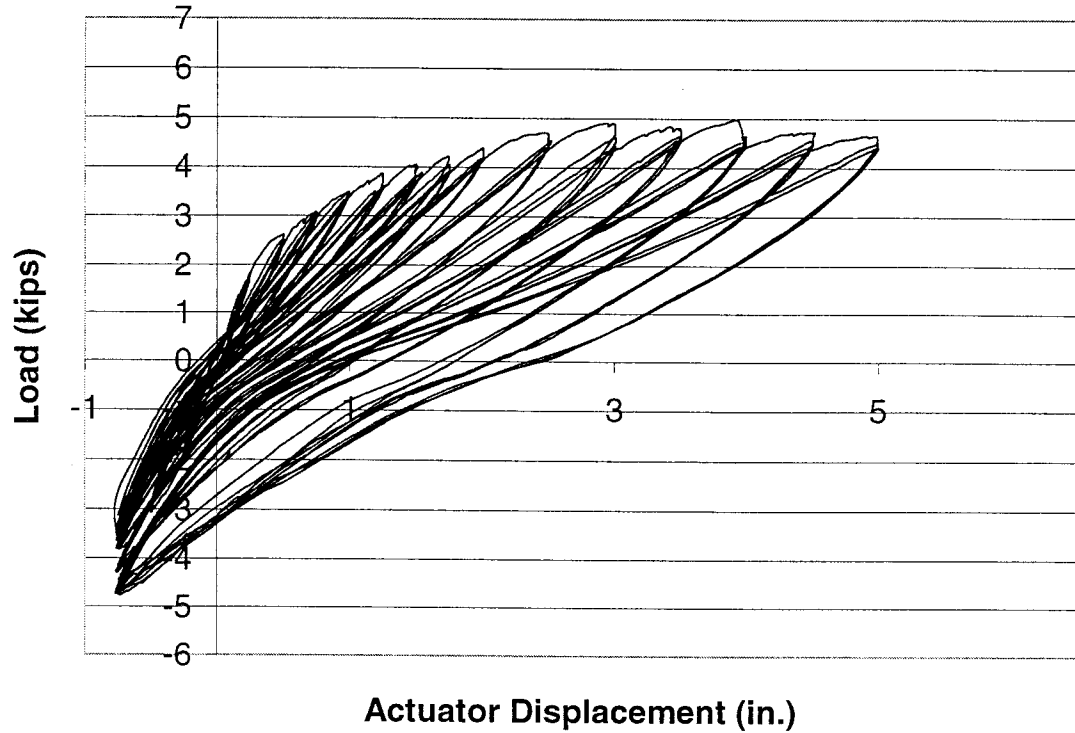


Figure 12 Load-Displacement Curves for Specimen AB1

The length of jacket resisting the opening forces is assumed to act over a distance  $Y$ , taken as  $B/2$ , where  $B$  is the width of one of the split sections in the direction of loading. Assuming a triangular stress distribution over the distance  $Y$  and with  $f_s = f_{yj}/2$ , where  $f_{yj}$  is the jacket yield strength, then the required jacket thickness is given by:

$$t_j = \frac{2V_p}{Bf_{yj}} \quad (\text{Equation 22})$$

Using this approach for Specimen SJ1, the required jacket thickness is 0.09 cm (0.035 in.). However, for practical applications, a minimum jacket thickness of 0.95 cm (0.375 in.) is used in the field. Therefore, for the one-third scale test specimens, a jacket thickness of 0.32 cm (0.125 in.) was used for the bottom section of Specimen SJ1.

The retrofit strategy for the two split sections of Specimen SJ1 focused on providing adequate confinement in the flexural hinging locations at the top and bottom of the split sections while at the same time preserving as much of the split between the two sections as possible to allow for lateral movement in the bridge. Following the design procedures developed by Priestley, et al (1996) for elliptical steel jackets as outlined earlier in this report, a required jacket thickness of 0.21 cm (0.081 in.) is required. As before, for practical considerations, a minimum jacket thickness of 0.32 cm (0.125 in.) was selected.

The jacketing was applied to the split sections of the specimen as semi-circular "D" jackets, as shown in Figure 14. Using steel-to-concrete epoxy, rectangular steel sheets were attached directly to the inside faces of the split columns. After the epoxy was fully cured, semi-circular steel shells were welded to the steel sheets. After positioning all of the steel jackets on the specimen, the gaps between the jackets and the concrete sections were filled with high-strength grout. Confinement of the potential flexural hinges required jacketing only in the hinge regions. However, steel jacketing was provided over the entire column height for aesthetic reasons. A gap of 1.9 cm (0.75 in.) (corresponding to 5cm (2 in.) in an actual column) was incorporated between the upper and lower steel jackets and between the steel jackets and the footing and column cap to prevent sections from bearing against each other at large drift angles. Retrofit details for Specimen SJ1 are shown in Figure 15.

Photographs of Specimen SJ1 during testing are shown in Figure 16. The resulting load-deflection hysteresis curves for the specimen are given in Figure 17. The peak applied load to the specimen was 29 kN (6.5 kips) and occurred at a lateral displacement at the top of specimen of 7.6 cm (3.0 in.). The specimen continued to carry approximately the same load up to a displacement of 15 cm (6 in.) when testing was stopped because the actuator reached its maximum displacement stroke. No significant damage of any kind was observed in the specimen. Ductile flexural hinges formed at the retrofitted bases of the split sections. No significant bulging of the steel jacketing inside the split was observed. Based upon a yield displacement of 1.5 cm (0.6 in.), the specimen demonstrated a displacement ductility capacity,  $\mu_{\Delta}$  of 10. The hysteresis curves indicate significant improvement in energy dissipation when compared to the hysteresis curves for the as-built Specimen AB1.

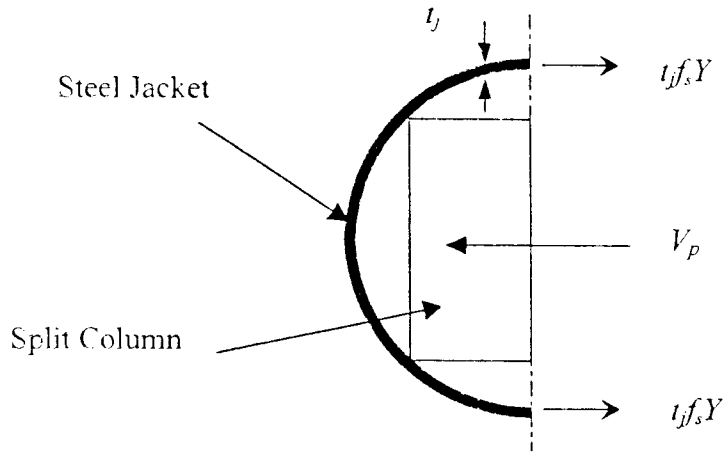


Figure 13 Basis of Retrofit to Prevent Crack Propagation from Split

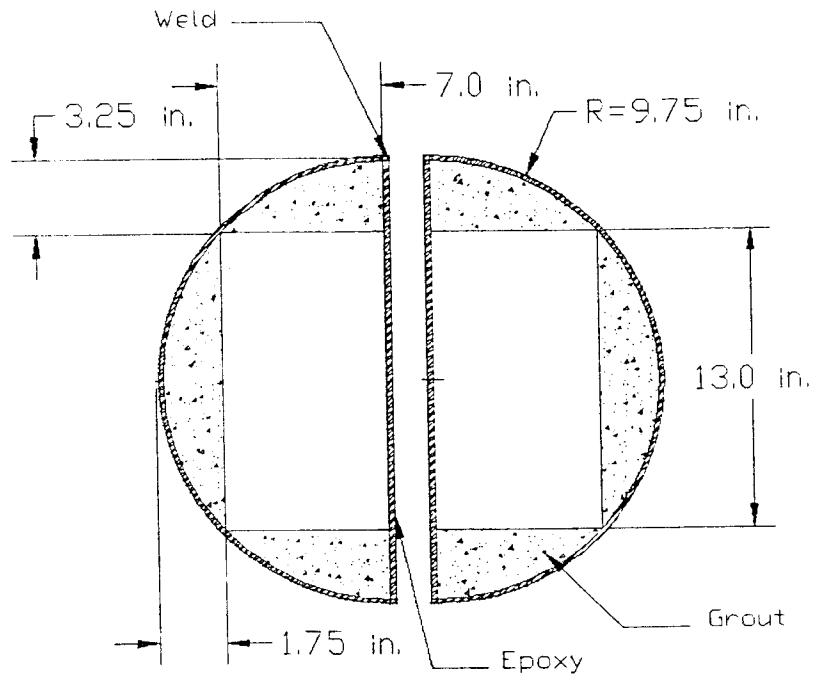


Figure 14 "D" Section Steel Jacket Retrofit of Split Sections

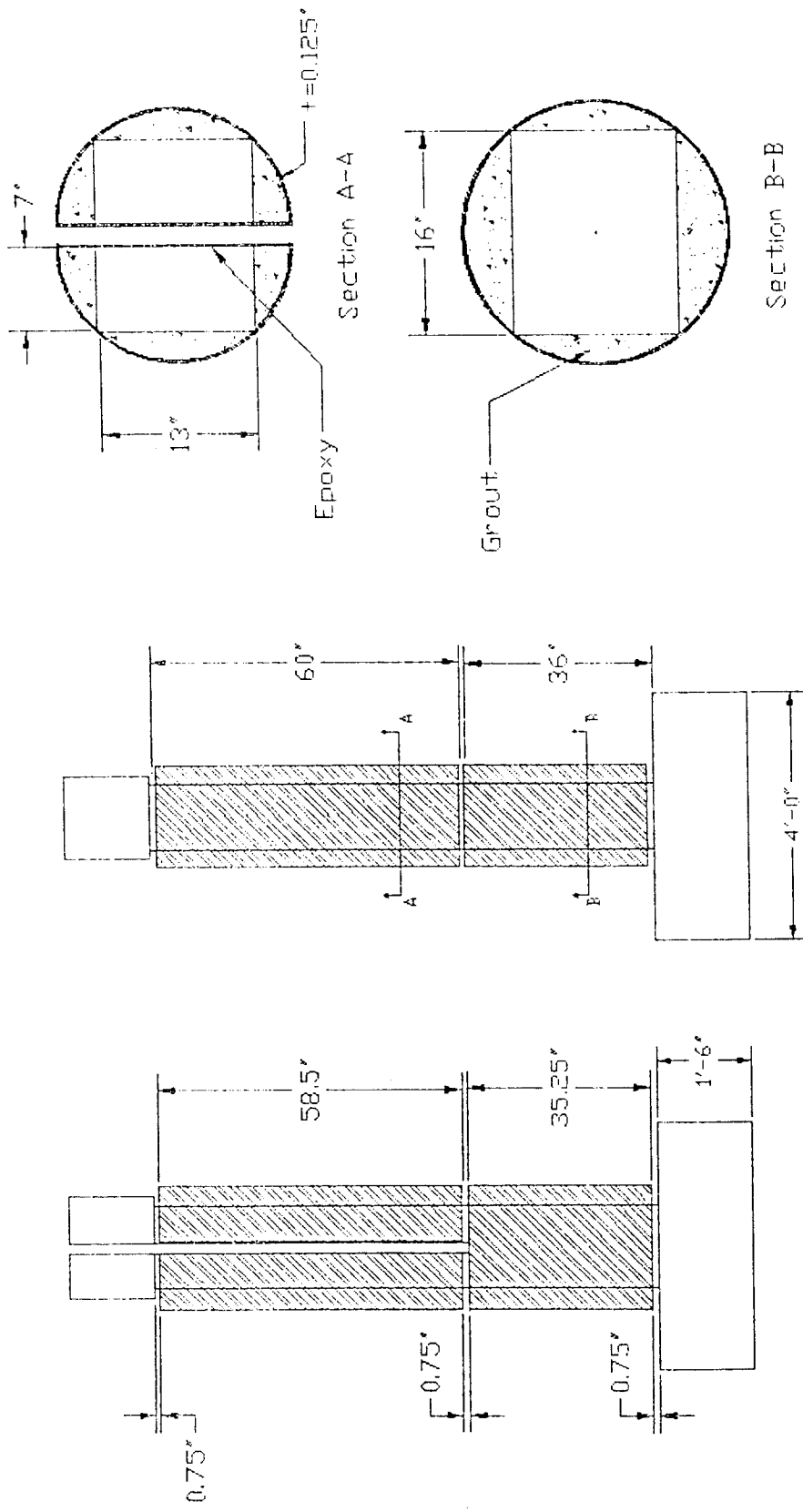


Figure 15 Retrofit Details for Specimen SJI

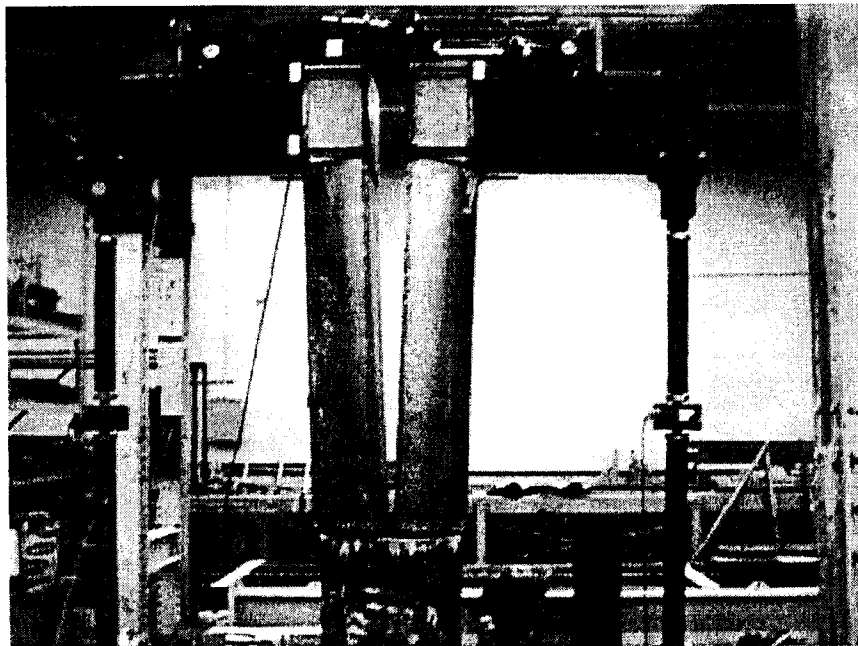
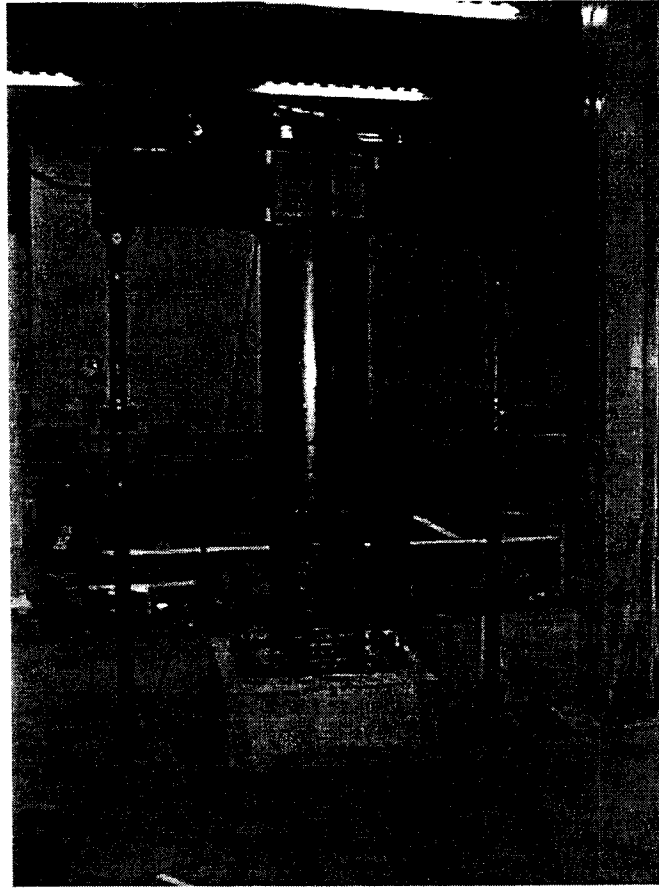


Figure 16 Specimen SJ1 Test Photographs

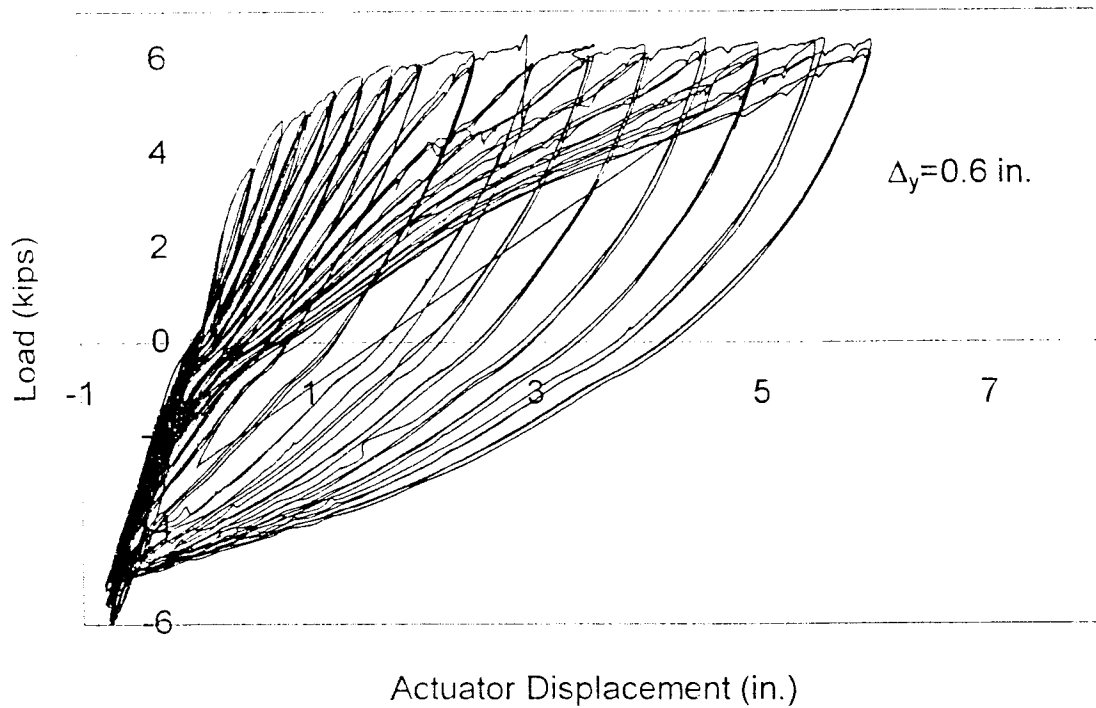


Figure 17 Load-displacement Curves for Specimen SJ1

**Specimen FW1 (Fyfe Company Retrofit)**

Specimen FW1 was constructed identically to the as-built specimen AB1, except that the specimen was retrofitted using the Fyfe Company retrofit system. The retrofit design was performed by the Fyfe Company. The full set of calculations for the retrofit design is given in Appendix A. A target displacement ductility,  $\mu_{\Delta}$ , of 6 was selected by the Fyfe Company for their design. Figure 18 provides a summary of the retrofit details for Specimen FW1.

No calculations were made to determine the retrofit requirements to prevent crack propagation at the base of the split sections. Through judgement on the part of the Fyfe Company engineers, it was assumed that

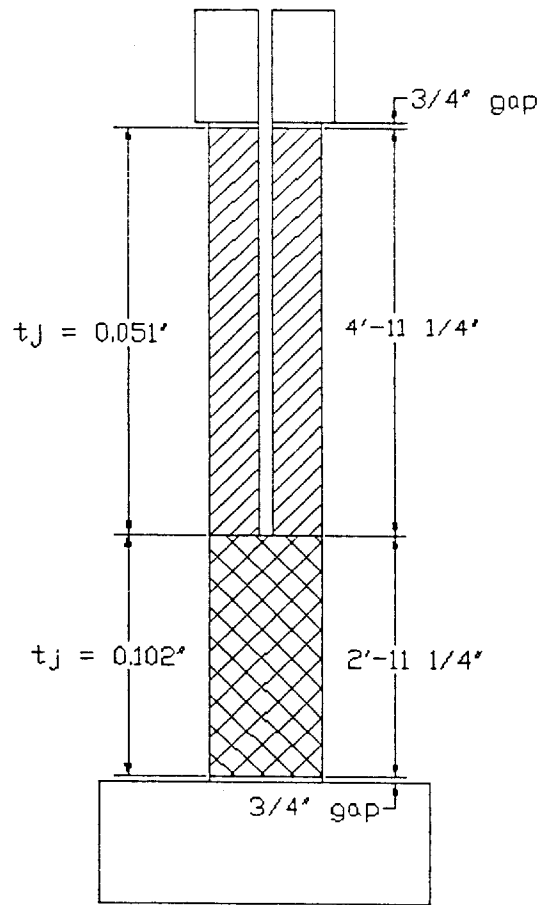
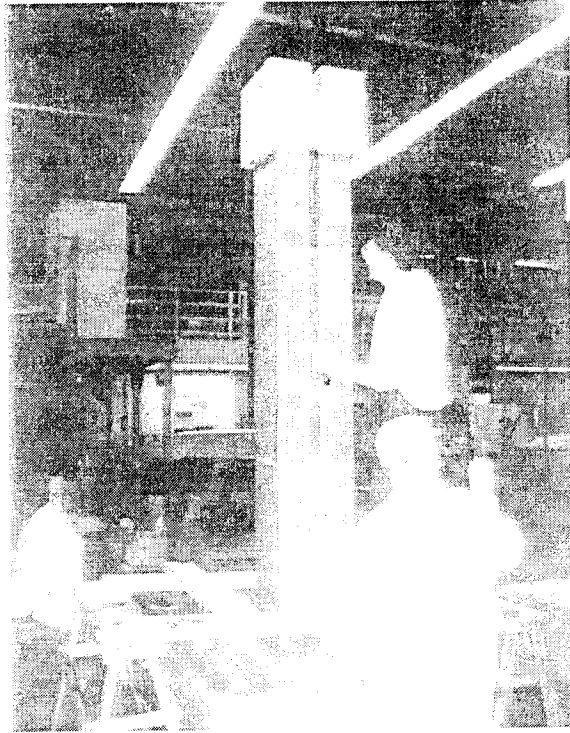


Figure 18 Retrofit Details for Specimen FW1.

two plies ( $t_j = 0.102$  in.) of composite material, installed on the entire unsplit portion of the column, would be sufficient to prevent crack propagation. The plastic hinge confinement design for the split sections of Specimen FW1 was done in accordance with the provisions set forth by Priestley, et al (1996). The controlling jacket thickness was due to a required ultimate compressive strain in the concrete of 0.00466. Fyfe Company installed one ply ( $t_j = 0.051$  in.) of material in the primary and secondary plastic hinge regions. Shear strength design for the specimen was performed in accordance with the SEQAD Provisions (1993). It was conservatively assumed that the composite material jacket would provide the entire shear strength required. Shear strength designs inside and outside of the plastic hinge regions were therefore identical, yielding a required jacket thickness of 0.06 cm (0.0239 in.). This corresponds to a requirement of one ply ( $t_j = 0.051$  in.) of composite material. Inside of the plastic hinge regions, one ply was required for plastic hinge confinement; therefore shear strength requirements did not control. Outside of the plastic hinge regions, one ply of material was installed.

Photographs taken during the installation of the retrofit of Specimen FW1 are shown in Figure 19. The Fyfe Company supplied all of the materials used during the installation process. The installation procedure is described below. The corners of the column were ground to a 2.5-cm (1-in.) radius and the column faces were roughened. The faces inside of the split were not roughened due to limitations imposed by the split. Epoxy was then applied to all of the column faces. The fiberglass material was saturated in the same epoxy and applied to the column. A roller was used to work out the air bubbles from under the material. Another coat of epoxy was then applied on top of the fiberglass material. This process was repeated as necessary until the desired number of layers was installed.

Photographs of Specimen FW1 during testing are shown in Figure 20. The load-displacement hysteresis curves for Specimen FW1 are presented in Figure 21. During initial testing, the loading caps on both split sections experienced severe cracking due to the applied moment. The test was terminated at a displacement of 10 cm (4 in.). The cap was repaired, the testing hardware was modified to prevent such failures, and the test was repeated. The data from the first test was used up to a displacement of 1.9 cm (0.75 in.), and the remainder of the data came from the second test. The peak horizontal load the specimen experienced was 27.6 kN (6.21 kips) at a displacement of 5.5 in. The specimen experienced no significant drop in load up to a final displacement of 15 cm (6 in.) with a corresponding displacement ductility, based on a yield

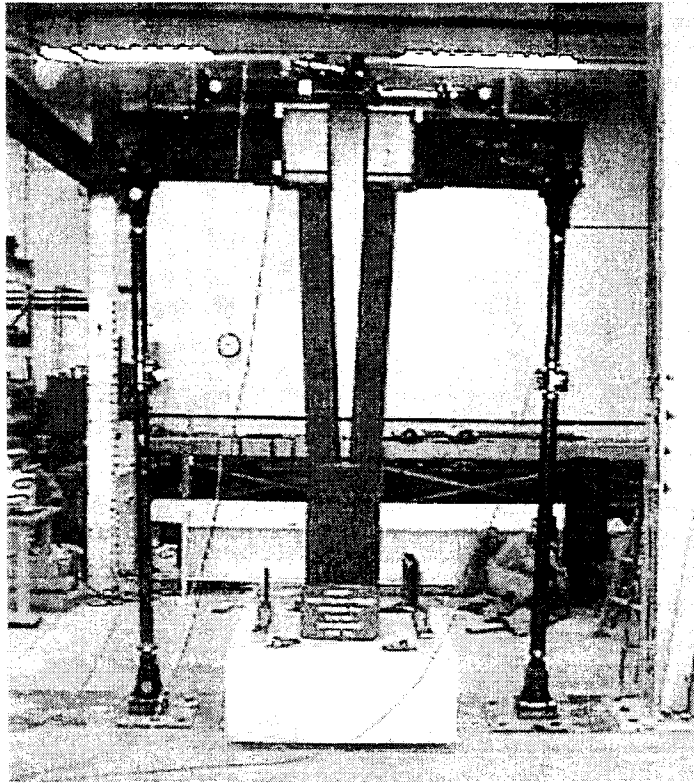


(a) Application of Epoxy

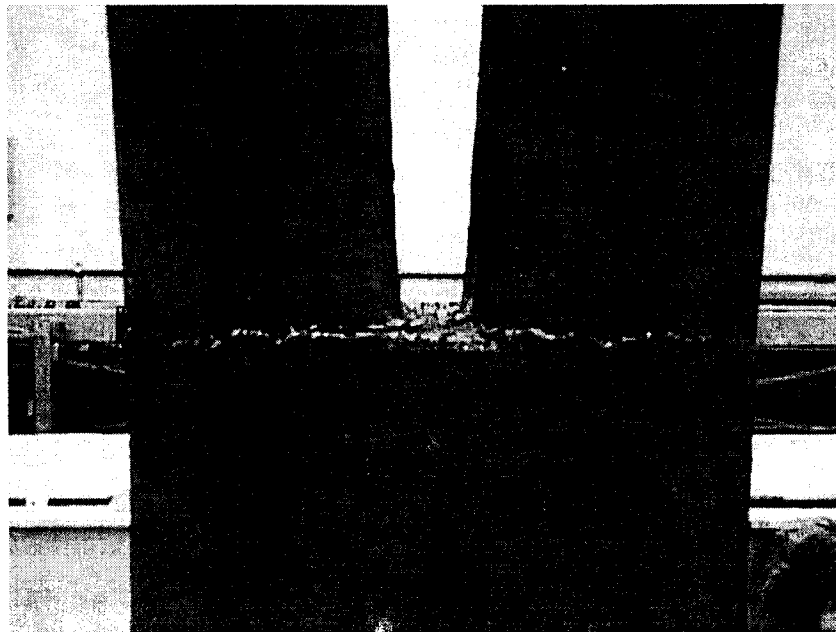


(b) Application of Fiberglass Material

Figure 19 Fyfe Company Retrofit Installation Photographs



(a) Testing of Specimen FW1



(b) Horizontal Flexure Cracking

Figure 20 Specimen FW1 Testing Photographs

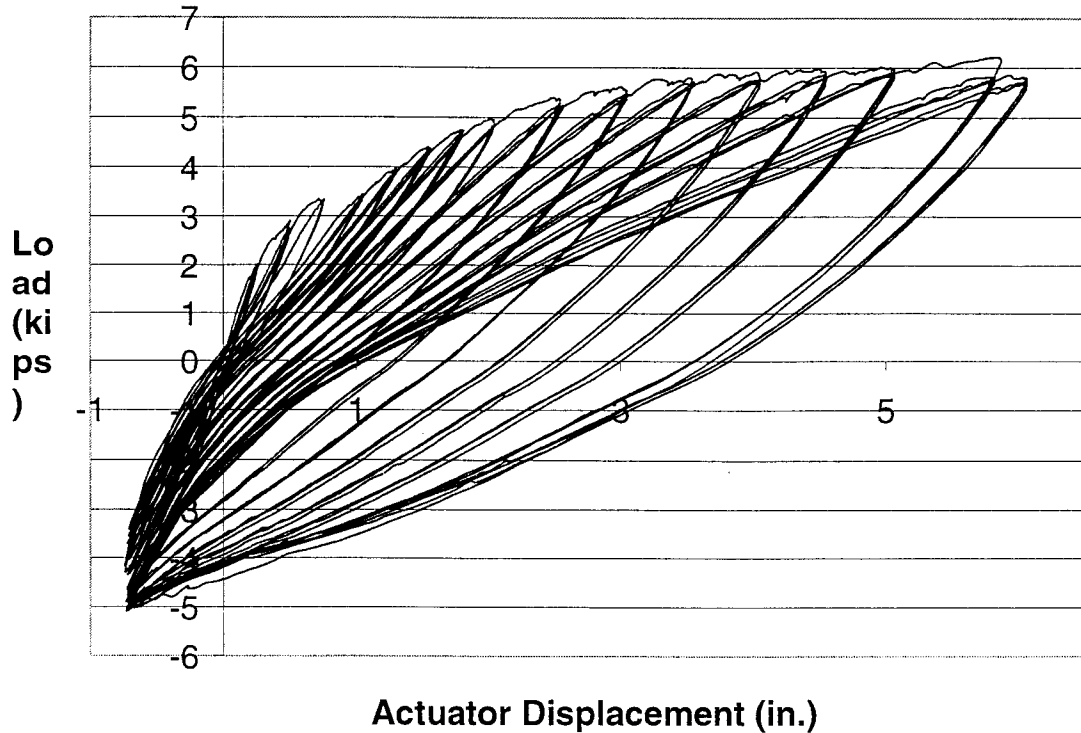


Figure 21 Load-Displacement Curves of Specimen FW1

displacement of 1.5 cm (0.6 in.), of approximately 10. Testing was terminated due to actuator stroke limitations.

The Fyfe Company retrofit prevented crack propagation at the base of the split. Significant horizontal flexure cracking occurred at the bottom and top of the split sections where there were gaps in the composite material and where the plastic hinges formed. There was no bulging of the composite material on the flat sections in the plastic hinge regions. From the load displacement hysteresis curves, it is clear that the retrofit installed on Specimen FW1 significantly increased energy dissipation when compared to that for the as-built specimen.

#### **Specimen FW2 (Sumitomo Retrofit)**

Specimen FW2 was constructed identically to the as-built specimen AB1, except that the specimen

was retrofitted using the Sumitomo retrofit system. The retrofit design was performed under the direction of the Sumitomo Company. Figure 22 provides a summary of the retrofit details for Specimen FW2. Sumitomo designed their retrofit systems based on providing for a displacement ductility,  $\mu_{\Delta}$ , of 8. The calculations for the Sumitomo retrofit design are shown in Appendix B.

Sumitomo determined that a shear force of 33 kN (7.4 kips) would have to be resisted at the base of the split to prevent crack propagation. The shear force was calculated based on the plastic moment capacity of the split sections. The jacket design was done in accordance with the ACTT-95/08 Provisions (Seible, et al, 1995) for shear strength enhancement. A 15 cm (6-in.) strip of 0.00264-in. composite material was installed directly below the split, and a 15 cm (6-in.) strip of 0.00132-in. composite material was installed directly below that. The plastic hinge confinement design for the split sections was performed using both the ACTT-95/08 Provisions (Seible, et al, 1995) and the provisions proposed by Priestley, et al (1996). The design with the Priestley, et al (1996) provisions controlled. However, the jacket thickness per the ACTT-95/08 Provisions (Seible, et al, 1995) was not doubled, as recommended for a rectangular cross-section, due to the results of previous testing conducted by Sumitomo. Further, ultimate jacket strains were limited to 0.004.

The controlling jacket thickness was due to a required ultimate compression strain in the concrete of 0.00526. A 15-cm (6-in.) strip of 0.0264-in. thick material was installed in the primary plastic hinge regions, and a 15-cm (6-in.) strip of 0.0132-in. thick material was installed in the secondary plastic hinge regions. In addition, one ply of material ( $t_j=0.0066$  in.) oriented in the longitudinal direction was applied to all sides in the split region and the plastic hinge regions. The purpose of this vertical material was to help distribute stresses evenly throughout the horizontally-oriented material. Shear strength design for the out-of-phase specimen was performed in accordance with the ACTT-95/08 Provisions (Seible, et al, 1995). The required jacket thickness for shear strength inside of the plastic hinge regions was 0.00096 cm (0.00376 in.) and therefore did not control. Outside of the plastic hinge regions, the required jacket thickness for shear strength was 0.005 cm (0.0021 in.) and one ply ( $t_j=0.0066$  in.) of material was installed.

Figure 23 shows photographs taken during the Sumitomo retrofit installation. Sumitomo supplied all of the materials used in the retrofit installation. The installation procedure for Sumitomo's carbon fiber/epoxy jackets went as follows. The corners of the columns were ground to a 2.5-cm (1-in.) radius. The smooth

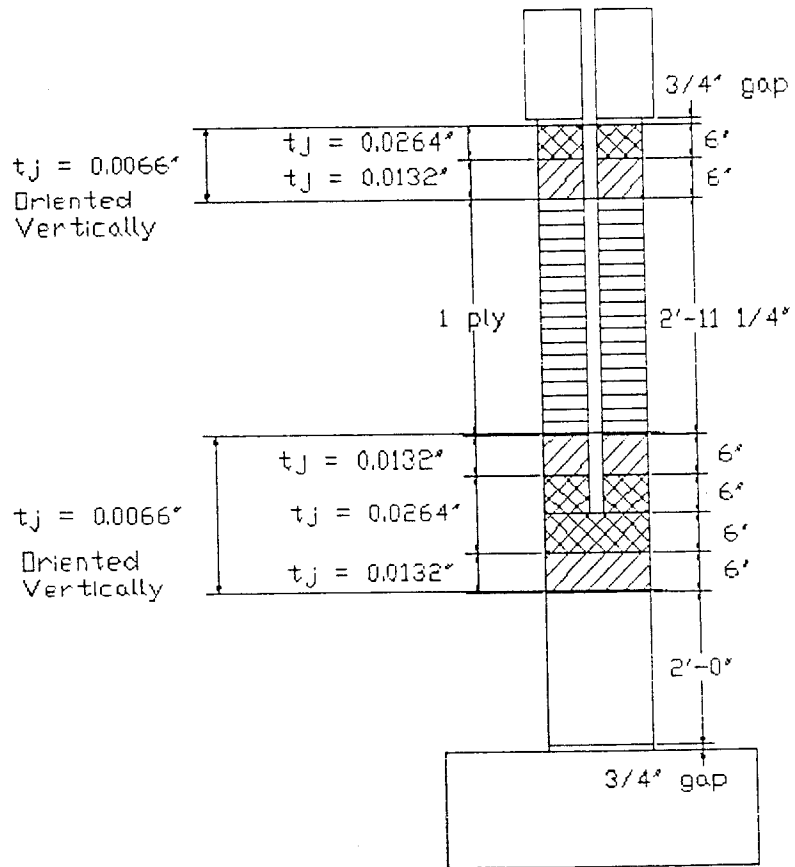
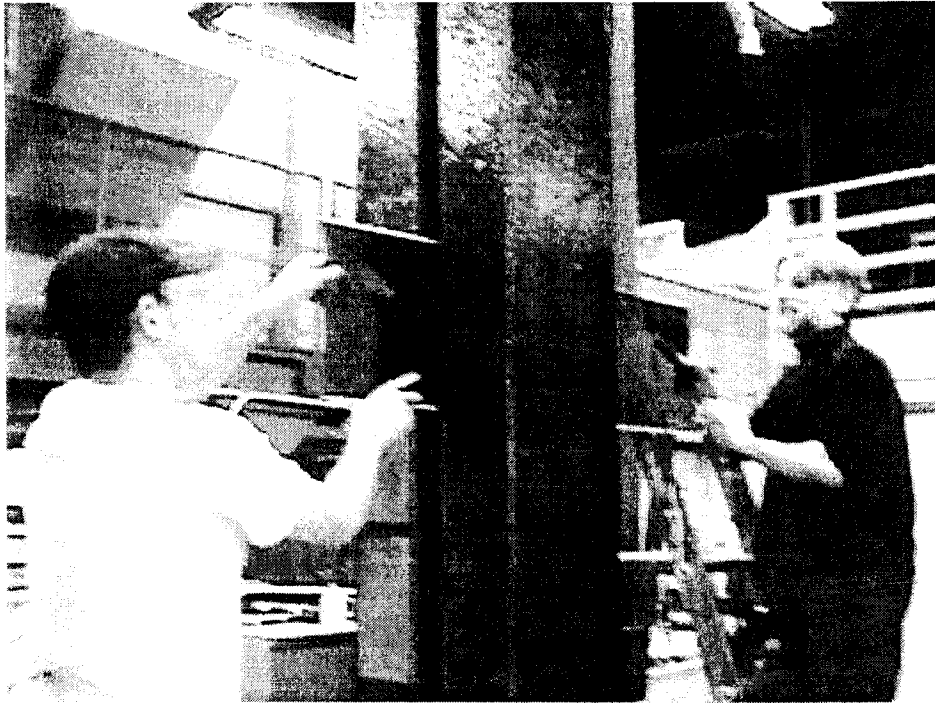


Figure 22 Retrofit Details for Specimen FW2



(a) Application of Epoxy



(b) Application of Carbon Fiber Material

Figure 23 Sumitomo Retrofit Installation Photographs

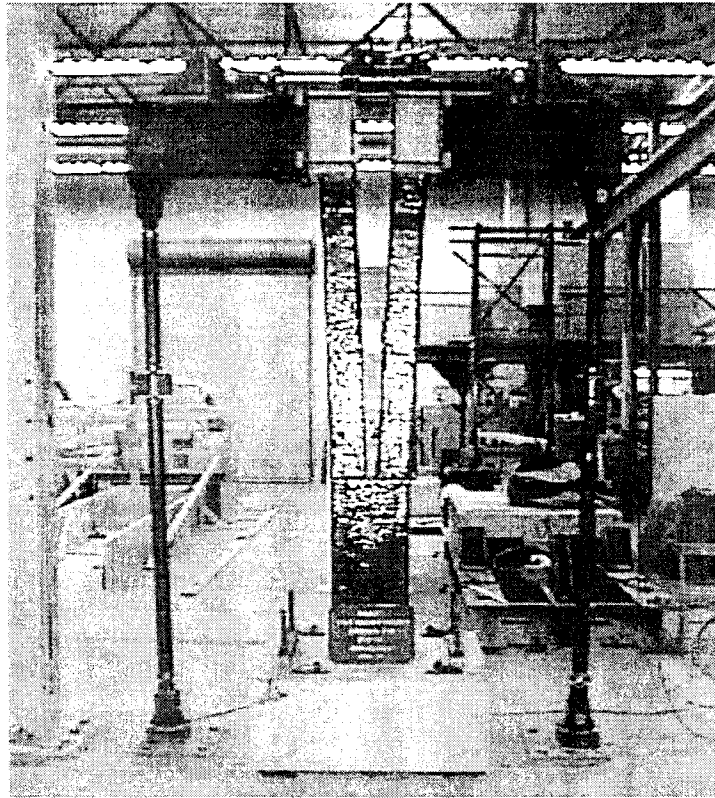
concrete surface of the column faces were roughened. Surface roughening was not possible on the inside of the split sections and these surfaces were not altered. The column surfaces were then covered with a layer of clear primer and the primer was allowed to dry. Epoxy was applied on top of the dry primer and one ply of carbon fiber material was applied by hand to the column on top of the epoxy. A roller was used to work the air bubbles out from under the material. Another coat of epoxy was applied on top of the carbon fiber and the next ply of carbon fiber was applied. The air bubbles were again worked out of the material with a roller. This continued until the required number of plies were installed. A final coat of epoxy was applied on top of the last layer of carbon fiber material.

Figure 24 shows testing photographs of Specimen FW2. Figure 25 shows the load-displacement hysteresis curves for Specimen FW2. The specimen reached a peak load of 26.6 kN (5.99 kips) at a displacement of 7.6 cm (3 in.). No significant drop in load occurred up to a final displacement of 15 cm (6 in.), when the test was terminated due to actuator stroke limitations. This displacement corresponds to a displacement ductility of approximately 10. No visible crack propagation occurred at the base of the split. Significant horizontal flexure cracking developed in the exposed concrete at the top and bottom of the split sections due to the formation of plastic hinges. The composite material experienced no bulging of the flat sections of the plastic hinge regions. By examining the load-displacement hysteresis curves shown in Figure 25, it is apparent that Specimen FW2 dissipated significantly more energy than the as-built specimen, AB1.

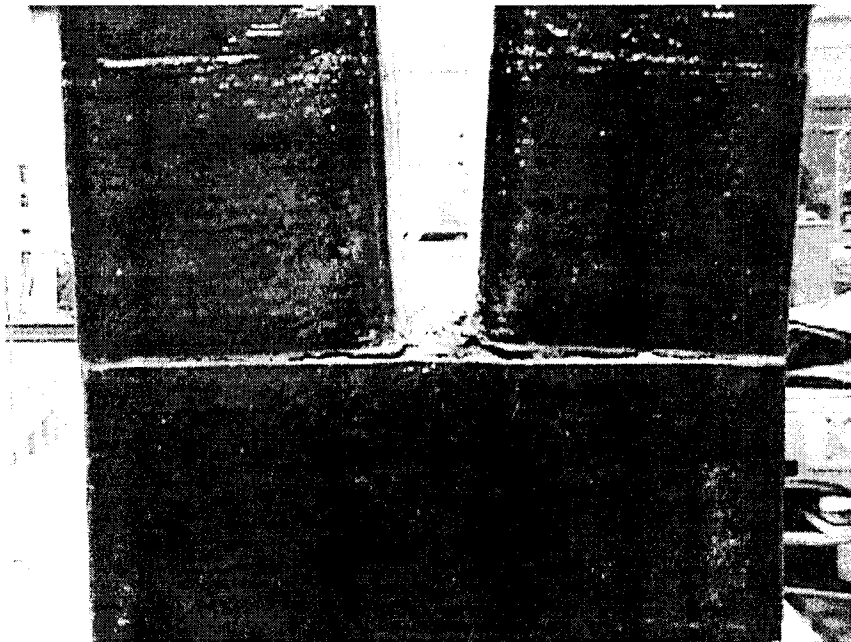
### **Specimen FW3 (XXSvs Retrofit)**

Specimen FW3 was constructed similarly to the as-built Specimen AB1, except that the specimen was retrofitted using the XXSvs retrofit system. A displacement ductility,  $\mu_{\Delta}$ , of 8 was used for the XXSvs retrofit designs. The calculations for the XXSvs retrofit design are shown in Appendix C. Figure 26 illustrates the retrofit details for specimen FW3.

XXSvs determined that a shear force of 131 kN (29.5 kips) would have to be resisted at the base of the split to prevent significant crack propagation from the base of the split. This was determined by limiting the crack width to 1 mm, resulting in a limiting jacket strain of 0.00246. The required jacket thickness was then determined using the ultimate stress of the composite material and assuming that the stress would be uniformly



(a) Testing of Specimen FW2



(b) Horizontal Flexure Cracking

Figure 24 Specimen FW2 Testing Photographs

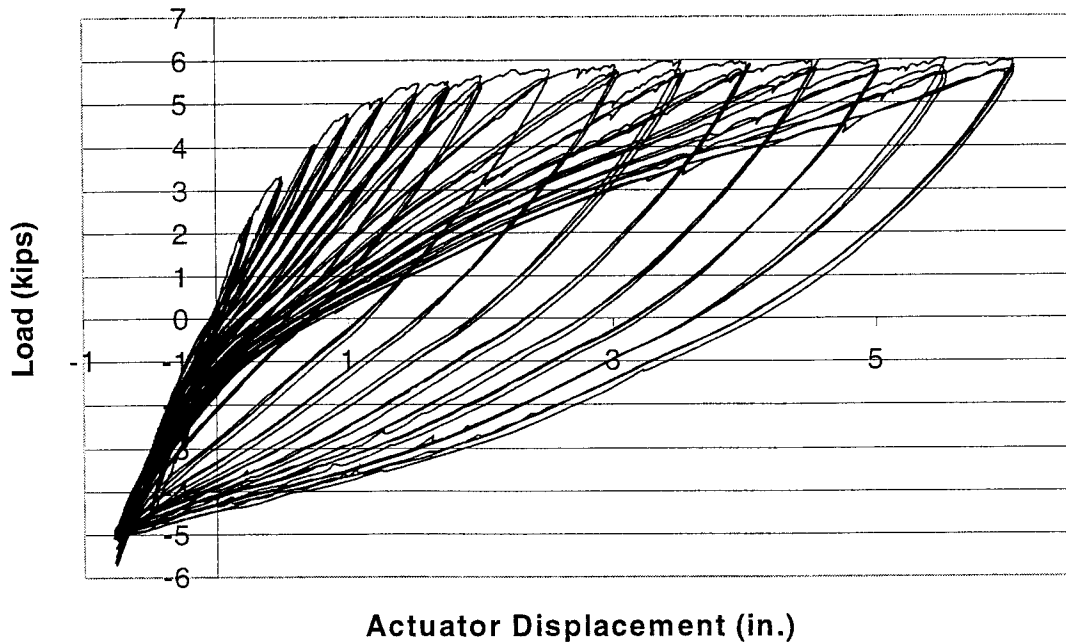


Figure 25 Load-Displacement Curves of Specimen FW2

distributed over a 15-cm (6-in.) deep region. A 15-cm (6-in.) strip of 0.053-in. thick material was installed directly below the split, and a 15-cm (6-in.) strip of 0.0266-in. thick material was installed directly below that. The plastic hinge confinement design in the split sections was also performed in accordance with the ACTT-95/08 Provisions (Seible, et al, 1995). The controlling jacket thickness was due to a required ultimate compression strain in the concrete of 0.0052. A 15-cm (6-in.) strip of 0.0268-in. thick material was installed in the primary plastic hinge regions, and a 15-cm (6-in.) strip of 0.0134-in. thick material was installed in the secondary plastic hinge regions. Shear strength design was done in accordance with the ACTT-95/08 Provisions (Seible, et al, 1995). The required jacket thickness for shear strength in the plastic hinge regions of the specimen was 0.02 cm (0.008 in.) and therefore did not control. Outside of the plastic hinge region no jacket was required or installed.

Photographs taken during the installation of the XXSys retrofit are shown in Figure 27. All of the materials used for retrofit installation were provided by XXSys. The installation procedure for the XXSys carbon fiber/epoxy retrofit is described below. The corners of the column were ground to a 2.5-cm (1-in.) radius. The smooth concrete surfaces were then roughened on all the column faces except the faces inside of the split. The first layer of carbon fiber material was either applied on top of a coat of adhesive or a coat of epoxy, depending on the retrofit region. The adhesive provides a better bond between the concrete and the composite material. In the crack propagation region of the specimen, a coat of adhesive was used. In the plastic hinge regions, a coat of epoxy was used. Following the installation of the first layer of carbon fiber, the air bubbles were worked out of the material with a roller. A coat of epoxy was then applied to the outside of the carbon fiber and another layer of carbon fiber was applied. Again, the air bubbles were worked out with a roller. This process continued until the required number of carbon fiber layers were installed. A final coat of epoxy was applied to the outside of the final layer of material.

Testing photographs of Specimen FW3 are shown in Figure 28. The load-displacement hysteresis curves for Specimen FW3 are provided in Figure 29. The specimen experienced a peak load of 26.3 kN (5.91 kips) at a displacement of 15 cm (6 in.), corresponding to displacement ductility of approximately 10. The peak load for each displacement interval was above 24.5 kN (5.5 kips) for all displacements greater than 5 cm (2 in.). The specimen experienced no significant drop in load and the test was terminated due to actuator stroke limitations. There was no visible crack formation at the base of the split. Significant horizontal flexure cracking at the top and bottom of the split sections developed due to plastic hinge formation at the location of gaps in the composite material. The material did not bulge in the flat sections of the plastic hinge regions. The load-displacement hysteresis curves for Specimen FW3 show a significant increase in energy dissipation when compared to the curves for the as-built specimen.

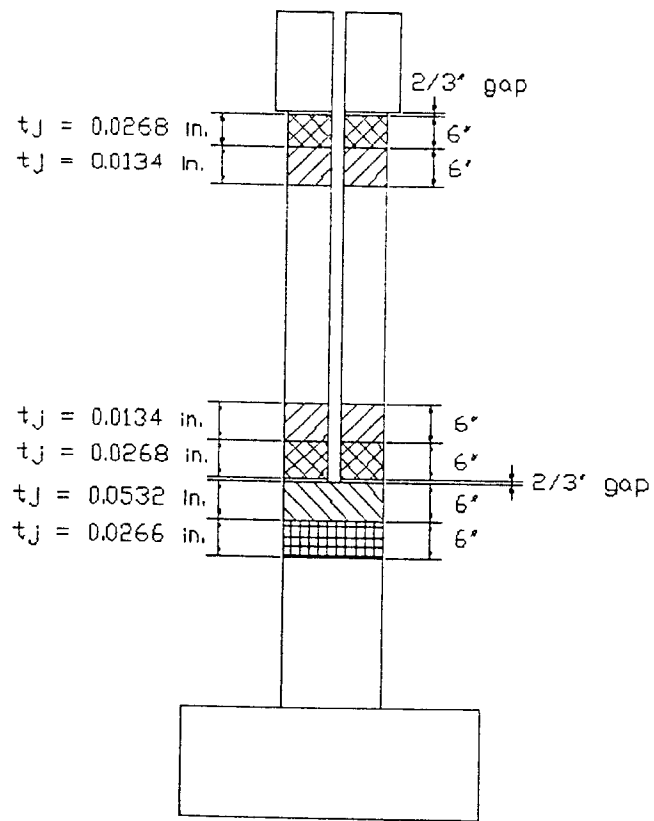
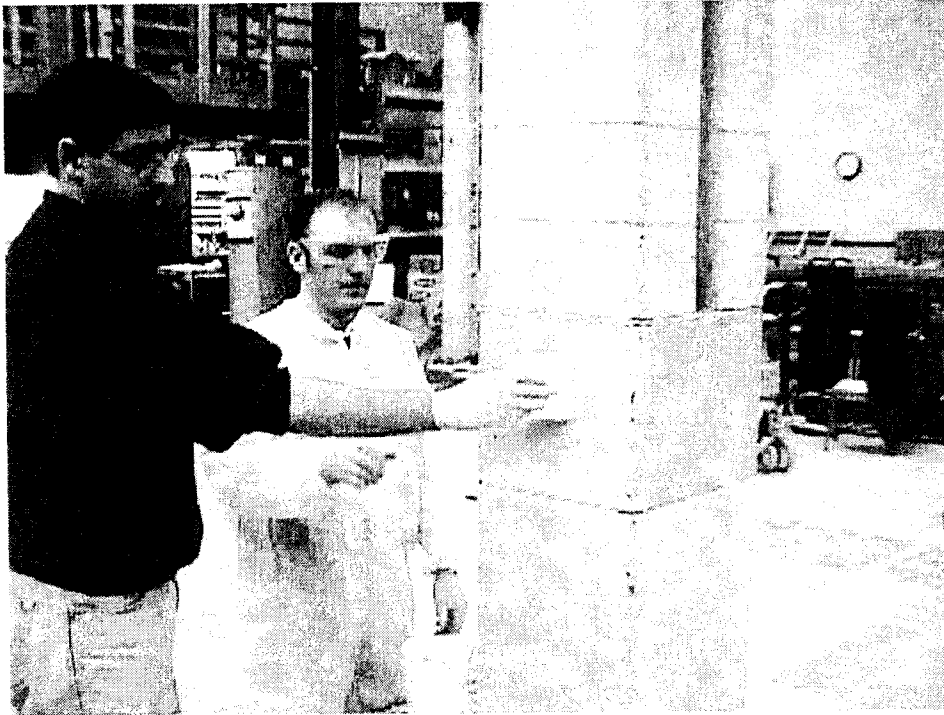
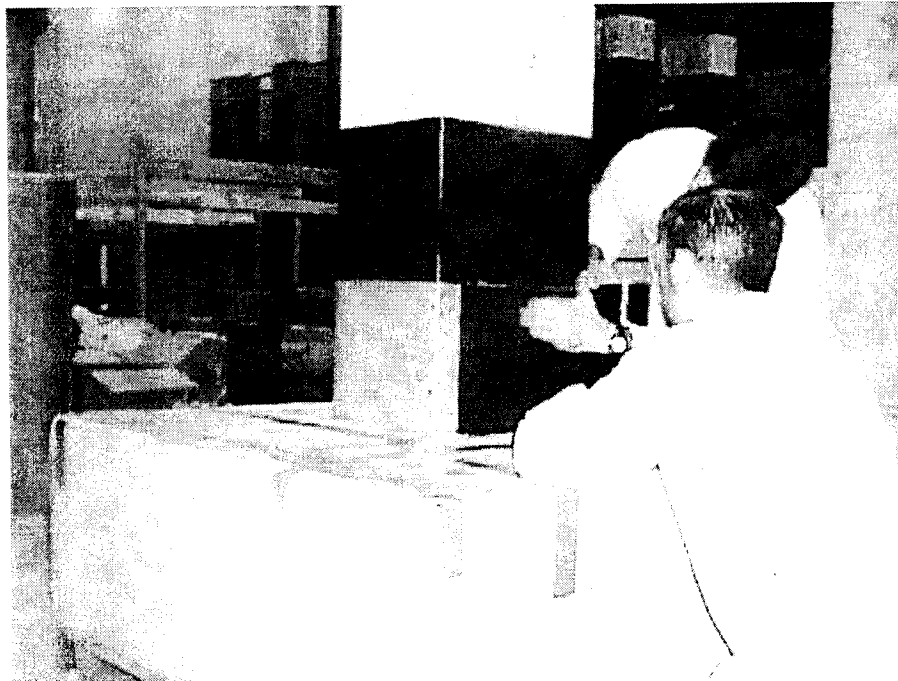


Figure 26 Retrofit Details for Specimen FW3

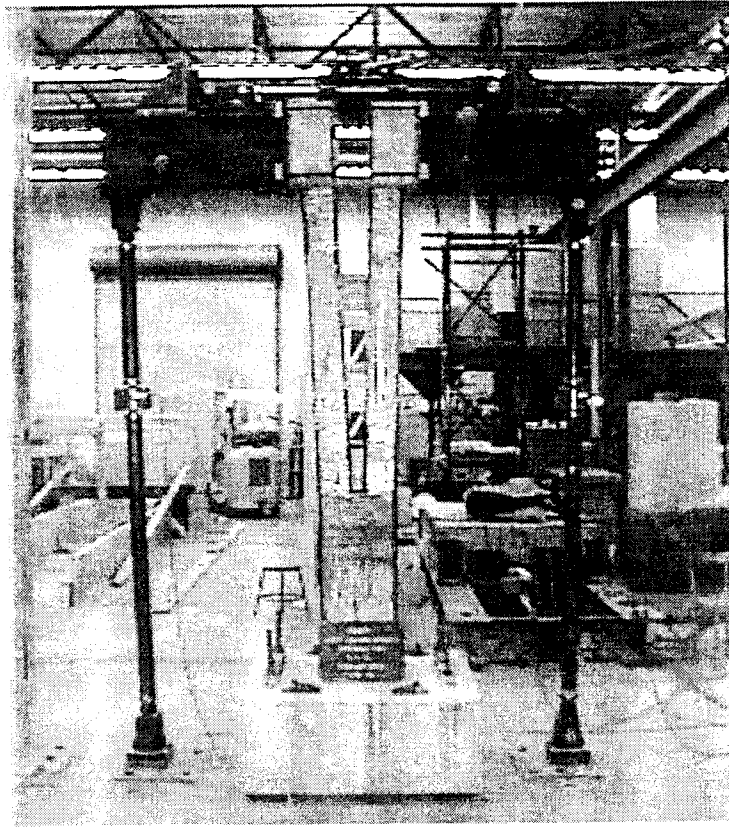


(a) Application of Adhesive

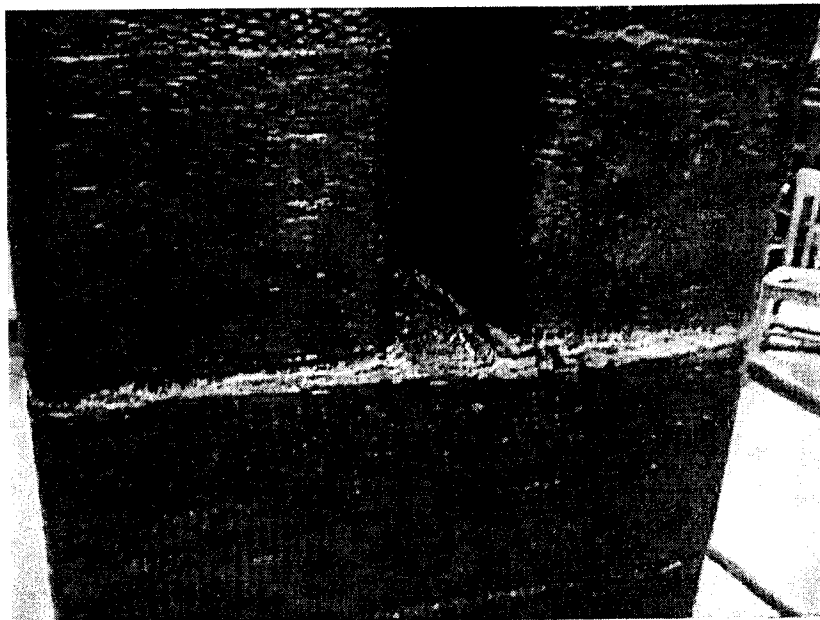


(b) Application of Carbon Fiber Material

Figure 27 XXSys Retrofit Installation Photographs



(a) Testing of Specimen FW3



(b) Horizontal Flexure Cracking

Figure 28 Specimen FW3 Testing Photographs

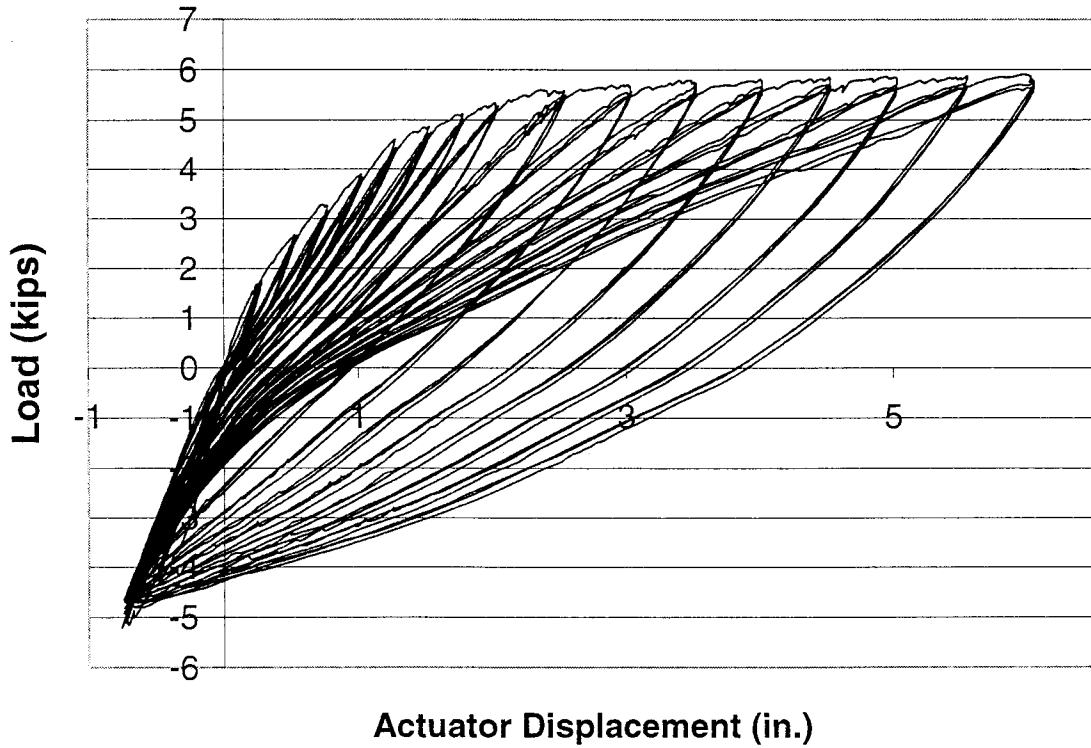


Figure 29 Load Displacement Curves of Specimen FW3

**Comparison of Out-of-Phase, Flexure-Critical Specimen Performance**

Table 3 summarizes the results from each of the out-of-phase, flexure-critical tests. Figure 30 compares the peak load-displacement envelopes of the four retrofitted specimens and the as-built specimen.

Table 3 Summary of Out-of-Phase, Flexure-Critical Test Results

Specimen	$\mu_{\Delta}$	Peak Load kN (kips)	Energy Dissipated KN-m (kip-in.)
AB1	Not Available	22.1 (4.96)	12.2 (108)
SJ1	10+	28.5 (6.41)	48.6 (430)
FW1	10+	27.6 (6.21)	32.9 (291)
FW2	10+	26.6 (5.99)	43.2 (382)
FW3	10+	26.3 (5.91)	33.9 (300)

All of the retrofit systems were successful in preventing crack propagation from the base of the split and in producing a ductile column response under the out-of-phase loading. From Table 3, all of the retrofitted specimens performed better than the as-built specimen in terms of both ductility and energy dissipation. The performance of the steel jacketed specimen, SJ1, and the Sumitomo specimen, FW2, exceeded the performance of the other two retrofitted specimens in terms of energy dissipation. The greater energy dissipation is a result of more confinement being provided in the plastic hinge regions by these retrofits. The different confinement stresses in the composite retrofit systems are a result of the design procedures used by the respective companies. The product  $t_j E_j$  can be used as a measure of the relative confinement pressure supplied by any jacket, with  $t_j$  being the jacket thickness and  $E_j$  the jacket modulus of elasticity. Table 4 compares the values of the product  $t_j E_j$  for the composite material jackets installed on the primary plastic hinge regions of specimens FW1, FW2, and FW3. It is clear from Table 4 that the Sumitomo jacket, as installed, supplies substantially more confinement pressure than the jackets of the other two companies.

Another design difference between the three retrofitted specimens was that XXSys included no material away from the plastic hinge regions of the specimen. The other two companies installed 1 ply of material in that region. This difference appeared to have no effect on specimen performance. No cracking was observed in the unretrofitted region of the XXSys specimen.

Table 4 Comparison of Relative Confinement Pressures in Composite Out-of-Phase Specimens

Specimen	Retrofit Company	$t_j E_j$ kN/m (kip/in.)
FW1	Fyfe Company	248 (204)
FW2	Sumitomo	1070 (882)
FW3	XXSys	391 (322)

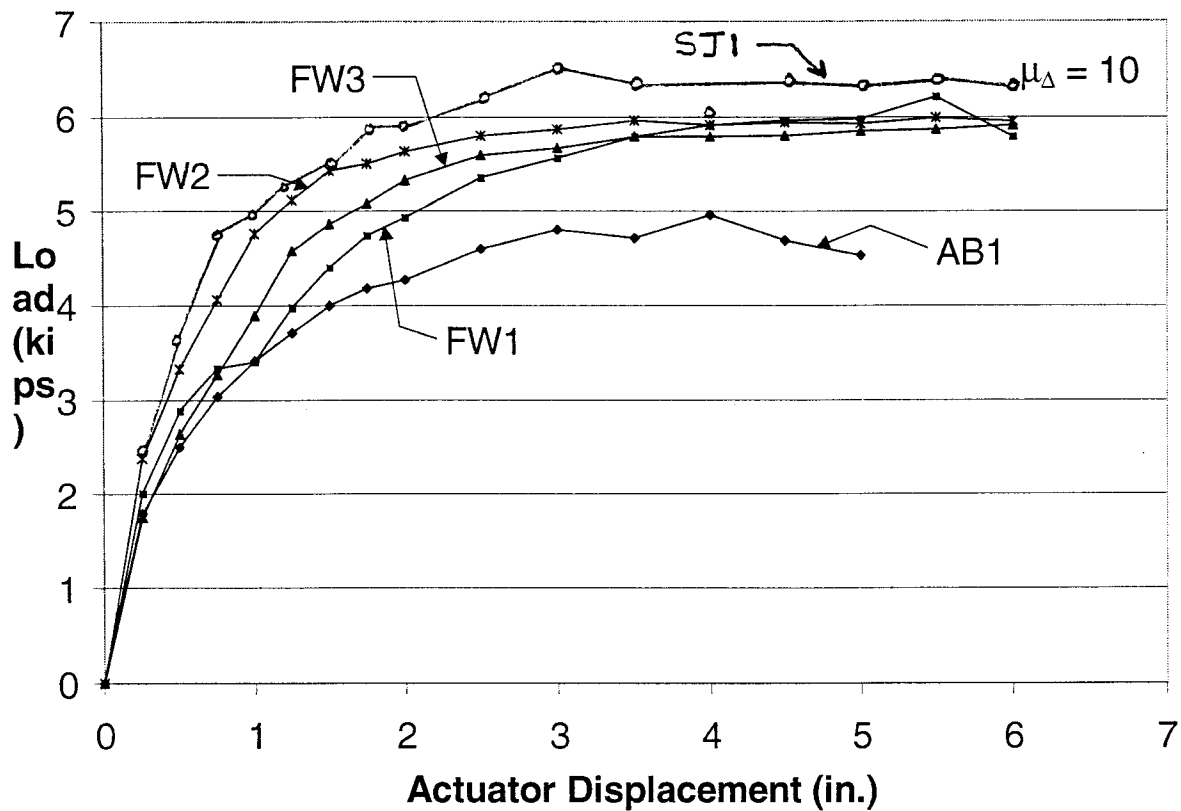


Figure 30 Peak Load-Displacement Envelope of Out-of-Phase Specimens

## OUT-OF-PHASE, SHEAR-CRITICAL TEST RESULTS

### Specimen AB3 (As-Built)

Specimen AB3 was constructed to be representative of the split columns in the Spokane Street Overcrossing, with a split over approximately half of the column height and for which there is concern of a brittle shear failure in the split sections. Details of the specimen are given in Figure 31. The column longitudinal reinforcing ratio was 0.037. The bottom non-split section was retrofitted with a 0.64-cm (0.25-in.) thick circular steel jacket to prevent crack propagation from the base of the split in order to reveal the shear response of the two split sections. Specimen AB3 was tested under out-of-phase loading.

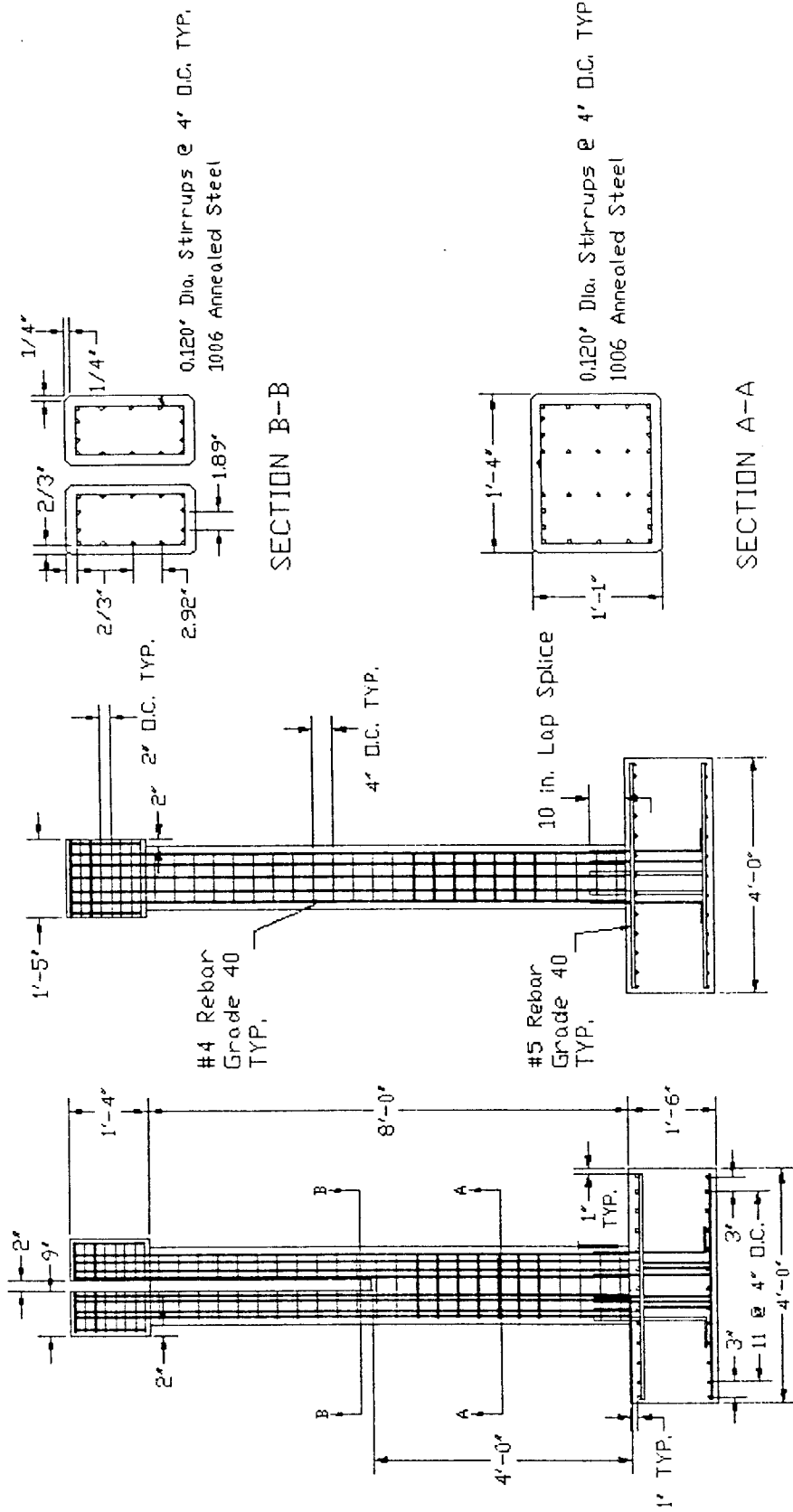


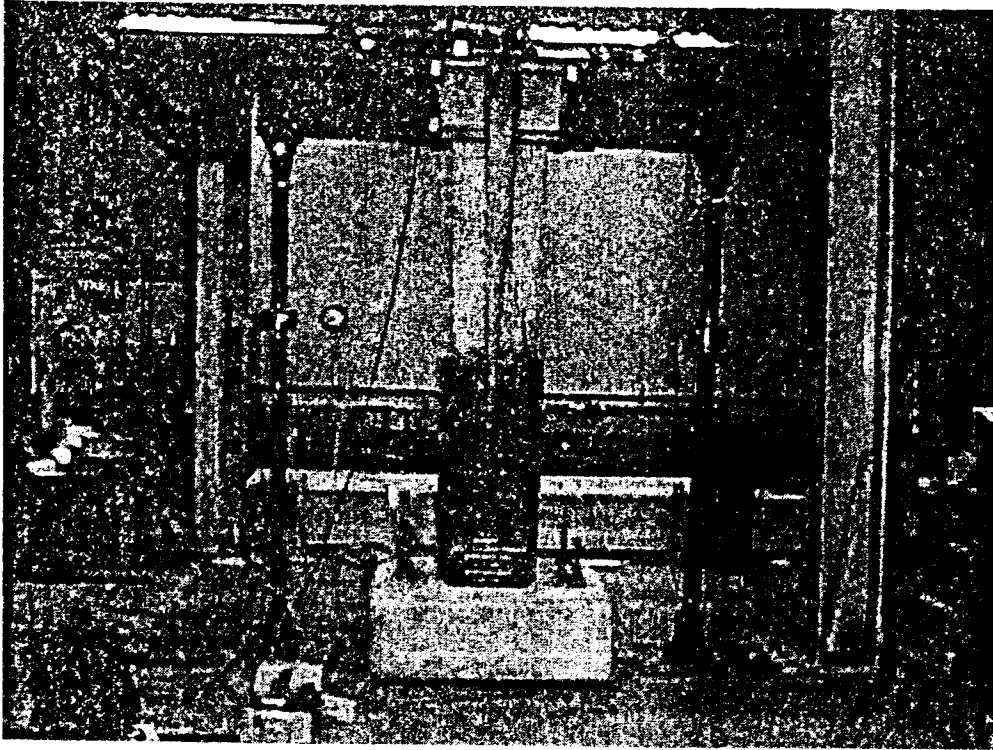
Figure 31 Details of Specimen AB3

Photographs taken during the testing of Specimen AB3 are shown in Figure 32. The load-displacement curves for the specimen are given in Figure 33. As was expected, Specimen AB3 failed in a shear mode. Inclined cracks at approximately  $45^\circ$  were observed at a displacement of 3.8 cm (1.5 in.). Brittle shear failure occurred at a displacement of 10.2 cm (4 in.) with an applied peak horizontal load of 73.8 kN (16.6 kips). No significant cracks were observed in the plastic hinge regions. The load-displacement curves indicate relatively poor energy dissipation.

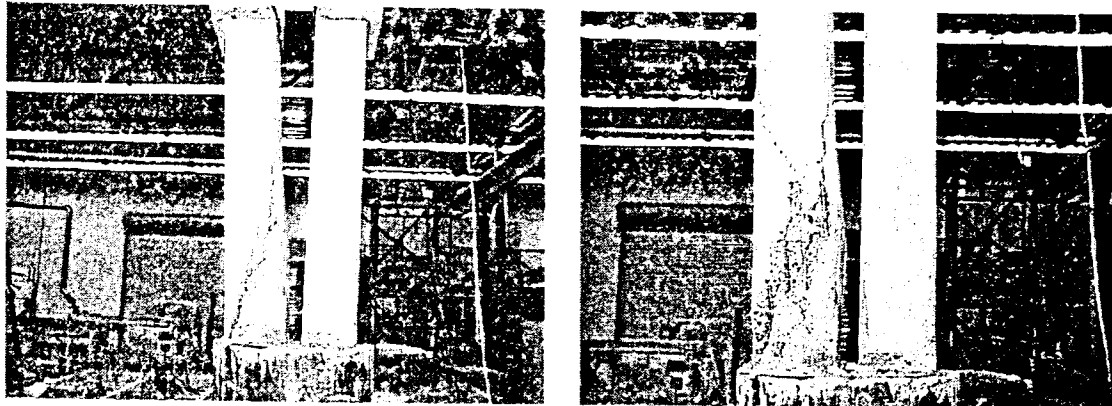
### **Specimen SJ3 (Steel Jacket Retrofit)**

Specimen SJ3 was constructed similarly to the shear-critical as-built specimen, AB3, except for being retrofitted with steel jacketing. Details of the retrofit for Specimen SJ3 are summarized in Figure 34. The objectives of the retrofit was to provide adequate shear strength and confinement to the flexural hinge regions in the split sections and to prevent crack propagation from the base of the split. Using the design procedures developed by Priestley, et al (1996) for enhancement of shear strength using steel jackets and hinge confinement, a steel jacket thickness of 0.01 cm (0.004 in.) is required. Therefore, the split sections of Specimen SJ3 were retrofitted with 0.32-cm (0.125-in.) thick "D" steel jackets along the entire split height. Following the procedures developed in this study for retrofitting to prevent the split opening, as discussed previously, a 0.25-cm (0.10-in.) thick circular steel jacket is required. Thus, a circular jacket with a thickness of 0.64 cm (0.25 in.) was applied around the bottom non-split section. A clearance of 1.9 cm (0.75 in.) was incorporated between the steel sections and between the steel jacket and the cap and footing.

A photograph of Specimen SJ3 during testing is shown in Figure 35. Load-displacement curves are given in Figure 36. The specimen carried a peak load of approximately 80 kN (18 kips) at a displacement of 18 cm (7 in.), when testing was stopped due to the actuator reaching its maximum stroke. Horizontal cracks were evident at the construction gaps at the top and bottom of the split sections. The retrofit was successful in converting the brittle shear failure observed in the as-built specimen to a ductile response with flexural hinging at the top and bottom of the split sections.



(a) Specimen AB4



(b) Shear Failure

Figure 32 Specimen AB3 Test Photographs

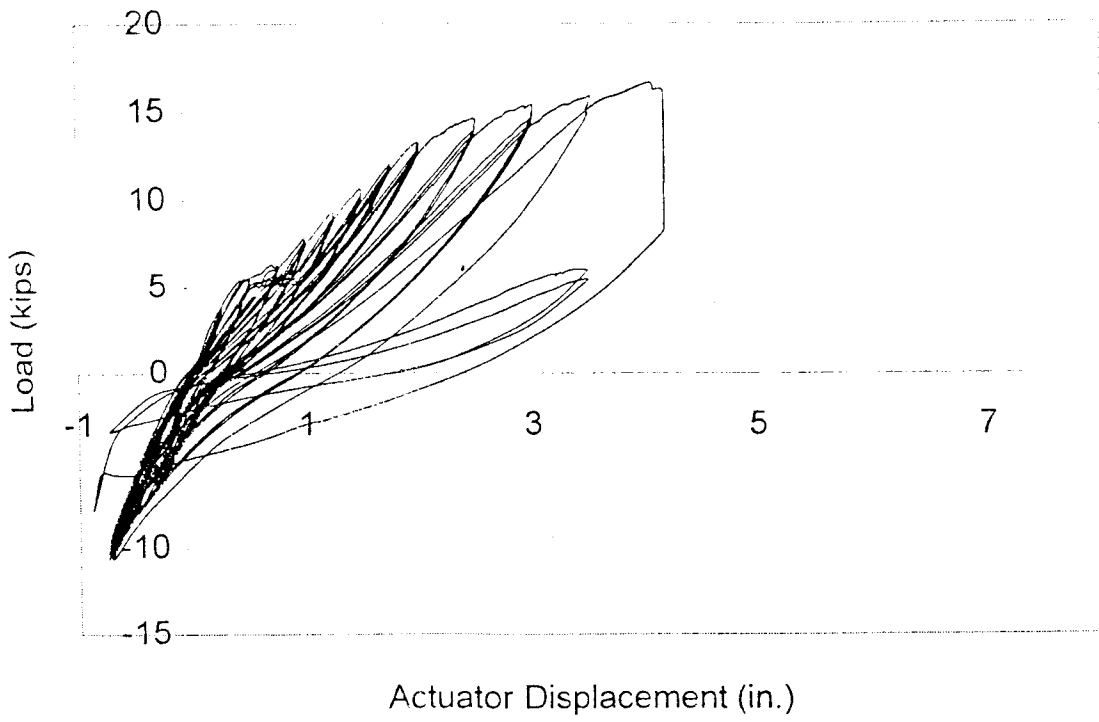


Figure 33 Load-displacement Curves for Specimen AB3

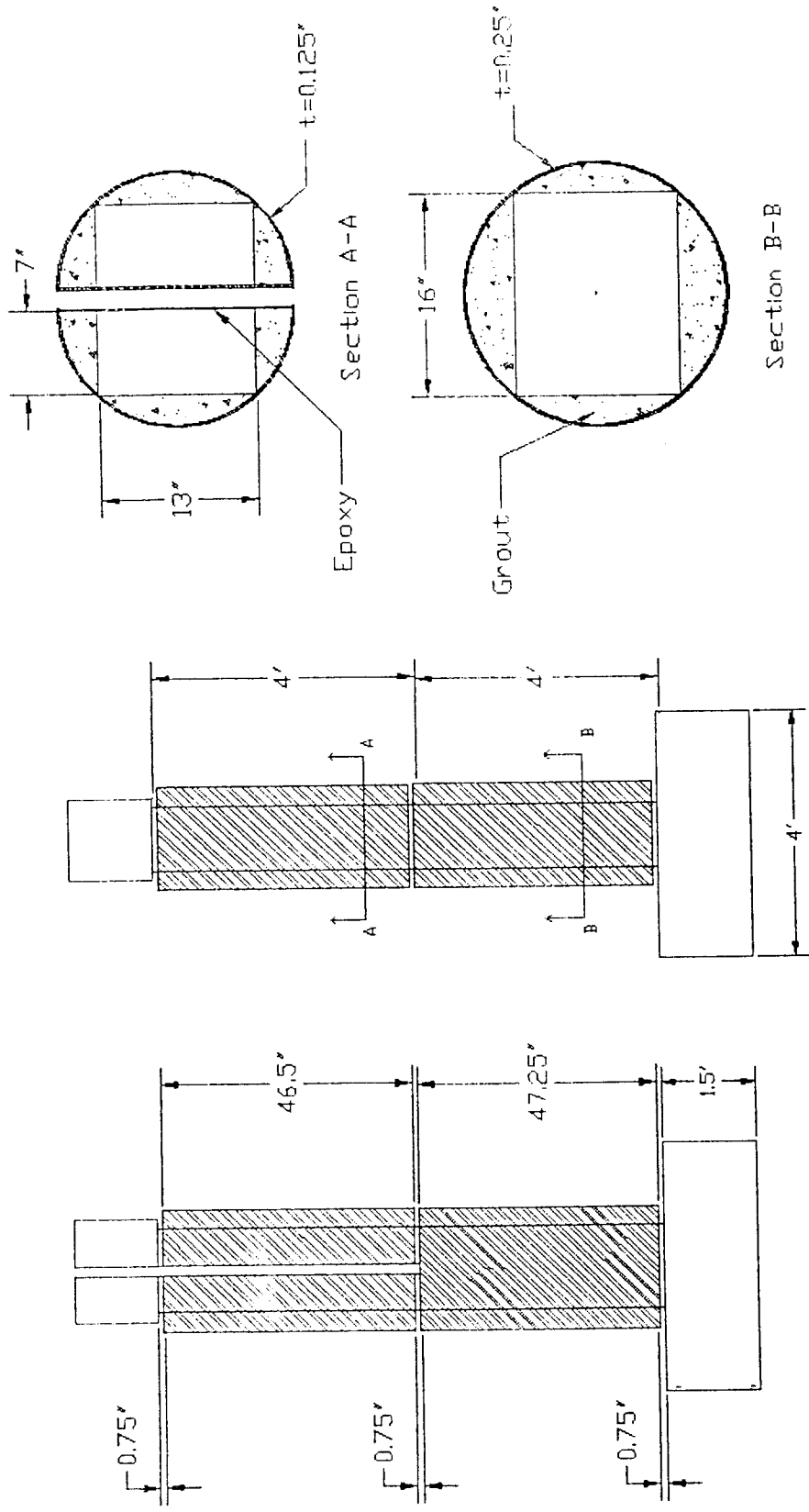


Figure 34 Retrofit Details for Specimen SJ3

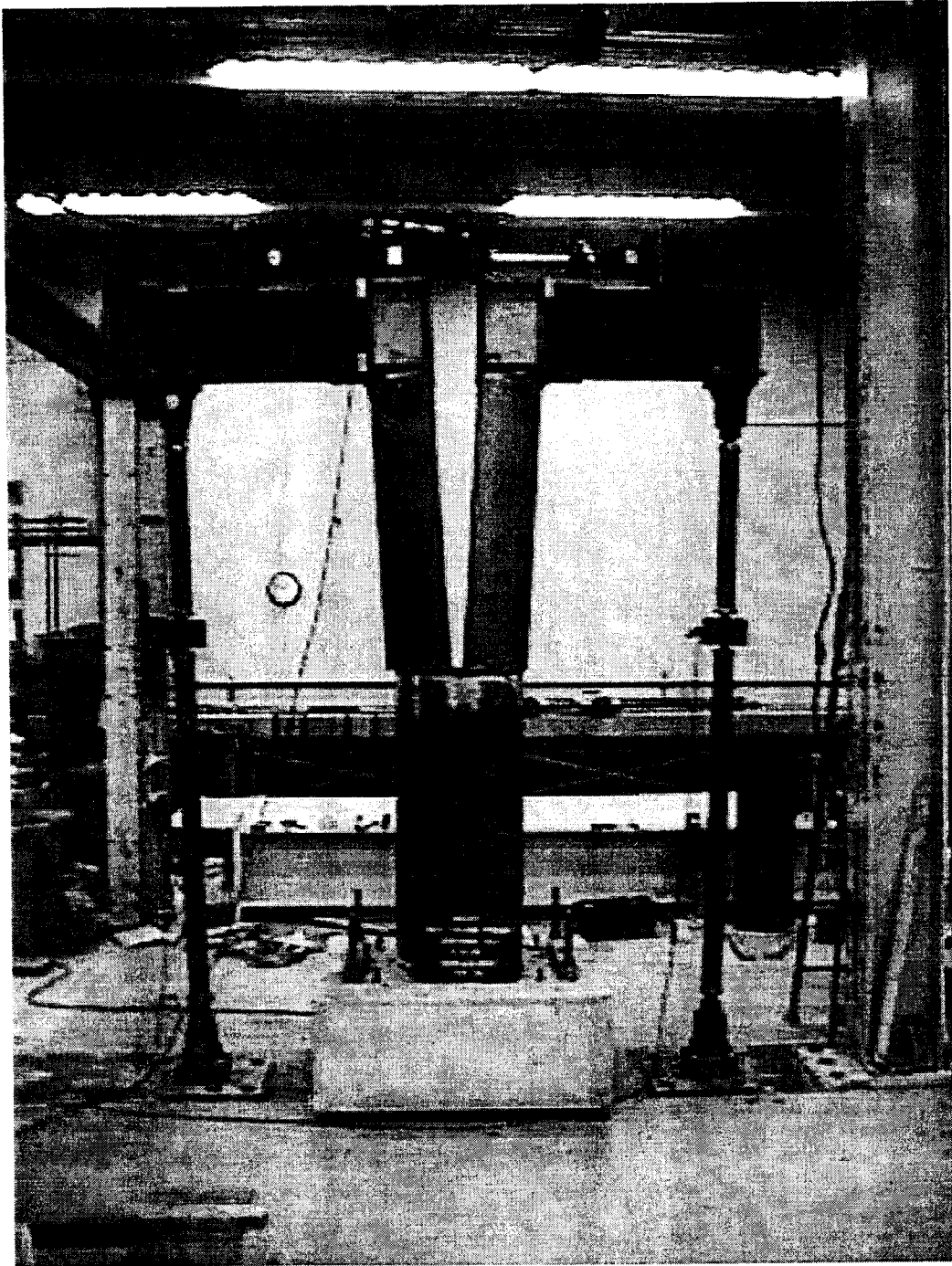


Figure 35 Specimen SJ3 Test Photograph

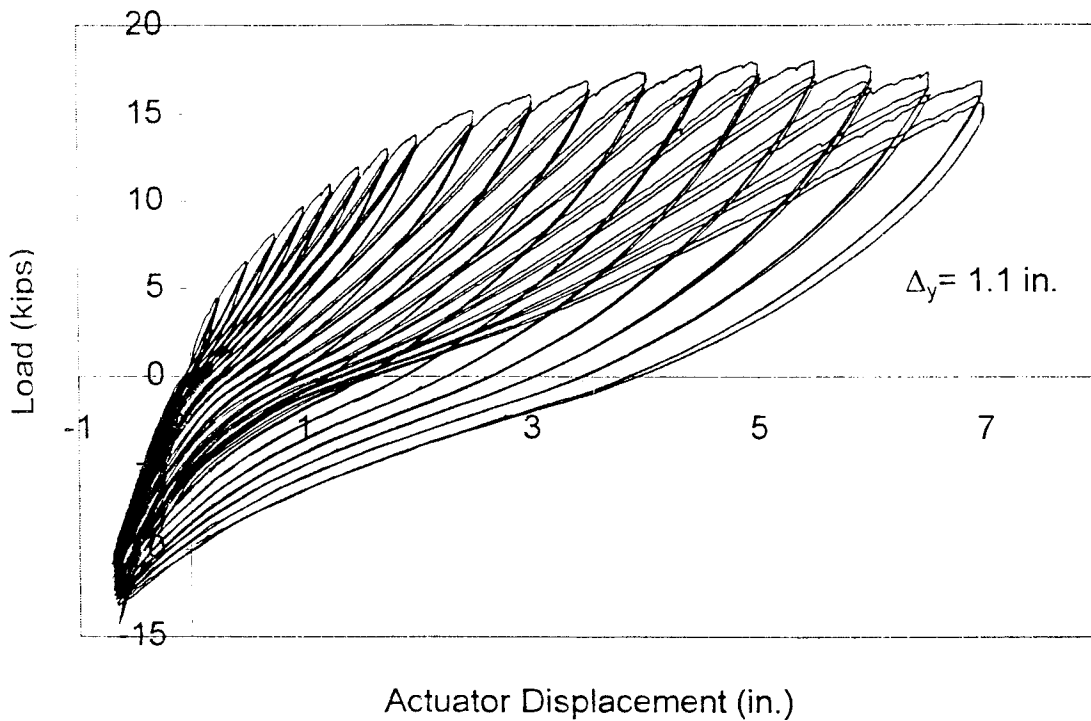


Figure 36 Load-Displacement Curves for Specimen SJ3

### **OUT-OF-PHASE, FOOTING-CRITICAL TEST RESULTS**

Specimen SJ2 was constructed similarly to the as-built Specimen AB1 except that a full height split was incorporated and the footing details were representative of the prototype footings in the Spokane Street Overcrossing. The footing in the scaled specimen was 0.30-m (1-ft) thick and had a single layer of reinforcement for positive bending only. The specimen was vulnerable to flexural hinge degradation at the top and bottom of the split sections as well as concerns regarding crack propagation from the base of the split into the footing. Loading was in the out-of-phase direction.

Retrofit measures were not applied to the footing. However, the concern regarding cracks propagating from the base of the split into the footing was addressed by applying a 0.32-cm (0.125-in.) thick circular steel

jacket around the two split sections up to a height of 0.46 m (1.5 ft) from the top of the footing. The application of the circular steel jacket around the two split sections near the footing will decrease the column effective height and will subsequently slightly increase the column lateral stiffness. The upper portions of the split sections were retrofitted with "D" steel jackets. Based upon earlier discussions, a steel jacket thickness of 0.64 cm (0.25 in.) was required for both the bottom circular jacket and the two "D" jackets. Figure 37 shows details of the retrofit.

A photograph of Specimen SJ2 during testing is shown in Figure 38. The load-displacement curves for the specimen are given in Figure 39. The specimen continued to carry slightly increasing load up to a displacement of 18 cm (7 in.), when loading was stopped due to the actuator reaching its maximum stroke. Horizontal cracks were observed in the gaps at the top of the split sections and between the upper and lower steel jackets. No cracks were observed at the column-footing connection or anywhere in the footing. The use of the circular steel jacketing around the base of the split columns was successful in preventing crack propagation into the deficient footing. Additionally, the "D" steel jackets around the split sections provided for ductile flexural hinge formation.

## **TRANSVERSE TEST RESULTS**

The transverse specimens were susceptible to lap splice failures and plastic hinge failures at the base of the full height split sections. The experimental yield displacement was found after testing to be 1.8 cm (0.7 in.) by fitting a bilinear load-displacement approximation to the hysteresis curves, as outlined by Priestley, et al (1996). The displacement ductility capacity,  $\mu_{\Delta}$ , and the energy dissipation were used to evaluate the seismic performance of each test specimen.

### **Specimen AB2 (As-Built)**

Specimen AB2 was constructed to be representative of a typical split column in the Spokane Street Overcrossing with a split over the full column height. A lap splice, with a lap length of 19 cm (7.5 in.) (20 bar diameters), was present at the base of the specimen making it vulnerable to lap splice degradation. Details of the specimen are given in Figure 40. The column longitudinal reinforcing ratio was 0.013. Specimen AB2 was

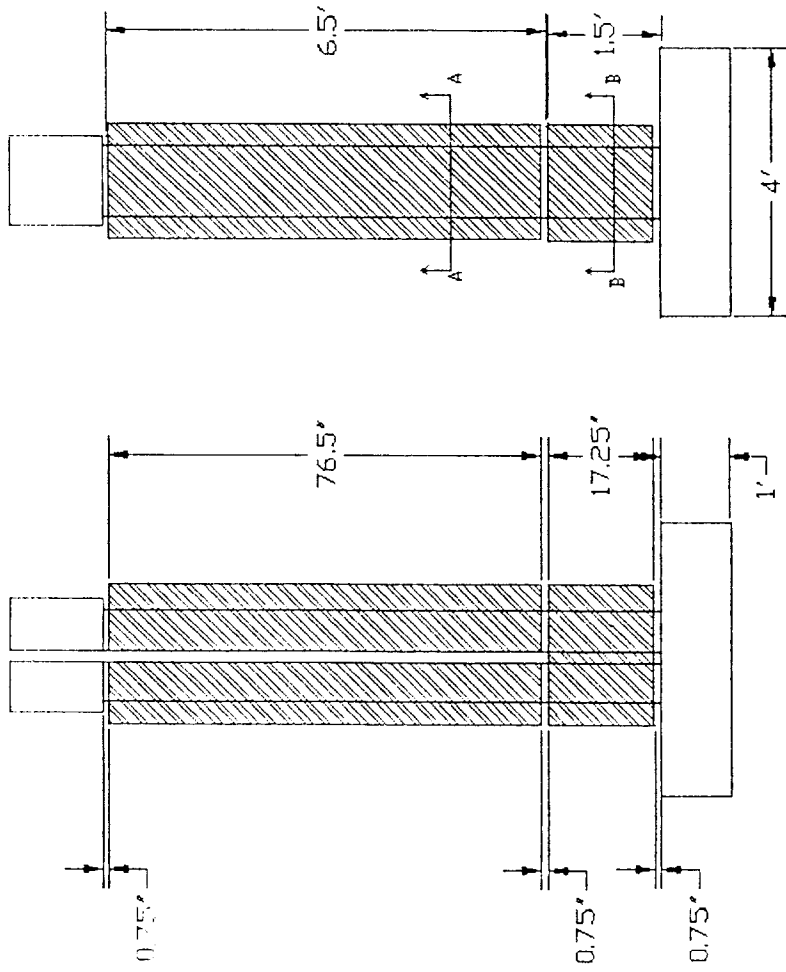
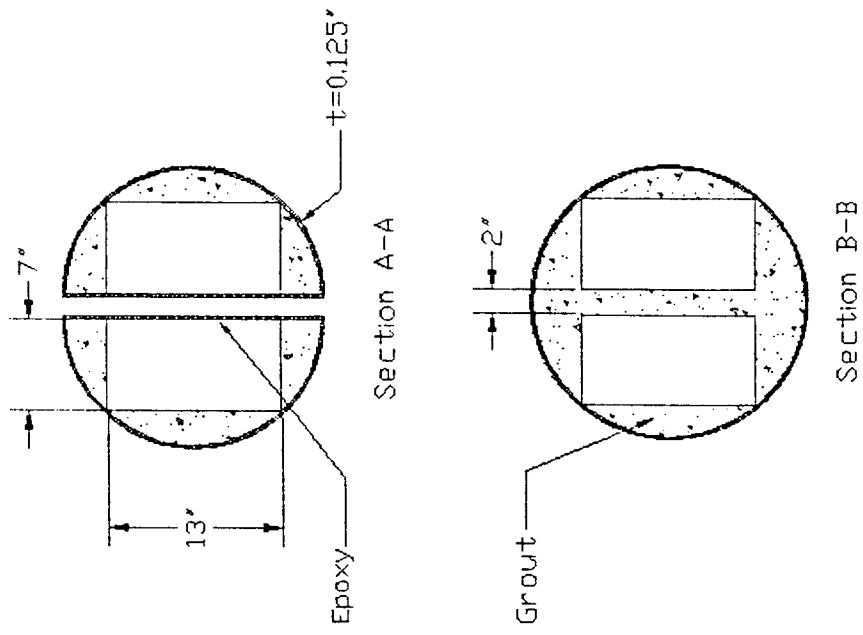


Figure 37 Retrofit Details for Specimen SJ2

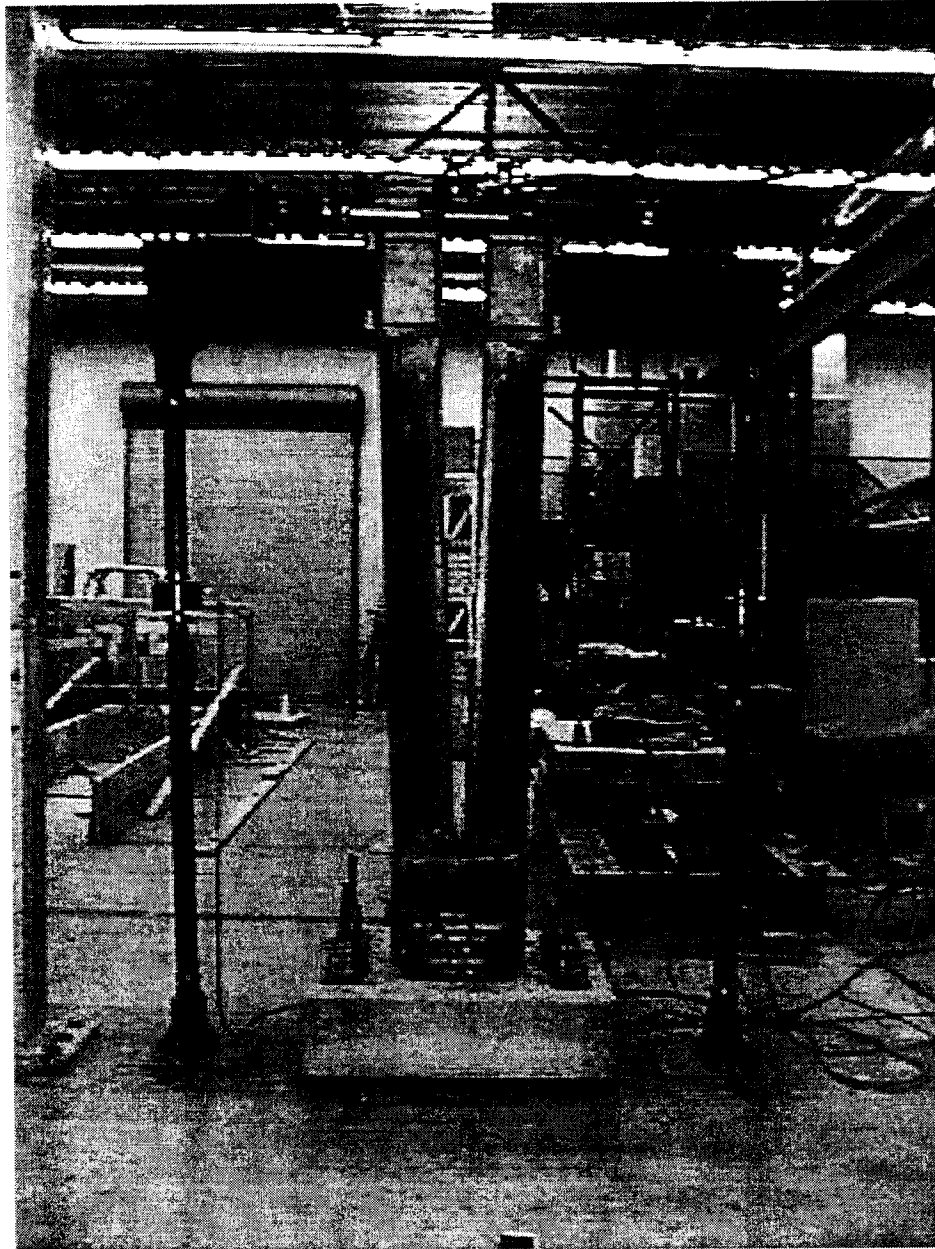


Figure 38 Photograph of Specimen SJ2 During Testing

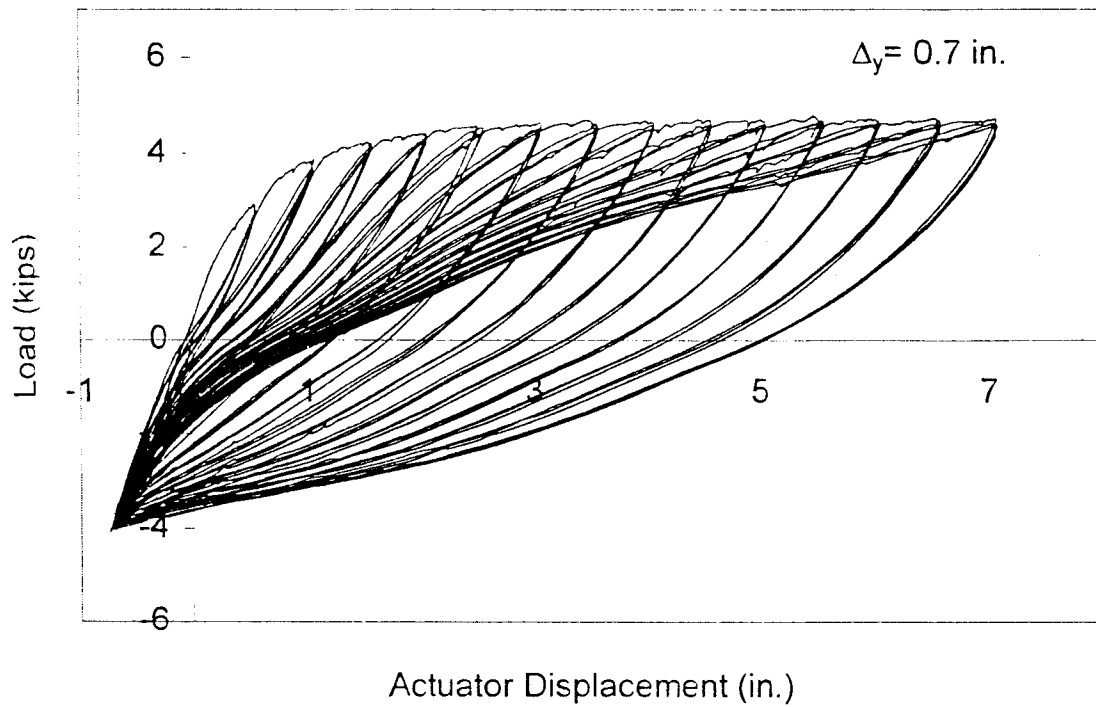


Figure 39 Load Displacement Curves for Specimen SJ2



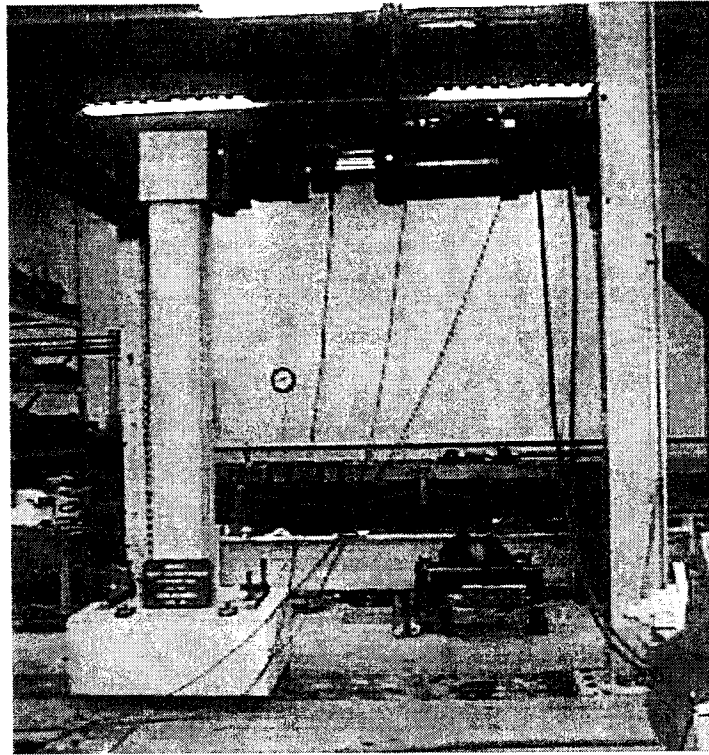
tested under out-of-phase loading.

Photographs of Specimen AB2 during testing are shown in Figure 41. The load-displacement hysteresis curves are given in Figure 42. The specimen experienced a 50% drop in lateral load capacity at a displacement of 5.1 cm (2 in.). This corresponds to a displacement ductility capacity of approximately 3. The peak load the column experienced was 21 kN (4.7 kips) at a displacement of 3.8 cm (1.5 in.). Vertical and horizontal cracking, indicative of lap splice degradation, occurred in the splice region at the base of each section, as shown in Figure 41. The small lap splice length and lack of adequate transverse confinement caused the bond between the starter bars and the concrete to degrade at a low level of displacement. Slippage of the longitudinal reinforcement was the cause of the vertical cracking and subsequent spalling of the concrete cover. The hysteresis curves indicate a low level of energy dissipation and rapid flexural strength degradation.

#### **Specimen SJ4 (Steel Jacketing)**

Specimen SJ4 was constructed similarly to the as-built specimen, AB2, except that it was retrofitted with steel jacketing to enhance confinement in the lap splice region. Following the design procedures for steel jacketing of deficient lap splices developed by Priestley, et al (1996), a jacket thickness of 0.25 cm (0.10 in.) is required. Based upon practical considerations, a jacket of 0.32 cm (0.125 in.) was used to confine the lap splice. To improve confinement, a full circular steel jacket rather than "D" jacketing was provided to a height of 0.46 m (1.5 ft) from the top of the footing, which fully covered the lap splice. Over this region, the 5-cm (2-in.) gap between the split sections was filled with grout. The remaining portions of the two split sections was retrofitted with "D" jacketing. Figure 43 provides a summary of the retrofit details for Specimen SJ4.

A photograph of Specimen SJ4 during testing is given in Figure 44. Load-displacement curves are presented in Figure 45. A peak applied load of 35 kN (7.9 kips) was reached at a displacement of 10.2 cm (4 in.). The specimen continued to resist this peak load until approximately 13 cm (5 in.) of displacement, at which time the load dropped. This corresponds to a displacement ductility capacity of approximately 7. Prior to the load dropping, a series of "popping" sounds were heard and "kinks" in the hysteresis curves were observed. The likely cause of these phenomena is reinforcement slippage in the lap splice region. By



(a) Testing of Specimen AB2



(b) Lap Splice Degradation Cracking

Figure 41 Specimen AB2 Testing Photographs

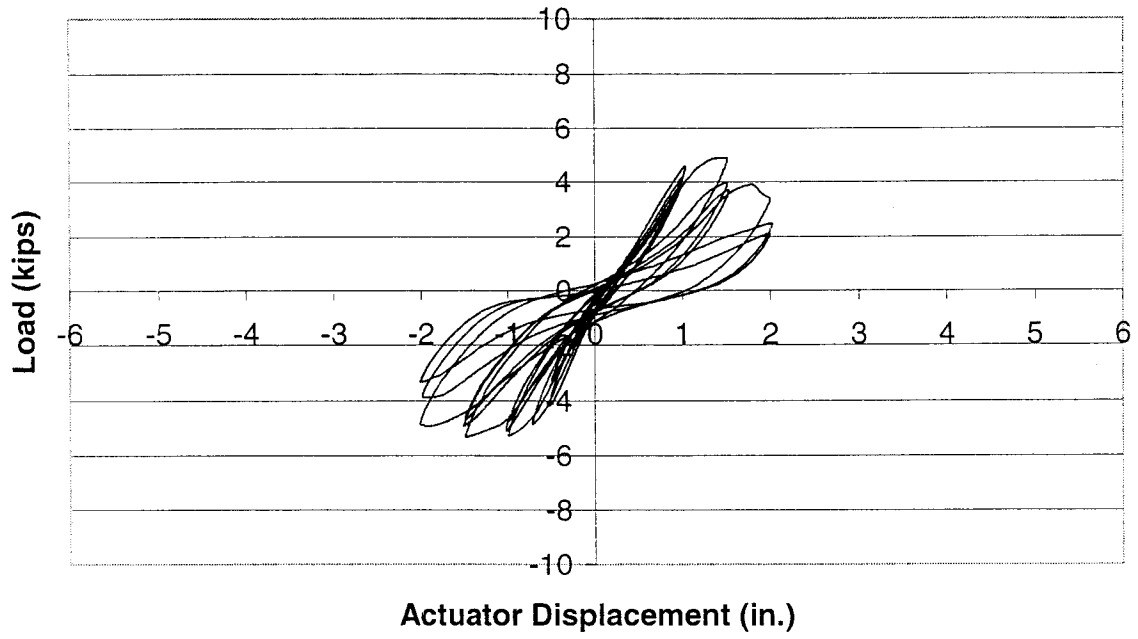


Figure 42 Load-Displacement Curves of Specimen AB2

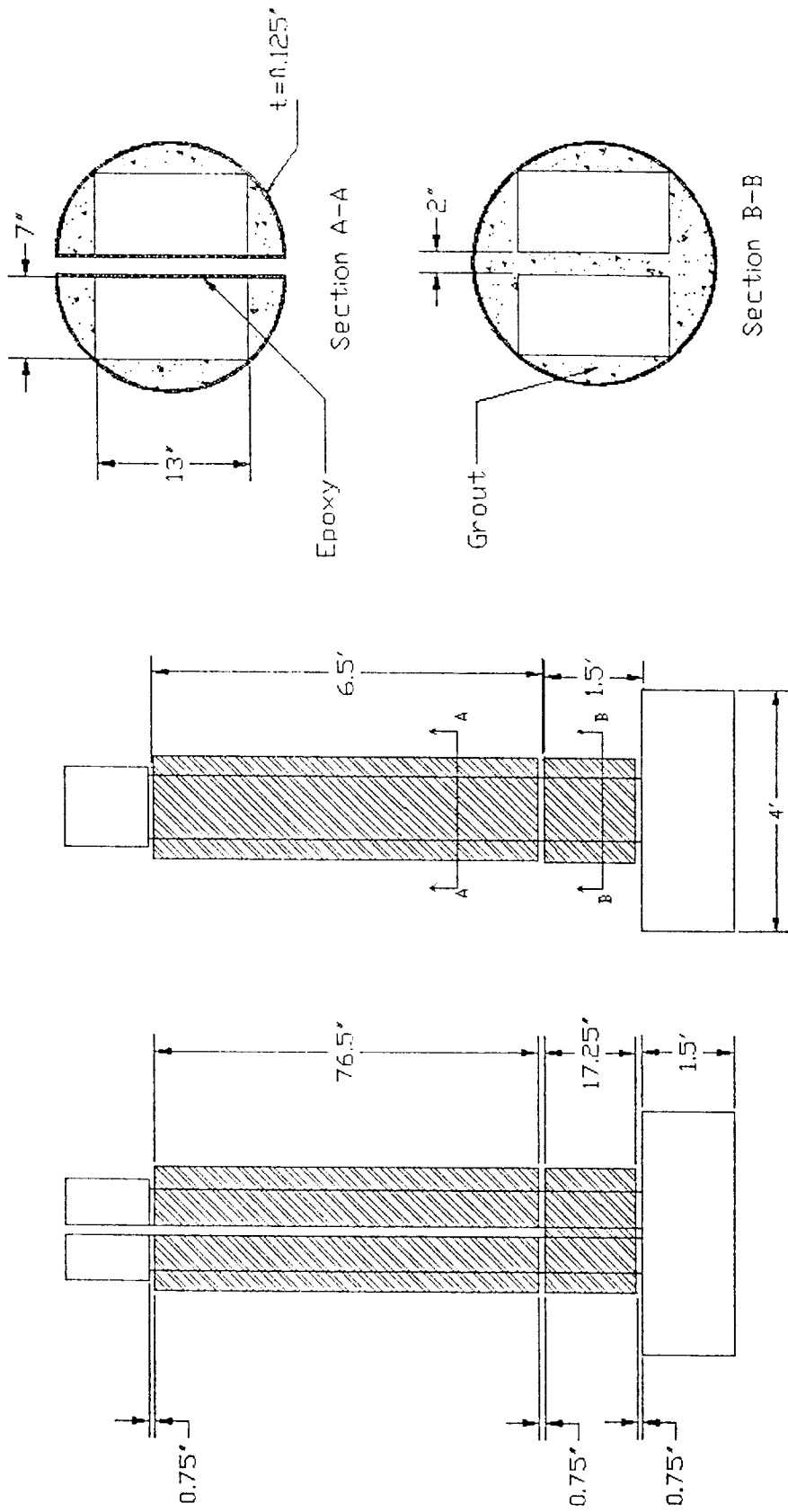


Figure 43 Retrofit Details for Specimen S14

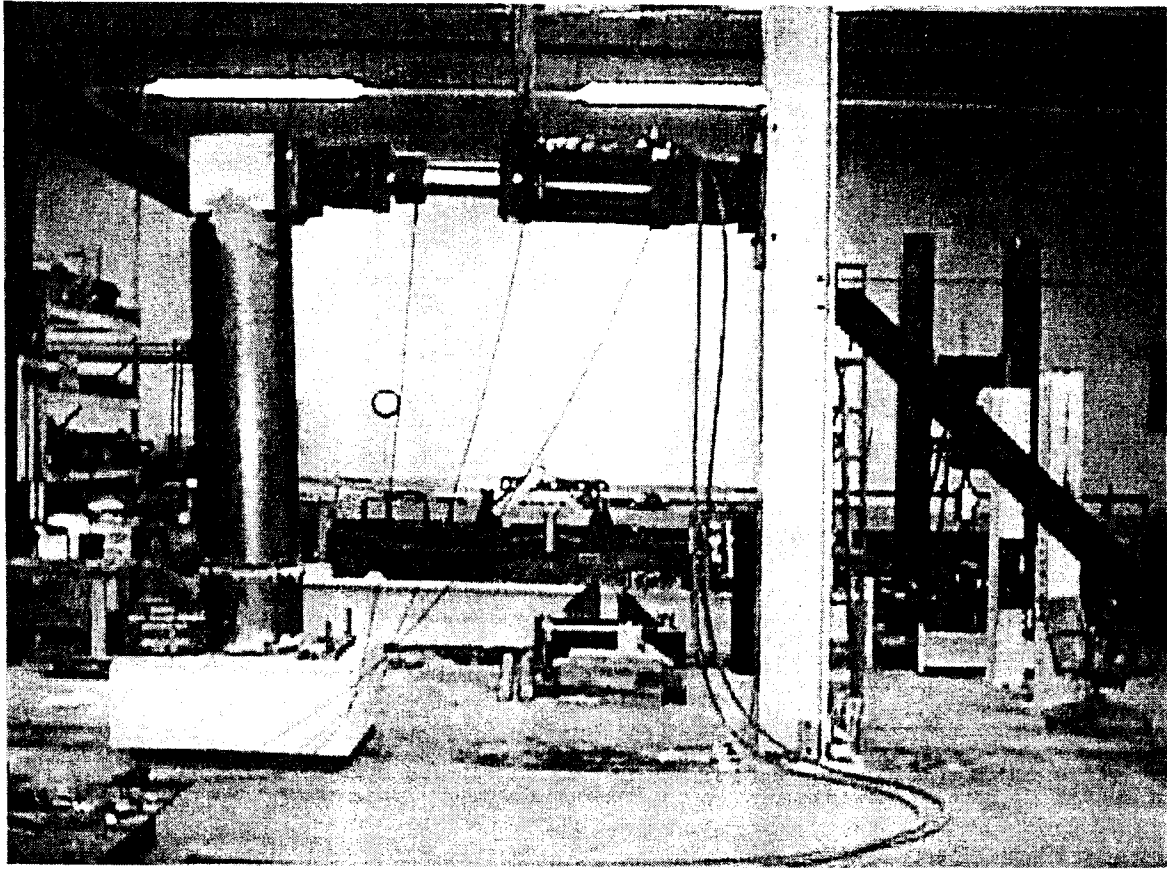


Figure 44 Specimen SJ4 Test Photograph

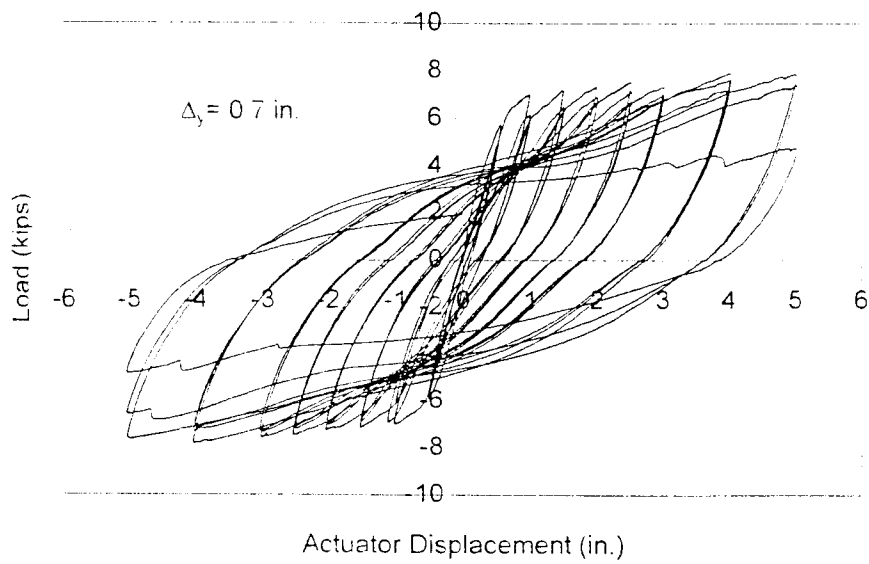


Figure 45 Load-Displacement Curves for Specimen SJ4

comparing the behavior of the steel jacketed specimen with that for the as-built specimen, significant improvement in ductility and energy dissipation is evident with the retrofitted specimen.

#### **Specimen FW4 (Fyfe Company Retrofit)**

Specimen FW4 was constructed similarly to the as-built specimen, AB2, except for being retrofitted using the Fyfe Company retrofit system. All retrofit design was performed by the company and is given in Appendix A. Flexural hinge confinement design was performed using Priestley, et al (1996) provisions. The controlling jacket thickness was that to produce an ultimate compression strain in the concrete of 0.0069. Only one ply ( $t_j = 0.051$  in.) material was required, but two plies ( $t_j = 0.102$  in.) were conservatively installed in both the primary and secondary plastic hinge regions. No lap splice confinement calculations were performed for the transverse specimen. The lap splice confinement that was provided was due to plastic hinge confinement design. Shear strength design for the transverse specimen was done in accordance with the SEQAD Provisions (1993). It was conservatively assumed that the composite material jacket would provide the entire shear strength required. Fyfe Company installed one ply ( $t_j = 0.051$  in.) of material in the shear-controlling region outside of the plastic hinge regions. A summary of the Fyfe Company retrofit for Specimen FW4 is given in Figure 46.

Figure 47 shows testing photographs of Specimen FW4. The load-displacement curves given in Figure 48. The peak horizontal load the specimen experienced was 31.4 kN (7.07 kips) at a displacement of 10.2 cm (4 in.). A 30% drop in lateral load capacity also occurred at a displacement of 10.2 cm (4 in.), resulting in a displacement ductility capacity of approximately 6. The failure was attributed to lap splice degradation at the base of each split section. The retrofit system of Specimen FW4 significantly improved the seismic performance of the column when compared to that of the as-built specimen, AB2. The retrofitted specimen was able to sustain a 100% increase in displacement ductility capacity, with wider hysteresis loops, allowing for a considerable increase in energy dissipation.

#### **Specimen FW5 (Sumitomo Retrofit)**

Specimen FW5 was constructed similarly to the as-built specimen AB2, except for being retrofitted

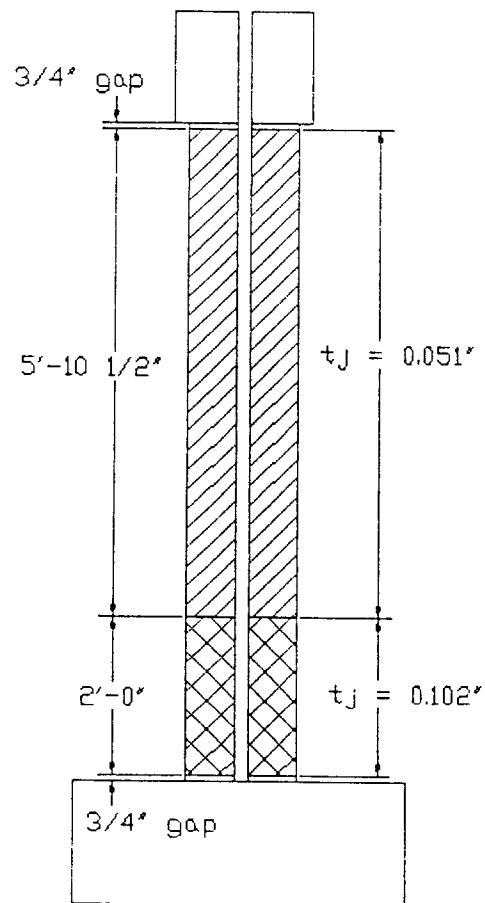
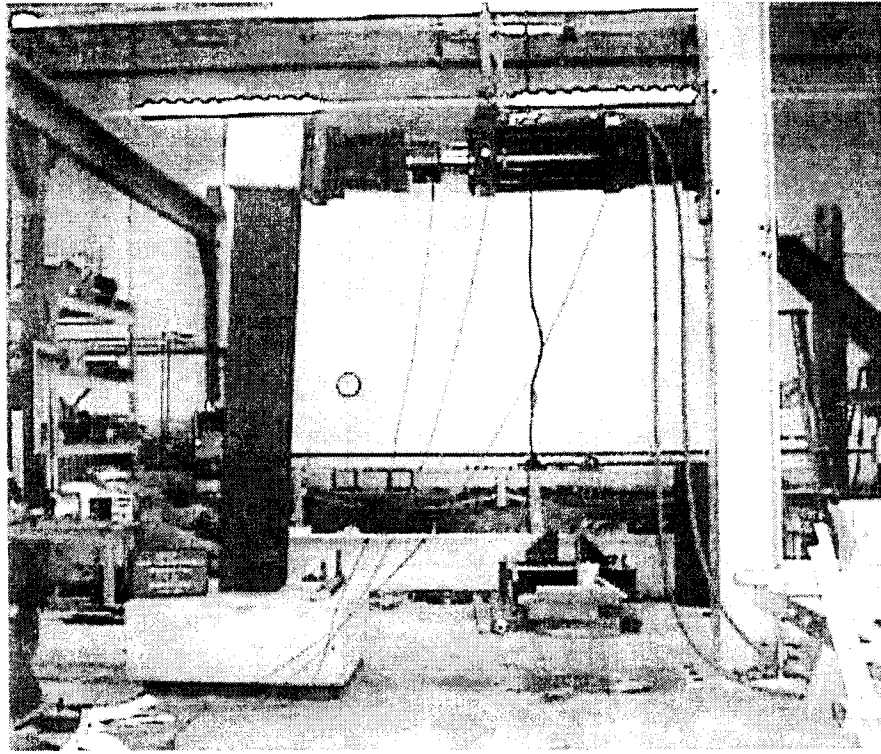
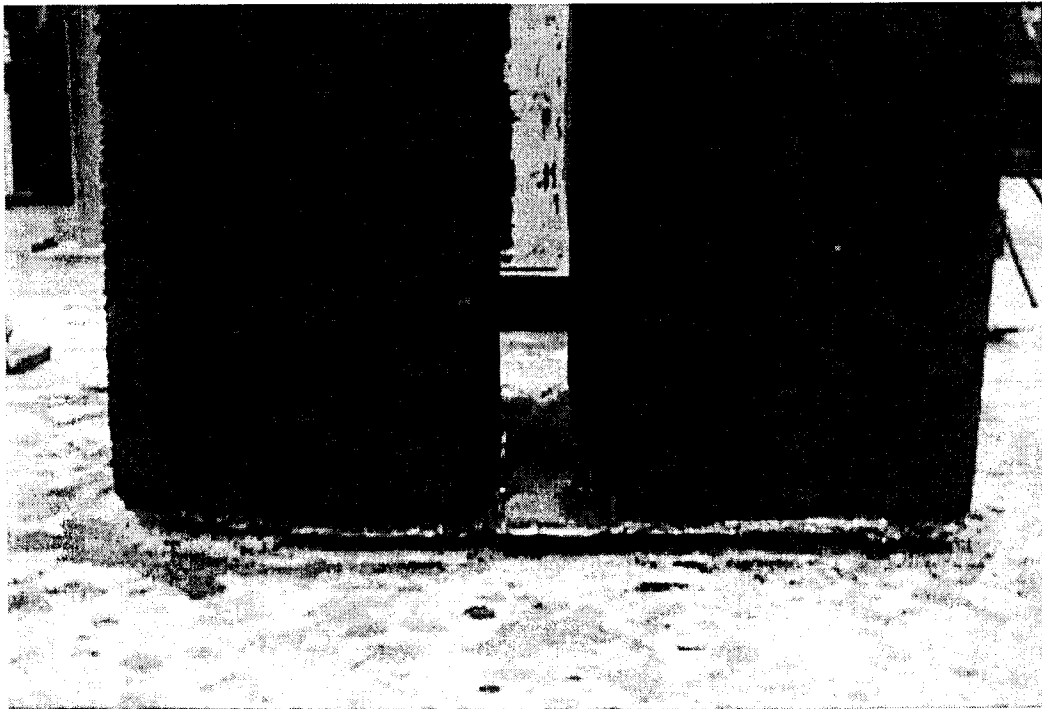


Figure 46 Retrofit Details for Specimen FW4



(a) Testing of Specimen FW4



(a) Opening at Base of Columns

Figure 47 Specimen FW4 Testing Photographs

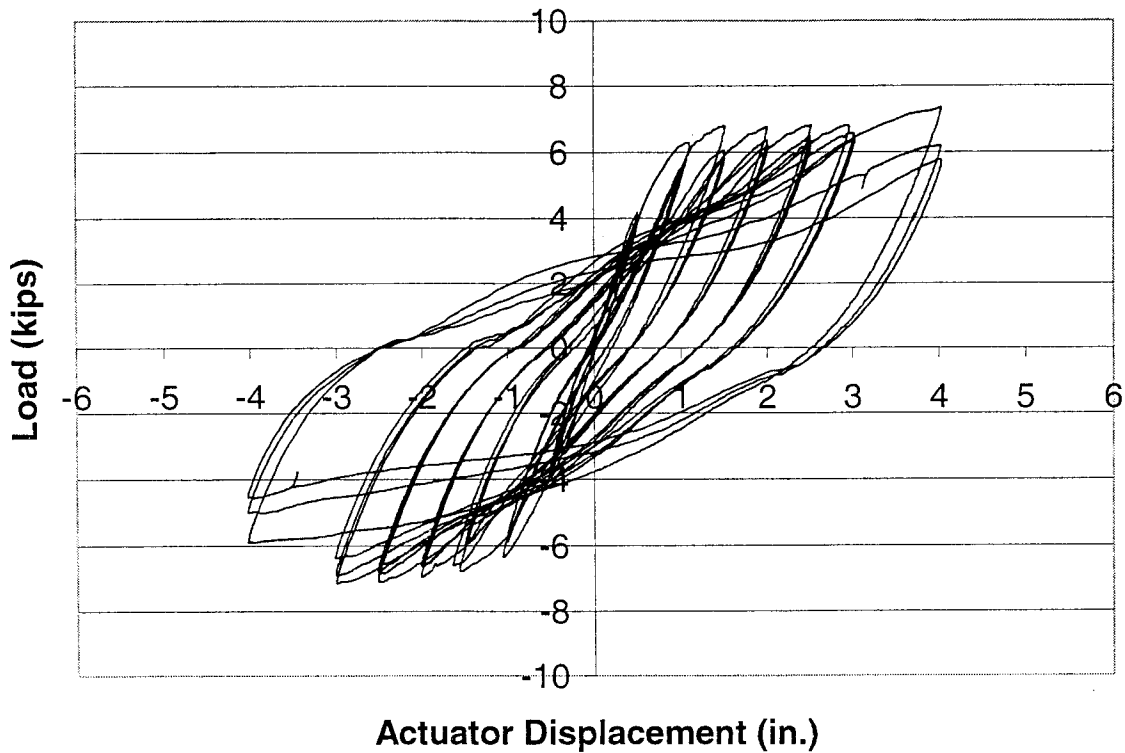


Figure 48 Load-Displacement Curves of Specimen FW4

using the Sumitomo retrofit system. The plastic hinge confinement design for the split sections was performed using both the ACTT-95/08 Provisions (Seible, et al, 1995) and the provisions proposed by Priestley, et al (1996). The controlling jacket thickness came from the Priestley, et al (1996) provisions. The jacket thickness was not doubled as recommended for a rectangular cross-section and jacket strains were limited to 0.004. The controlling jacket thickness was due to a required ultimate compression strain in the concrete of 0.00575. For Specimen FW5, a 33-cm (13-in.) strip of 0.00396-in. thick material was installed in the primary plastic hinge region, and a 33-cm (13-in.) strip of 0.00198-in. thick material was installed in the secondary plastic hinge region. Sumitomo installed one ply ( $t_j=0.0066$  in.) of vertically oriented material on all sides of the bottom 0.9 m (3 ft) of the column to help distribute stresses. Lap splice confinement calculations, per the ACTT-95/08

Provisions, for the transverse specimen yielded a required jacket thickness of 0.186 cm (0.0733 in.). The lap splice calculations were performed after the retrofit was installed and were not included in the final retrofit design or installation. Shear strength design for the transverse specimen was done in accordance with the ACTT-95/08 Provisions. The required jacket thickness for shear strength in the plastic hinge region was 0.0019 cm (0.00076 in.) and therefore did not control. Outside of the plastic hinge region no jacket was required, but Sumitomo conservatively installed one ply of material. The retrofit details for Specimen FW5 are summarized in Figure 49.

Testing photographs of Specimen FW5 are shown in Figure 50. Load-displacement hysteresis curves given in Figure 51. The specimen reached a peak lateral load of 33.9 kN (7.63 kips) at a displacement of 10.2 cm (4 in.). This corresponds to a displacement ductility capacity of approximately 7. The lateral load capacity of the specimen dropped by 60% at a displacement of 15 cm (5 in.) due to lap splice degradation. During the 15-cm (5-in.) displacement cycles, “popping” noises were heard and were attributed to the lap splice bars slipping relative to the concrete core. This slippage also produced “kinks” in the load-displacement hysteresis curves, as can be seen in Figure 51. The performance of Specimen FW5 was improved significantly compared to Specimen AB2 as a result of the retrofit measures. The load-displacement hysteresis curves show a large increase in displacement ductility and resulting seismic energy dissipation.

#### **Specimen FW6 (XXSys Retrofit)**

Specimen FW6 was constructed similarly to the as-built specimen AB2, except that it was retrofitted with the XXSys retrofit system. The split in the plastic hinge region was filled with grout prior to retrofit installation to provide confinement on the inside faces of the split. The plastic hinge confinement design was again based on the ACTT-95/08 Provisions (Seible, et al, 1995). The controlling jacket thickness was due to a required ultimate compression strain in the concrete of 0.0053. A 30-cm (12-in.) strip of 0.0400-in. thick material was installed in the primary plastic hinge region, and a 30-cm (12-in.) strip of 0.0199-in. thick material was installed in the secondary plastic hinge region. Lap splice confinement calculations for the transverse specimen were done in accordance with the ACTT-95/08 Provisions, yielding a required jacket thickness of

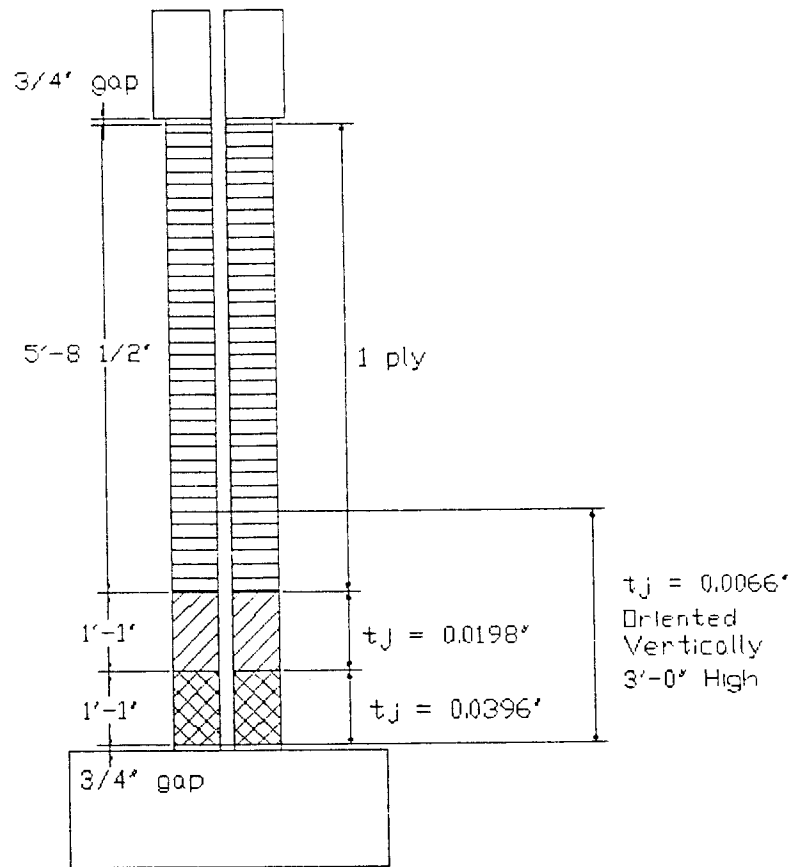
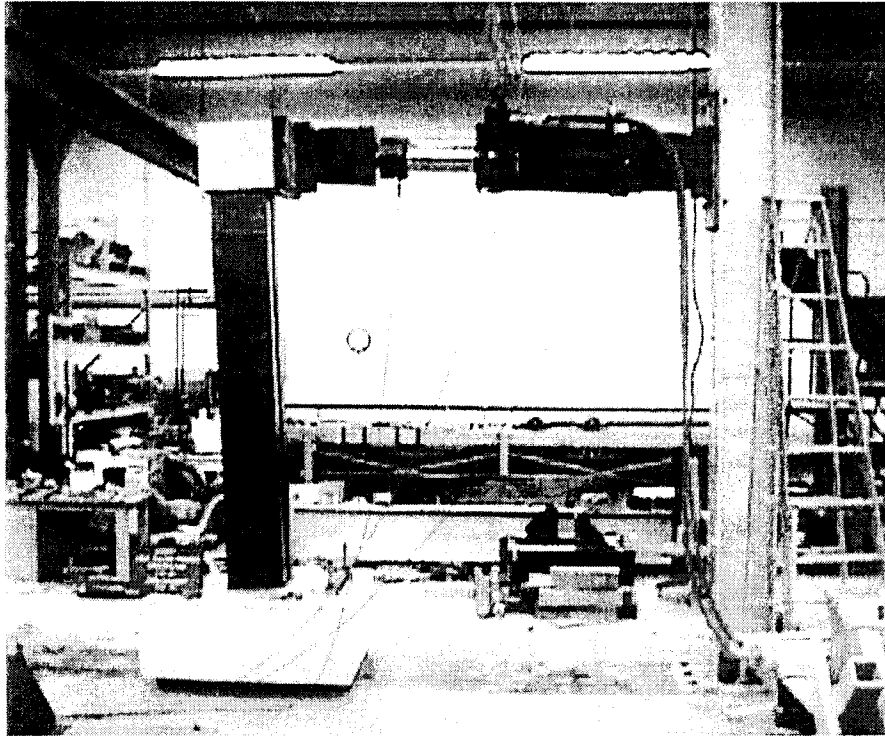
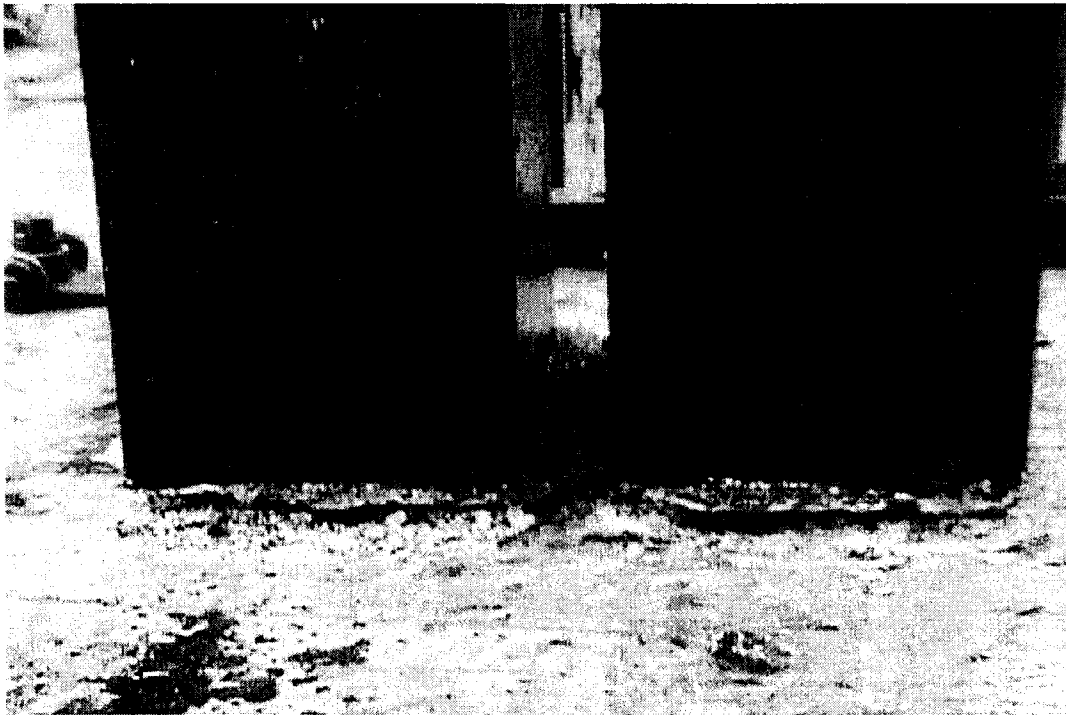


Figure 49 Retrofit Details for Specimen FW5



(a) Testing of Specimen FW5



(a) Opening at the Base of the Columns

Figure 50 Specimen FW5 Testing Photographs

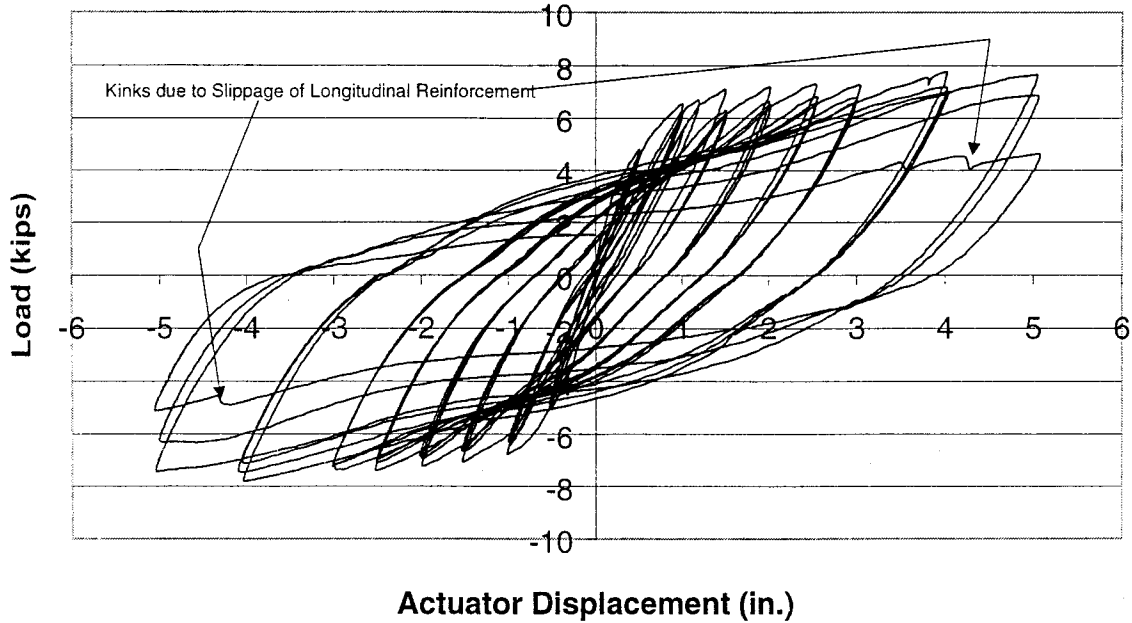


Figure 51 Load-Displacement Curves of Specimen FW5

0.71 (0.28 in.). XXSys decided that this jacket thickness was likely not to be economical and that the jacket thickness requirements for plastic hinge confinement would provide reasonable confinement for the lap splice as well. The final retrofit design considered only plastic hinge failure in the lap splice region. The ACTT-95/08 Provisions were used for shear strength design of the transverse specimen. The required jacket thickness for shear strength in the plastic hinge region was 0.0015 cm (0.0006 in.) and therefore did not control. Outside of the plastic hinge region, no jacket was required or installed. Figure 52 provides a summary of the retrofit details applied to Specimen FW6.

Testing photographs of Specimen FW6 are shown in Figure 53. The load-displacement hysteresis curves for Specimen FW6 are given in Figure 54. The specimen experienced a peak load of 30.9 kN (6.94 kips) during the first loading cycle at a displacement of 10.2 cm (4 in.). During the following two loading cycles at a 10.2-cm (4-in.) displacement, the specimen experienced a 65% drop in lateral load capacity. Lap splice degradation at the base of the split section was judged to be the cause of the failure, with a displacement

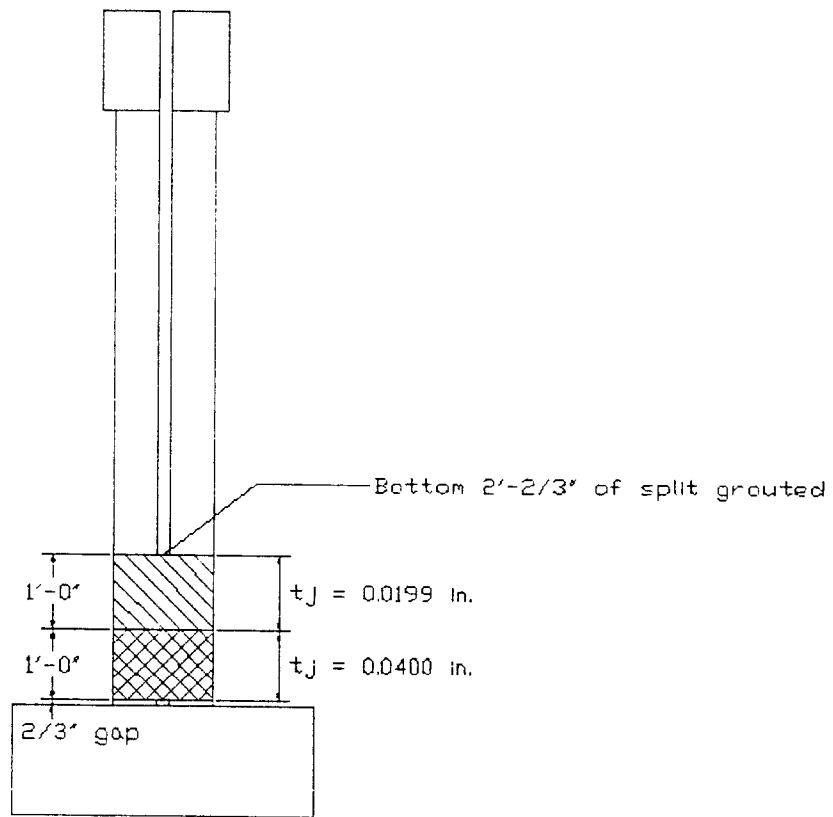
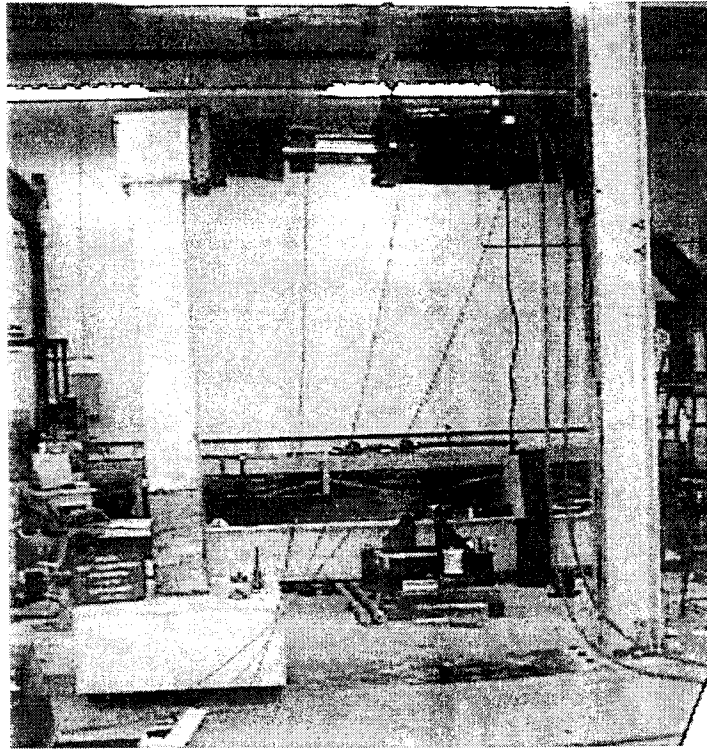
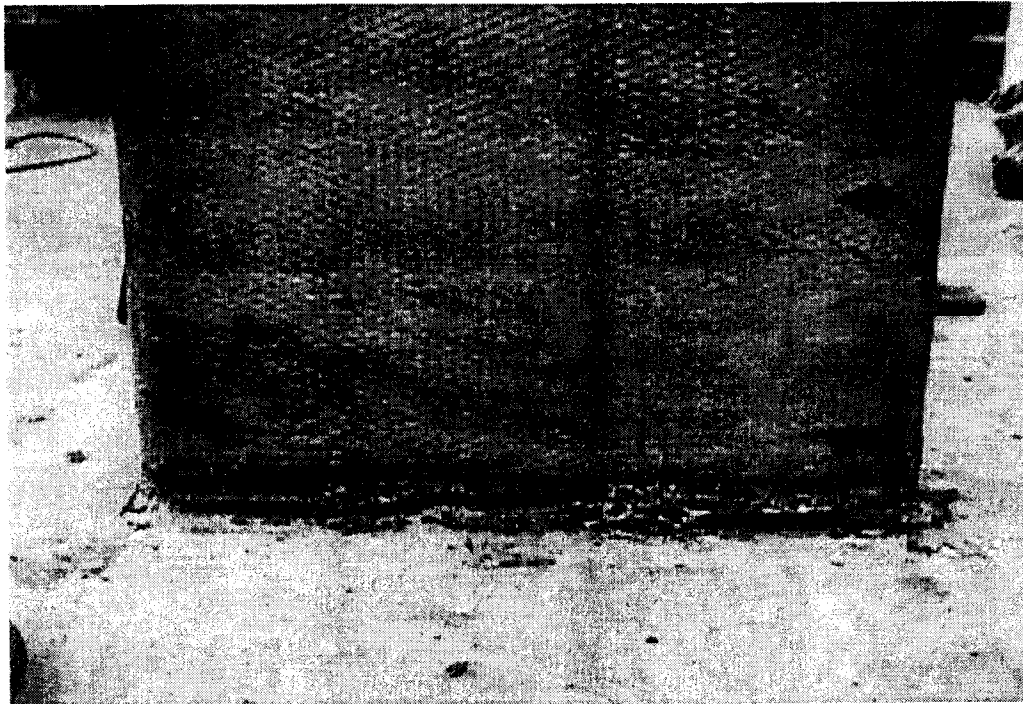


Figure 52 Retrofit Details for Specimen FW6



(a) Testing of Specimen FW6



(b) Crack Opening at Base of Columns

Figure 53 Specimen FW6 Test Photographs

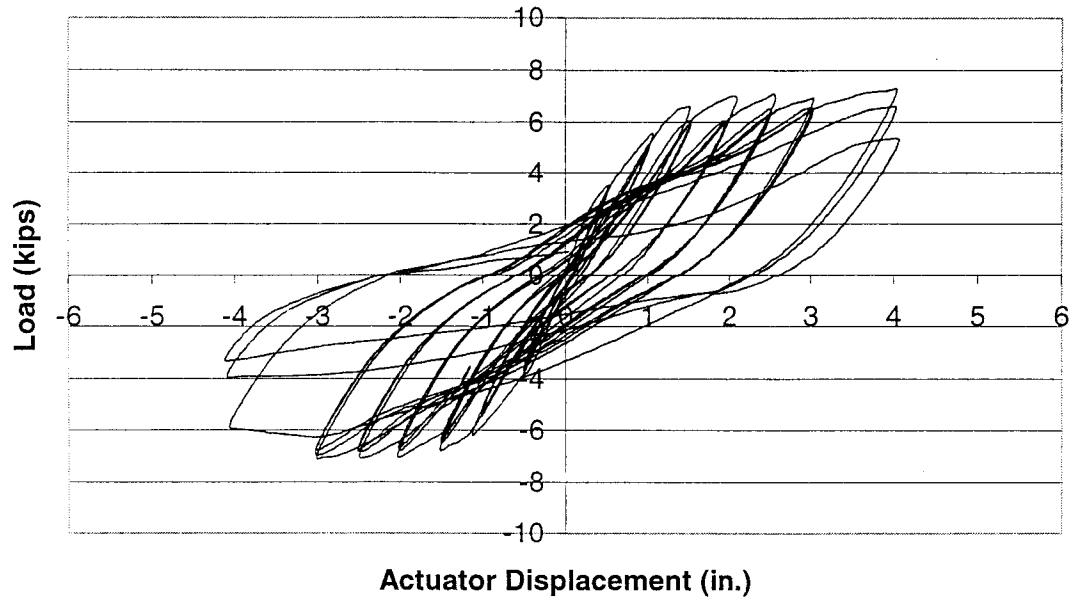


Figure 54 Load-Displacement Curves of Specimen FW6

ductility capacity of approximately 6. Compared to the as-built specimen, AB3, the retrofit system significantly increased the specimen's seismic performance. The additional confinement doubled the displacement ductility capacity and allowed for more seismic energy dissipation.

**Comparison of Transverse Specimen Performance**

The results of the transverse tests are summarized in Table 5. The peak load-displacement envelopes for all four retrofitted specimens and the as-built specimen under transverse loading are shown in Figure 55.

Table 5 Summary of Transverse Test Results

Specimen	$\mu_{\Delta}$	Peak Load kN (kips)	Energy Dissipated kN-m (kip-in.)
AB2	3	21.6 (4.87)	3.6 (32)
SJ4	7	34.6 (7.79)	63.7 (564)
FW4	6	31.4 (7.07)	33.6 (297)
FW5	7	33.9 (7.63)	58.9 (521)
FW6	6	30.9 (6.94)	25.0 (221)

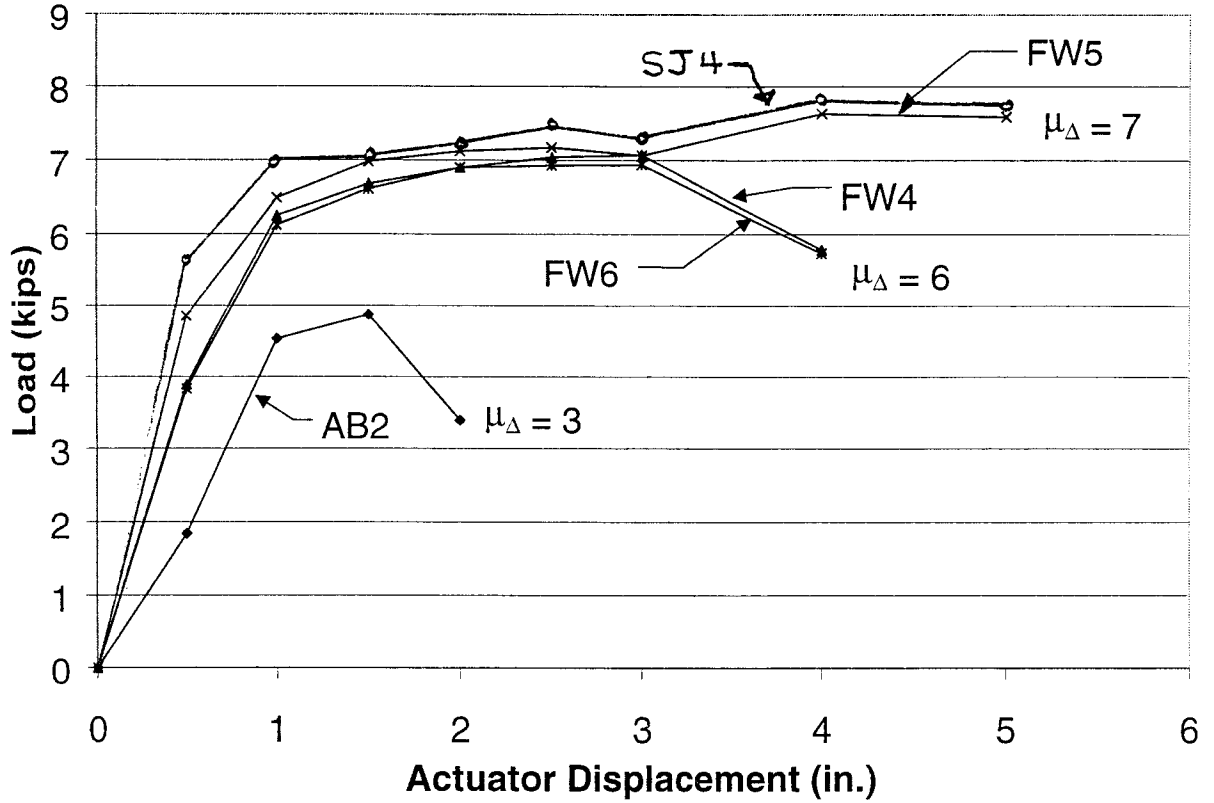


Figure 55 Peak Load-Displacement Envelope of Transverse Specimens

The performance of all four retrofitted specimens exceeded the as-built performance in terms of ductility and energy dissipation. All retrofit specimens reached or exceed a ductility capacity of 6. The curves for the Fyfe Company specimen, FW4, and the XXSys specimen, FW6, are very similar. Both specimens failed due to lap splice degradation at a displacement of 10.2 cm (4 in.). The steel jacketed specimen, SJ4, and the Sumitomo specimen, FW5, also failed due to lap splice degradation, but both specimens reached a higher level of ductility and dissipated substantially more seismic energy. This behavior can be attributed to higher confinement stresses in the lap splice region for those two specimens. None of the commercial companies

incorporated full lap splice confinement into their final retrofit designs. The provided lap splice confinement is only for flexural hinge confinement design. The different confinement stresses present in the specimens are a result of the plastic hinge design processes used by the respective companies. Sumitomo limited the ultimate stress and ultimate strain in the jacket based on a strain limit of 0.004. Fyfe Company and XXSys used the ultimate stress and ultimate strain of their respective materials. With a ply thickness of 0.0066 in., Sumitomo would only be required to install two plies of material, instead of the six plies that were installed. This would result in a significant decrease in the confinement pressure supplied by the jacket. As noted previously, the product  $t_j E_j$  can be used to measure the relative confinement pressure supplied by any jacket. The values of this product for the primary plastic hinge regions of each retrofit system are listed in Table 6. It is clear that the confinement pressure supplied by the Sumitomo jacket is substantially larger than the pressure supplied by the other two retrofit systems.

Table 6 Comparison of Relative Confinement Pressures in Composite Transverse Specimens

Specimen	Retrofit Company	$t_j E_j$ kN/m (kip/in.)
FW4	Fyfe Company	496 (408)
FW5	Sumitomo	1609 (1323)
FW6	XXSys	584 (480)

Another design difference between the three retrofit systems was that XXSys grouted the split in the plastic hinge region and installed no composite material in the shear-controlling region. The grouting of the split appears to have had no significant effect on the specimen performance. Horizontal flexure cracks formed in the concrete directly above the plastic hinge region but did not contribute to the failure mechanism.

## CONCLUSIONS

The experimental test results of this study indicate that split reinforced concrete columns typical of those present in the Spokane Street Overcrossing will likely perform poorly in a significant earthquake event. Crack propagation from the base of the split can be expected, resulting in the potential for major damage or even collapse of the columns. Tests conducted on specimens representing as-built conditions indicate that cracks will propagate from the base of the split at low displacement levels and will continue to propagate through the non-split section. The crack propagation into the non-split section increases the effective height of the column and, as a result, the column becomes more flexible. In the case of out-of-phase motion in the longitudinal direction of the bridge, there will be little ability to dissipate energy and the split columns can be expected to pound against each other. Split columns with deficient lap splices at their bases are also expected to perform poorly in a large earthquake. Tests on as-built specimens showed rapid splice degradation due to short lap length and insufficient confinement steel. In addition, for columns with full-height splits, existing footings may be vulnerable to crack propagation from the split into the footing.

This research showed that circular steel jacketing around the bottom non-split section is effective in inhibiting crack propagation from the base of the split. The use of "D" shaped steel jacketing of the split sections enabled preservation of split function as well as enhancing the flexure and shear performance of the columns. Circular steel jacketing at the column base was used to improve the performance of the deficient lap splice regions. Tests showed that the steel jacketing retrofit scheme used in this study was effective in improving ductility and energy dissipation when compared to the as-built response. All steel jacketed columns reached or exceeded a displacement ductility capacity of 7, which would generally be regarded as acceptable performance for retrofit design.

Results from this research indicate that the design guidelines developed by Seible, et al (1995), Priestley, et al (1996), and SEQAD (1993) for composite materials can be utilized to successfully address split column vulnerabilities using rectangular jackets. All three commercial composite material retrofit systems investigated in this study successfully prevented crack propagation at the base of the split and plastic hinge degradation in the split sections. Under out-of-phase loading, all retrofitted out-of-phase specimens reached

composite material jackets be those as set forth by the ACTT-95/08 Provisions (Seible, et al, 1995) and by Priestley, et al (1996). The ACTT-95/08 Provisions (Seible, et al, 1995) specify a required jacket thickness based on an equivalent circular diameter; that thickness is then multiplied by a factor of 2 to account for the reduced effectiveness of rectangular jackets. The provisions of Priestley, et al (1996) address rectangular jackets directly. Both of these design procedures were used by the companies involved in this project and both resulted in satisfactory specimen performance.

As for all older columns, when deficient lap splices are present, retrofit measures should be designed to provide confinement over the length of the lap splice. For steel jacketing, a circular jacket should be applied over the lap, with the jacket thickness selected based upon provisions developed by Priestley, et al (1996). Rectangular composite material jackets provide confinement stresses only at the corners and are therefore less effective than circular or elliptical jackets. However, rectangular jackets will improve specimen performance if controlled debonding is permissible. For rectangular jacketing of deficient lap splices using composite materials, ACTT-95/08 Provisions (Seible, et al, 1995) should be used. Of note is that none of the companies participating in this project used the jacket thickness required for lap splice confinement per these Provisions. However, jacketing based upon plastic hinge confinement design did provide the specimens with some degree of lap splice confinement. If the lap splice confinement jacket thickness requirement is judged to be not economical, and controlled debonding of the lap splice is acceptable, then providing lap splice confinement via the plastic hinge confinement design is a viable alternative. It is recommended that further tests be conducted to investigate the effectiveness of using rectangular composite material jackets for lap splice confinement.

#### **ACKNOWLEDGMENTS**

This research project was funded by the Washington State Department of Transportation. The investigators gratefully acknowledge the contributions of the engineers in the WSDOT Bridge Office, particularly those of Hongzhi Zhang, Chuck Ruth and Ed Henley. The grout and epoxy materials used in this study were donated by the Sika Corporation through the efforts of Thad Brown. The authors also thank the Pacific Earthquake Engineering Research (PEER) Center for support received as a PEER Graduate Fellowship.

a displacement ductility level of 10 without any significant drop in load. In addition, the energy dissipated by the retrofitted specimens significantly exceeded that for the as-built specimen.

All retrofitted specimens with deficient lap splices eventually failed due to lap splice degradation at the base of the column sections. None of the composite material retrofit designs met the recommendations for lap splice confinement set forth in the ACTT-95/08 Provisions (Seible, et al, 1995). Rather, the provided lap splice confinement with the composite systems was that for plastic hinge confinement design. However, the performance of the retrofitted specimens exceeded the as-built performance in terms of displacement ductility capacity and energy dissipation. All retrofit specimens with deficient lap splices reached or exceeded a displacement ductility capacity of 6.

While some differences in performance were obtained with the various retrofit systems, all retrofitted specimens showed significant improvements in performance when compared to that for the as-built specimens. Performance differences in the retrofitted specimens were attributed to the different design procedures and assumptions used by each retrofit company.

## **RECOMMENDATIONS/APPLICATIONS/IMPLEMENTATION**

The results from this research provide a basis for designing retrofit measures to improve the seismic performance of split reinforced concrete columns. Both steel jacketing and composite material jacketing is effective in improving ductility capacity and ability to dissipate seismic energy of the split columns. An assessment must first be made of the seismic deficiencies present in the existing split columns. Deficiencies will include the presence of the split and, depending upon the age of the bridge, may also include inadequate flexural hinge confinement, shear strength, and lap splices. Guidelines for performing these assessments are provided in Priestley, et al (1996) and the FHWA *Seismic Retrofitting Manual for Highway Bridges* (1995).

In columns containing a partial height split, crack propagation from the base of the split must be prevented. A procedure was developed in this study for designing a circular steel jacket to be applied to the column immediately below the split in order to prevent the split from propagating. The required steel jacket thickness,  $t_j$ , is given by:

$$t_j = \frac{2V_p}{Bf_{yj}} \quad (\text{Equation 22})$$

where  $V_p$  is the shear force required to develop a plastic hinge mechanism in one split section,  $B$  is the width of one of the split sections measured in the direction of loading, and  $f_{yj}$  is the yield strength of the steel jacket. For columns with a full-height split, this circular jacketing should be applied at the column base over a height equal to the larger of the column cross-sectional dimensions.

With composite jacketing, the design calculations varied with the three companies regarding how to address the vulnerability of crack propagation from the base of the split. Fyfe Company used engineering judgment without any supporting calculations. Sumitomo designed for the shear force required to reach the plastic moment capacity of the split sections. XXSys based their design on a limiting crack width of 1 mm, which resulted in a design shear force much larger than the shear force required to develop the plastic moment capacity of the split sections.. From a mechanics standpoint, the method Sumitomo used appears the most reasonable, and it is similar to the procedure proposed in this study for steel jacketing. The following design steps are therefore recommended for composite retrofitting, based on the results from this research:

- Design for the shear force required to develop the plastic moment capacity of the split sections.
- Design a strip of composite material, to be installed directly below the split, which will resist the total shear force. The effective depth of this strip should be approximately equal to one-half of the unsplit column dimension measured on the face perpendicular to the split.

Retrofit measures should be applied to the split columns for flexural hinge confinement design if the column transverse reinforcement in the hinge regions is inadequate. The gap between the two split sections must be maintained in order to continue to allow movement in the bridge. Rectangular split sections can be retrofitted with "D" shaped steel jacketing in the potential hinge locations. For columns deficient in shear, full height "D" jacketing should be used. For aesthetic reasons, full height jacketing may be desired for all retrofit applications. The thickness of the "D" jacketing can be determined based upon provisions developed for elliptical steel jackets by Priestley, et al (1996).

It is recommended that design guidelines for retrofitting for flexural hinge confinement using

## REFERENCES

- California Department of Transportation (1992). "Memo to Designers, 20-4," April.
- Chai, Y.H.; Priestley, M.J.N.; and Seible, F. (1991). "Retrofit of Bridge Columns for Enhanced Seismic Performance," *Seismic Assessment and Retrofit of Bridges, SSRP 91/03*, pp. 177-196.
- Priestley, M.J.N. (1991). "Seismic Assessment of Existing Bridges," *Seismic Assessment and Retrofit of Bridges, SSRP 91/03*, University of California, San Diego, pp. 84-149.
- Priestley, M.J.N. and Seible, F. (1991). "Design of Seismic Retrofit Measures for Concrete Bridges," *Seismic Assessment and Retrofit of Bridges, SSRP 91/03*, University of California, San Diego, pp. 197-234.
- Priestley, M.J.N. and Seible, F. (1994). "Seismic Assessment of Existing Bridges," Proceedings of the Second International Workshop, Queenstown, New Zealand, Earthquake Commission of New Zealand, August 9-12.
- Priestley, M.J.N., Seible, F. and Calvi, G.M. (1996). *Seismic Design and Retrofit of Bridges*, John Wiley & Sons, Inc., New York.
- Seismic Retrofitting Manual For Highway Bridges* (1995). Federal Highway Administration, Report No. FHWA-RD-94-052, May.
- Seible, F., and Innamorato, D., *Earthquake Retrofit of Bridge Columns with Continuous Carbon Fiber Jackets*, Advanced Composites Technology Transfer Consortium, Report No. ACTT-95/08, La Jolla, California, August, 1995.
- SEQAD Consulting Engineers, *Seismic Retrofit of Bridge Columns Using High Strength Fiberglass/Epoxy Jackets*, Solana Beach, California, August, 1993.
- Zhang, H., Knaebel, P.J., Coffman, H.L., VanLund, J.A., Kimmerling, R.E. and Cuthbertson, J.G. (1996). "Seismic Vulnerability Study of the SR99 Spokane Street Overcrossing," Washington State Department of Transportation, January.